FACULTY OF PHYSICS

ADAM MICKIEWICZ UNIVERSITY

NANOBIOMEDICAL CENTRE

DEPARTMENT OF MEDICAL PHYSICS

POZNAŃ

Synthesis and evaluation of superparamagnetic iron oxide nanoparticles containing doxorubicin as a potential targeted drug delivery system

Magdalena Hałupka – Bryl

Supervisor: Prof. dr hab. Ryszard Krzyminiewski

Assistant supervisor: Dr Bernadeta Dobosz

Doctoral thesis

Acknowledgments

I would like to thank my supervisor Prof. Ryszard Krzyminiewski for help, useful advice and scientific support throughout the course of this work.

I sincerely thank Prof. Stefan Jurga for giving me the possibility to carry out my doctoral thesis in the NanoBioMedical Centre and encouragement on this project.

I wish to express my gratitude to my co-supervisor Prof. Yukio Nagasaki for giving me the best opportunity to work in his group. I thank him for providing me with the numerous possibilities to carry out scientific research, outstanding supervision in the experiments and stimulating discussions on our experimental results. I thank him and members of his group for sharing their knowledge, fruitful discussions and excellent time we spent together.

Special thanks go to Kei Asai and Sindhu Thangavel who helped and guided me to start up my research project, for their invaluable help, scientific and non-scientific support.

I want to thank Dr Bernadeta Dobosz for her help, suggestions and discussions throughout Electron Paramagnetic Resonance studies.

Many thanks to all my colleagues from the NanoBioMedical Centre, especially I would like to thank Dr Barbara Maciejewska, Dr Alicja Warowicka, Martyna Michalska and Mikołaj Grzeszkowiak for their help, friendly atmosphere, scientific and non-scientific support.

I thank my friend, Magdalena Bednarowicz for her endless support, enthusiastic encouragement throughout this PhD project and unforgettable time we spent together during our secondment.

Finally, my deepest gratitude goes to my husband Jarek for his love, continuous support during the last four years, motivation and that you always believed in me.

To my husband Jarek

List of Abbreviations

CLSM	Confocal Laser Scanning Microscope
DLS	Dynamic Light Scattering
DMEM	Dulbecco's Modified Eagle's Medium
DOX	Doxorubicin
EPR effect	Enhanced Permeability and Retention Effect
EPR	Electron Paramagnetic Resonance
FBS	Fetal Bovine Serum
HRTEM	High-Resolution Transmission Electron Microscope
LC-MS	Liquid Chromatography – Mass Spectroscopy
MRI	Magnetic Resonance Imaging
NMR	Nuclear Magnetic Resonance
NPs	Nanoparticles
PBS	Phosphate Buffered Saline
PEG	Poly(ethyleneglycol)
PEG-*b*-PVBP	Poly(ethylene glycol)-*block*-poly(4-vinylbenzylphosphonate) Block Copolymer
PEG-PIONs	Iron Oxide NPs covered with PEG-*b*-PVBP
PEG-PIONs/DOX	Iron Oxide NPs covered with PEG-*b*-PVBP containing DOX
RES	Reticuloendothelial System
SEC	Size Exclusion Chromatography
SPIONs	Superparamagnetic Iron Oxide NPs
SQUID	Superconducting Quantum Interference Device
XRD	X-ray Diffraction

Table of contents

Abstract

One of the biggest challenges in antitumor therapy is to deliver chemotherapeutic drug directly to the desired location, at the lowest dose possible and thus to increase the effectiveness of treatment and decrease strong adverse effects of chemotherapy. Anticancer drugs, which are the pharmacological ground for approaches to antitumor therapy, usually exhibit high cytotoxic properties, however they are not specific in reaching the desired location in the body. This results in a systemic distribution of cytotoxic agents, which provoke well known strong side effects. Advances in nanotechnology offer new approaches for targeted delivery of anticancer agents, which may reduce or prevent side effects by targeting the drug molecules directly to the tumor region.

Iron oxide nanoparticles (NPs) have drawn great interest in recent years because of their unique physical and chemical properties. Administration of functionalized magnetic iron oxide NPs became one of the strategies to improve safety and sensitivity to cancer chemotherapy, and these nanostructures are attractive materials that could be used in various bioapplications, including diagnostic imaging and targeted therapy.

Magnetic NPs were synthesized by alkali co-precipitation of iron salts followed by coating with surface modification agent, poly(ethylene glycol)-*block*-poly(4-vinylbenzylphosphonate) block copolymer (PEG-PIONs). An anticancer drug DOX, which clinical use is associated with severe cardiotoxicity, was loaded onto PEG-PIONs surface (PEG-PIONs/DOX), and to my knowledge, this formulation showed higher drug encapsulation efficiency than other formulations previously reported. PEG-PIONs/DOX were examined in terms of their physicochemical and magnetic properties using different methods. Synthesized NPs were stable in physiological mimicking conditions and had a hydrodynamic diameter appropriate for biomedical use. The present findings of characterization of magnetic properties demonstrated that synthesized nanosystem is promising tool for potential magnetic drug delivery. *In vitro* studies showed that PEG-PIONs/DOX exhibit stable and continuous *in vitro* drug release and antiproliferative effects on cancer cells. Fluorescent imaging indicated internalization of the PEG-PIONs/DOX in cancer cells. Moreover, *in vivo* biodistribution studies showed that PEG-PIONs/DOX preferentially accumulate in the tumor region *via* enhanced permeability and retention effect. In addition, analysis of the serum levels of enzymes indicated that PEG-PIONs/DOX reduced the cardiotoxicity associated with free DOX.

The results presented in this dissertation suggest that PEG-PIONs/DOX have a potential for their future bioapplications and may lead to obtain tissue selective and/or externally guided targeted delivery system of antitumor drugs.

Summary

Due to their unique physical and chemical properties, superparamagnetic iron oxide nanoparticles (SPIONs) have drawn a great interest in recent years. Administration of appropriately functionalized magnetic iron oxide nanoparticles (NPs) became one of the strategies to improve safety and sensitivity to cancer chemotherapy by targeting the drug molecules directly to the tumor region. These NPs are attractive materials that could be used in various bioapplications, including diagnostic imaging and targeted therapy. Although advances in nanotechnology offer new nanoparticle-assisted drug delivery systems, the therapeutic efficacy of these materials remains to be clarified. One of the major issues is low accumulation efficiency of NPs in the tumor region, also their stability and drug loading capacity have still some scope for improvement. To have the best possible control of quality of produced nanosystem, I decided to synthesize and characterize the material from the basic step − the biocompatible block copolymer PEG-derivative to functionalized SPIONs containing anticancer drug doxorubicin (DOX). The main aim of this work was to design and characterize a stable, biocompatible and injectable nanocarrier with antiproliferative effect on cancer cells and high drug loading efficiency and to explore their usefulness as a potential targeted drug delivery system.

This dissertation is divided into 5 chapters. The *Introduction* reviews previous work and basic concepts of SPIONs, their most important properties and the possibility for their application in biomedicine. In particular, the methods of SPIONs synthesis and their surface modification, which is crucial for *in vivo* administration have been introduced and characterization of SPIONs for bioapplications has been presented. Next, magnetic properties of these materials and characterization of SPIONs as drug delivery systems are described. Finally, the enhanced permeability and retention effect is discussed in detail.

The second chapter introduces the reader to the main *experimental methods* used in this work and it is subdivided into 6 subsections to facilitate reading and arrange all the techniques used. Materials used in my research are presented in first subsection. Then, synthesis of block copolymer is described. Next, synthesis and complete physicochemical characterization of functionalized magnetic NPs are discussed. The two last subsections of this chapter include their presentation of performed *in vitro* as well as *in vivo* experiments.

The third chapter reports *Results and discussion* of this work; characterization of block copolymer is presented, the physicochemical properties of synthesized and appropriately functionalized NPs containing DOX are described: size, stability in physiological conditions,

drug loading efficiency; magnetic properties, their superparamagnetic and crystalline nature indicated that prepared NPs are promising tool for their potential bioapplication; i*n vitro* studies demonstrated stable and continuous drug release profile, antiproliferative effects on cancer cells and internalization of NPs in cancer cells; *in vivo* biodistribution studies showed preferred accumulation in the tumor region *via* enhanced permeability and retention effect and reduction of the cardiotoxicity associated with free DOX.

The fourth chapter comprises general *conclusions,* a short summary of the work performed and goals achieved.

The fifth chapter includes bibliography.

Streszczenie

Jednym z głównych założeń rozwoju i doskonalenia współczesnej terapii przeciwnowotworowej jest dostarczenie leku bezpośrednio do wybranej lokalizacji w organizmie, stosując jego możliwie jak najmniejszą dawkę oraz kontrolując jego uwalnianie. Osiągnięcie tego celu umożliwiłoby zmniejszenie toksyczności chemioterapii i wpłynęłoby korzystnie na efektywność leczenia. W literaturze znajdujemy wiele raportów naukowych o nowoczesnych systemach dostarczania leków, także tych, opartych na zastosowaniu różnych nanomateriałów, jednakże ich skuteczność jest ciągle dyskusyjna. W celu udoskonalenia ww. układów nanonauki zaproponowały nowe kierunki celowanych terapii. Jednym z nich są, będące tematyką mojej pracy doktorskiej, magnetyczne nanocząstki jako nośnik leku przeciwnowotworowego. Superparamagnetyczne nanocząstki tlenku żelaza (SPIONs) są dziś przedmiotem intensywnych badań ze względu na ich unikalne właściwości fizyczne i chemiczne. Dzięki możliwości stosowania licznych modyfikacji powierzchniowych (np. powlekanie nanocząstek biozgodnymi polimerami, dołączanie leków i innych biomolekuł) można manipulować ich własnościami i kontrolować ich parametry. Zabiegi takie korzystnie wpływają na biodegradowalność i biokompatybilność w ustroju, zmniejszają toksyczność oraz zwiększają stabilność wprowadzanych nanoukładów. Obecnie trwają intensywne prace badawcze nad potencjalnym zastosowaniem SPIONs w celowanej terapii przeciwnowotworowej i diagnostyce medycznej. Jednakże głównym problemem jest ich niska kumulacja w rejonie guza, a stabilność układów w warunkach odzwierciedlających naturalne oraz stopień enkapsulacji leku wciąż podlegają dyskusji.

Głównym celem przeprowadzonych badań była synteza oraz kompleksowa charakterystyka fizykochemiczna i biologiczna magnetycznych SPIONs pokrytych oryginalnym, biokompatybilnym polimerem - pochodną polietylenoglikolu, zawierających lek przeciwnowotworowy - doksorubicynę (PEG-PIONs/DOX). Przeprowadzone przeze mnie badania miały na celu stworzenie biokompatybilnego układu do wstrzykiwania dożylnego, o wysokim stopniu enkaspulacji środka cytostatycznego i działaniu antyproliferacyjnym na komórki nowotworowe, mającego w przyszłości potencjalne zastosowanie w terapii celowanej leczenia nowotworów.

PEG-PIONs/DOX otrzymano stosując metodę koprecypitacji soli żelazowych w środowisku zasadowym. Następnie, w wyniku funkcjonalizacji zsyntetyzowanym wcześniej biozgodnym polimerem blokowym, otrzymano hydrofilowy materiał, do którego powierzchni podłączono lek przeciwnowotworowy – doksorubicynę.

Zweryfikowano parametry fizykochemiczne, właściwości magnetyczne i biologiczne uzyskanych nanocząstek. Właściwości fizyczne otrzymanych układów scharakteryzowano metodami dynamicznego rozpraszania światła, spektroskopii UV-Vis oraz wysokorozdzielczej transmisyjnej mikroskopii elektronowej. Właściwości magnetyczne określono metodami elektronowego rezonansu paramagnetycznego, magnetometrii SQUID oraz dyfraktometrii promieni rentgenowskich. Przeprowadzono analizę cytotoksyczności układów za pomocą testu żywotności MTT na komórkach nowotworowych raka jelita grubego C-26 oraz zbadano biodystrubycję DOX z otrzymanych NPs w badaniu *in vivo* na mysim modelu zwierzęcym.

Niniejsza praca podzielona jest na pięć rozdziałów. W pierwszym paragrafie zatytułowanym *Introduction* opisano wcześniejsze prace badawcze i podstawy dotyczące SPIONs, ich najważniejsze właściwości oraz możliwości ich potencjalnego zastosowania w biomedycynie. W szczególności przedstawiono różne metody syntezy SPIONs oraz dokładnie opisano stosowane do tej pory metody modyfikacji ich powierzchni, który to etap jest niezbędny dla ich administracji *in vivo*. Następnie szczegółowo sklasyfikowano cechy SPIONs jako układu do bioaplikacji, na które należy zwrócić uwagę przy ich projektowaniu, t.j. stabilność, średni rozkład wielkości, toksyczność oraz właściwości magnetyczne. Przedstawiono właściwości SPIONs jakie muszą spełniać jako nośniki leków w terapiach celowanych oraz szczegółowo opisano fizjologiczne zjawisko zwiększonej przepuszczalności naczyniowej i retencji zachodzące w guzie.

Drugi rozdział, *Experimental methods*, opisuje krótką charakterystykę większości technik eksperymentalnych użytych do badań i został podzielony na sześć podrozdziałów w celu uporządkowania metodyki badań oraz ułatwienia czytania pracy. Materiały użyte w badaniach zostały wymienione w pierwszym podrozdziale. Następnie opisana została synteza polimeru blokowego, użytego w kolejnym etapie do opłaszczenia magnetycznych NPs. W dalszej części przedstawiona została synteza i kompletna charakterystyka fizykochemiczna sfunkcjonalizowanych PEG-PIONs/DOX. Ostatnie dwa podrozdziały zawierają prezentację wyników uzyskach z badań PEG-PIONs/DOX przy użyciu technik *in vitro* na komórkach nowotworowych oraz *in vivo* na mysim modelu zwierzęcym.

W rozdziale trzecim zatytułowanym *Results and discussion* przedstawiono rezultaty wraz z dyskusją przeprowadzonych badań. W rozdziale tym opisuję charakterystykę zsyntetyzowanego polimeru blokowego. Następnie, uzyskane wyniki z pomiarów właściwości fizykochemicznych otrzymanych i odpowiednio sfunkcjonalizowanych magnetycznych NPs zawierających lek przeciwnowotworowy, średni rozkład wielkości, stabilność w warunkach odzwierciedlających fizjologiczne, stopień enkapsulacji substancji aktywnej; właściwości

magnetyczne PEG-PIONs/DOX, wykazanie superparamagnetyzmu oraz krystalicznej struktury. Badania i*n vitro* przedstawiają stopniowy profil uwalniania DOX z NPs w kwaśnym pH odzwierciedlającym środowisko w rejonie tkanki nowotworowej, działanie antyproliferacyjne na komórki nowotworowe oraz internalizację NPs do komórek rakowych. Następnie zostały przedstawione wyniki z badań *in vivo* biodystrybucji leku w poszczególnych organach po podaniu PEG-PIONs/DOX i wolnego roztworu DOX oraz porównanie toksyczności *in vivo* wolnej DOX w porównaniu do układu PEG-PIONs/DOX.

Rozdział czwarty, *Conclusions*, podsumowuje wyniki badań. Stwierdzono utworzenie stabilnych magnetycznych NPs w warunkach fizjologicznych, o odpowiednim do zastosowań biomedycznych profilu hydrodynamicznym, wąskim rozkładzie wielkości, o wysokim stopniu enkapsulacji leku i jego przedłużonym uwalnianiu z układu PEG-PIONs/DOX. Badania właściwości magnetycznych PEG-PIONs/DOX potwierdziły ich superparamagnetyczną naturę oraz strukturę krystalograficzną. Badania *in vitro* wykazały skuteczną internalizację przez komórki nowotworowe oraz efektywne zmniejszenie ich żywotności. Wychwyt DOX z PEG-PIONs/DOX w tkance guza myszy był większy niż równoważne dawki wolnego roztworu DOX, a związana z zastosowaniem leku kardiotoksyczność była znacznie mniejsza w przypadku zastosowania układu PEG-PIONs/DOX.

W rozdziale piątym, *References*, zawarto spis literaturowy.

Aim Of The Work

The aim of this work was to design a stable, biocompatible and injectable nanocarrier with antiproliferative effect on cancer cells and high drug encapsulation efficiency. The general objective was to examine the physical and biological properties of synthesized superparamagnetic iron oxide nanoparticles (SPIONs) with anticancer agent. That allowed to confirm the usefulness of these composites as potential targeted drug delivery systems.

1. Introduction

1.1. Literature review of Superparamagnetic Iron Oxide Nanoparticles

Over the past three decades, scientists and engineers have reached the possibility to measure and construct structures on the scale of atoms and molecules. Nanotechnology holds great opportunities to create materials with enhanced features and attributes by penetrating to the nanoscale − one billionth of a meter. Nanomaterials are already being used or tested in a wide range of products such as cosmetics, clothing, sport equipment, medical and electronic devices, among others. Nowadays, it is possible to synthesize, characterize and specifically modify the functional properties of nanostructures in variety of applications (Figure 1), including the biomedical use, for example as contrast agents for magnetic resonance imaging (MRI) [Schweiger *et al.* 2011; Ling *et al.* 2011; Rosen *et al.* 2012;] or for drug delivery in targeted therapy [Butoescu *et al.* 2009; Arnold *et al.* 2007; Y. Liu *et al.* 2010]. Over 50 years ago, Freeman *et al.* [(Freeman, Arrott, and Watson 1960)] presented the pioneering concept of using an external magnetic field coupled with magnetic carriers. Since then, much research has been done in this field, leading to the design of various magnetic particles and vectors, to deliver drugs to required area *in vivo* [A. S. Lübbe *et al.* 1996; a S. Lübbe, Alexiou, and Bergemann 2001]. Recently, the special interest is focused on superparamagnetic iron oxide nanoparticles (SPIONs). They show unique physical and chemical properties such as superparamagnetism, and can be delivered to the specific site through external magnets [Kodama 1999]. A particle of the magnetic material below a critical diameter (for maghemite γFe_2O_3 or magnetite Fe_3O_4 of about 5 - 20 nm) (A. K. Gupta and Gupta 2005], contains only one single magnetic domain, thus it is at a state of uniform magnetization at any field without interaction with neighbour domains in a well dispersed material. An object consisting of many of these nanoscale particles displays magnetic properties under an applied external magnetic field, however magnetization would not remain after its removal [Harris *et al.* 2003]. The reason for this phenomenon, called superparamagnetism, is that these domains will return to disordered status by having enough space to refuse the interaction between each other while there is no extra magnetic field applied. This feature is especially necessary in biomedical applications, because it enables to maintain colloidal stability of SPIONs and protects against potential clogging of the vessels and capillaries. The current research on SPIONs is opening up broad horizons for their use in the biomedical sciences. They have been used for both diagnostic as well as therapeutic purposes. The utility of SPIONs as MRI contrast agents has been studied for more than two decades,

allowing diagnosis of progressive diseases in their early stages [Weinstein *et al.*2010]. *Via* intravenous injection of the contrast agent, SPIONs are injected into a blood vessel and taken up by the solid cancer cell during circulation. This leads to clear images of soft tissue with magnetic agents. MRI may also play important role in thero-diagnostic purpose. In a recent preclinical study, specific tumoral accumulation of intravenously injected magnetic nanoparticles (NPs) labeled with a near-infrared dye and covalently linked to small interfering RNA (siRNA) was demonstrated by *in vivo* MRI and optical imaging; specific silencing of an apoptosis inhibitor protein was achieved, leading to increased tumor apoptosis and necrosis [Medarova *et al.*2007]. From a therapeutic point of view, targeting of cancer is the most pursued area, with emphasis on treatment using hyperthermia [Ling *et al.*2011] or delivery of chemotherapeutics to required site [Cao *et al.* 2009]. Tumor cells have shown a greater sensitivity to heat compared to healthy cells. This has led to the use of hyperthermic therapies in the clinic, often in combination with other treatments [Neuberger *et al.*2005]. Hyperthermia is a therapeutic procedure that promotes the increase of temperature in body tissues in order to change the functionality of the cellular structures. Temperature increase between 41°C and 42°C can induce tumor cell death, as the tumor cells are less resistant to sudden increases in temperature than the normal surrounding . The rise in temperature changes the functioning of many enzymatic and structural proteins in cells, in turn altering cell growth and differentiation, which can induce apoptosis [Silva et al. 2011; Laurent and Mahmoudi 2011;]. Advances in the area of nanotechnology have contributed to the development of superparamagnetic materials, which are well recognized as promising hyperthermia method for cancer treatment [Laurent and Mahmoudi 2011], however it is still limited by the fact that the anticipated heating distribution is difficult to control [Salloum, Ma, and Zhu 2008]. The main disadvantage of the majority of available chemotherapies is that they are comparatively non-specific. The intravenous administration of the drugs gives rise to an overall distribution in the body, producing harmful side-effects due to the non-selectivity between tumor and healthy cells. Therefore, one of the biggest challenges is to deliver chemotherapeutic directly to the desired location, at the lowest dose possible and thus to increase the effectiveness of treatment and decrease strong adverse effects of chemotherapy. Using SPIONs as the new nanocarriers may provide a physical and chemical targeting method for drug delivery [Debrassi *et al.*2011; Maver *et al.*2009; Zou *et al.*2010;]. Increasing importance of SPIONs applications have also been found in the areas of gene delivery [Prijic *et al.*2012; Cheong *et al.*2009], cell death with the help of local hyperthermia, and delivery of peptides and antibodies to their site of action [Wahajuddin 2012].
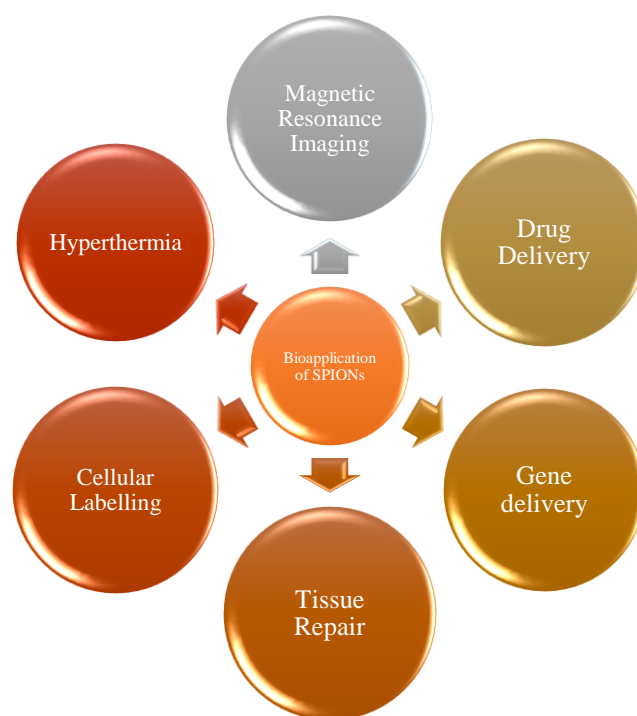
Figure 1. Bioapplications of SPIONs.

1.1.1. Superparamagnetic Iron Oxide Nanoparticles synthesis

It has been a great scientific and technological challenge to produce magnetic NPs that fulfil the requirements for biomedical applications. Iron oxides, both γFe_2O_3 or Fe_3O_4, occur naturally as nano-sized crystals in the earth's crust generated by various environmental sources such as volcanoes and fires. SPIONs, either γFe_2O_3 or Fe_3O_4, can be generated as air pollution or industry, but for their bio-applications they are appropriately synthesized [Karlsson, Holgersson, and Möller 2008]. Existing primarily used methods are mainly physical and chemical routes of synthesis. The main aim in SPIONs fabrication is to control the reaction conditions in a way to enable synthesis of NPs with a narrow size distribution, high level of monodispersity and homogenous composition [Bulte *et al.*2001]. In order to maximally facilitate use of SPIONs in therapeutic applications, MRI or drug delivery, their high magnetization values are required. Hydrodynamic particle size is an important parameter that influences magnetization values as well as dissolution and stability [A. K. Gupta and Gupta 2005]. Therefore, the reaction conditions during their synthesis should have the opportunity to be modulated, to generate particle size with large surface area, which in turn allows SPIONs to exhibit high magnetic susceptibility [Goya *et al.*2003]. A variety of methods (Figure 2) can be

employed in SPIONs synthesis, however chemical methods are much simpler and more efficient.

Chemical
- Coprecipitation
- Microemulsion
- Thermal decomposition
- Sonochemical
- Hydrothermal

Physical
- Gas phase deposition
- Electron beam litography
- Pulsed laser ablation

Biological
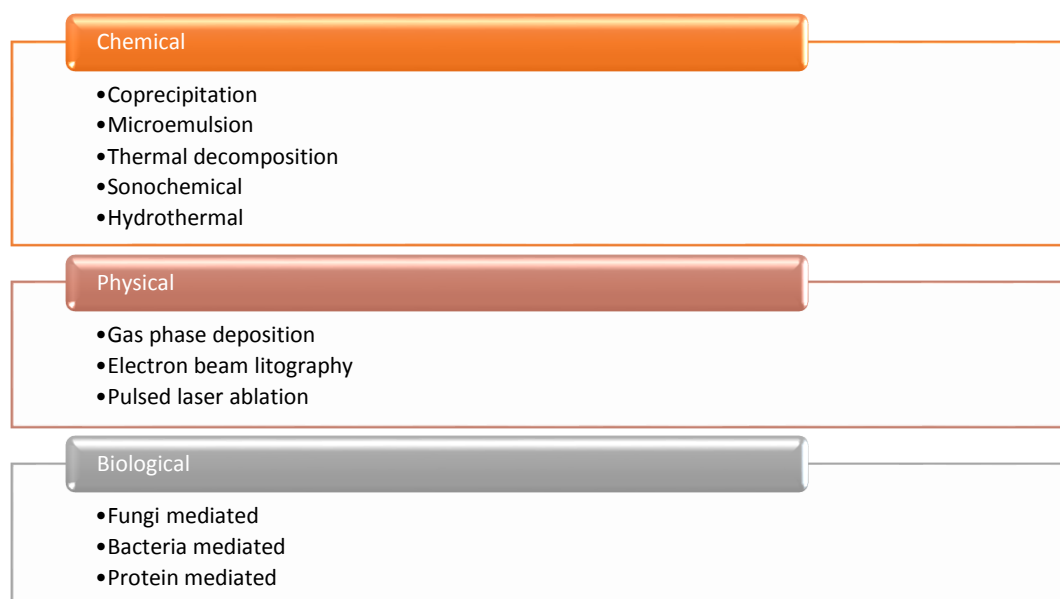- Fungi mediated
- Bacteria mediated
- Protein mediated

Figure 2. Three different routes of SPIONs synthesis.

Most of chemical methods allow to modulate conditions of the synthesis reaction in order to achieve SPIONs with desired physicochemical properties. The most remarkable advantage of chemical methods is that they have appreciable control of particle size, composition and particle shape [A. K. Gupta and Gupta 2005]. Physical methods are elaborated procedures that often suffer from the inability to control the size of particles in the nanometer range [C. S. Lee, Lee, & Westervelt, 2001;]. Once the core of SPIONs has been synthesized, the appropriate surface modification with biocompatible molecules [Bulte *et al.*2001; A. K. Gupta and Curtis 2004; Catherine C. Berry *et al.*2003;] should follow, which can either be performed *in situ* or *via* post-synthesis methods [Laurent *et al.*2008].

One of the most popular procedures to fabricate SPIONs, that has been widely used during last years, is co-precipitation technique [A. K. Gupta and Gupta 2005]. Conventionally, in this method magnetite is prepared by the addition of base to an aqueous solution of Fe^{2+} and Fe^{3+} ions in a 1:2 stoichiometry, which produces a black precipitate of spherical magnetite NPs of uniform sizes. The overall reaction may be written as follows:

$$Fe^{2+} + 2Fe^{3+} + 8OH^- \longrightarrow Fe_3O_4 + 4H_2O$$

According to the thermodynamics of this reaction, a complete precipitation of magnetite can be expected between pH 9 and 14, while maintaining a molar ratio of Fe^{2+}/Fe^{3+} is 1:2 [A. K. Gupta and Gupta 2005]. In order to prevent them from possible oxidation in air as well as from agglomeration, Fe_3O_4 produced by reaction presented above are usually coated with organic or inorganic molecules *in situ*. In this technique, the type of salts used (e.g. chlorides, sulphates, nitrates, etc.), Fe^{2+} and Fe^{3+} ratio, pH and ionic strength of the media determines size, shape and composition of generated NPs. SPIONs are crystalline structures that are governed by the principles of crystal formation and growth. Precipitation from a solution is a fundamental method of crystallization, which involves two processes, nucleation and growth, which are the principle pathways for the formation of solids. In general, for precipitation to occur, there must be a saturated medium, in which addition of any excess solute will cause precipitation and the formation of nanocrystals (Burda *et al.*2005]. Formation of tiny crystalline nuclei occurs when the solution is supersaturated [Jun, Lee, and Cheon 2007], leading to a short single burst of nucleation, followed by the decrease of concentration and stopping of nucleation. Then, the nuclei can grow uniformly by diffusion from the solution to their surfaces, until an equilibrium concentration is achieved [Lodhia *et al.*2010]. The main advantages of co-precipitation method are it is mild and simple synthesis procedure, typically carried out in aqueous media under ambient conditions and the amount of produced NPs per one batch is large. However, problems arise from the particle size distribution, which are strongly dependent on a large number of procedural parameters, including pH, the concentration and ratio of reactants, ionic strength and temperature of the reaction mixture. In an attempt to produce ideally controllable and reproducible particles, many research groups have experimented with a variety of these parameters to establish the best conditions for co-precipitation method [Valenzuela *et al.*2009; Iida *et al.*2007]. Taking into consideration all of the obtained assumptions, this route directly generates hydrophilic monodisperse SPIONs with narrow size distribution. Controlling the size of the particles in co-precipitation method is the key step to producing SPIONs with narrow size distribution.

Due to that challenge, alternative synthesis techniques such as the microemulsion (water-in-oil) method were developed. In this technique, the aqueous phase is dispersed as microdroplets in a continuous hydrocarbon phase (oil) surrounded by a monolayer of surfactant molecules [K. Gupta and Wells 2004]. Iron precursors in the form of soluble metal salt can precipitate as iron oxide in the water phase specifically located in the center of the micelles. Iron oxides do not precipitate in organic phase as the iron precursors are unreactive in this phase. The main advantage of utilizing of microemulsion system for NPs formation is that their size can be

controlled by modulating the size of the aqueous micellar core [D. Zhang *et al.*2008]. However the primary drawback is that the large-scale success of the microemulsion technique has been limited by low production yields compared to co-precipitation and thermal decomposition method [Z. L. Liu *et al.*2004; Y. Lee *et al.*2005]. Microemulsion synthesis may also prove problematic due to the complex purification steps required for *in vivo* application to remove surfactants that have adhered to the particles [Lu, Salabas, and Schüth 2007]. The surfactants are required during fabrication process for separating and controlling the growing SPIONs, however some thought must be devoted considering the toxicity and biocompatibility of these molecules for pharmaceutical applications.

Highly monodispersed NPs can be also synthesized using the thermal decomposition of organometallic precursors. This process includes two techniques: liquid phase and gas phase. The first one involves high-temperature decomposition of a metal-surfactant complex such as iron-oleate [J. Park *et al.*2004], iron pentacarbonyl [Fe(CO)5] or ferric acetylacetonate [Fe(acac)3] in the presence of an organic solvent and is similar to the microemulsion methods, with surfactants to aid in the dispersion and prevent the aggregation of the oleophobic iron oxide particles [Amara *et al.*2009]. The thermal decomposition synthesis method produces monodisperse, highly crystalline and non-aggregated SPIONs [Yoffe *et al.*2013], however more elaborated equipment and chemicals have to be used in the process and production yield is quite low comparing to simple co-precipitation method. It also shares the difficulty of the microemulsion technique of fabricating hydrophobic SPIONs which must be further processed for applications requiring the NPs to be dispersed in water phase.

A recent development in the synthesis of SPIONs is the use of sonochemical route [Vijayakumar *et al.*2000; Kumar *et al.*2001]. This method involves the application of powerful ultrasonic radiation that creates acoustic cavitations which provides localized heat with a temperature of about 5000 ºC. At high temperature, the rapid formation, growth of nuclei and the implosive collapse of bubbles takes place. This method is an inexpensive and non-toxic way to synthetize SPIONS and it enables preparation of monodisperse NPs of a variety of shapes. However, it is unlikely that it will be industrially relevant as it lacks large scale synthesis and requires both specialized equipment and high-energy input in the form of ultrasonic irradiation [Yoffe *et al.*2013].

The hydrothermal method is typically performed at higher pressures and reaction temperatures, where iron precursors in aqueous medium can be heated. It produces naturally hydrophilic SPIONs due to the aqueous solvent and is a universal process that can be performed with a variety of starting reactants and their proportions and reaction conditions (temperatures,

pressure) and also can be easily scaled up. [Wu *et al.*2009; Yan *et al.*2009]. It allows to obtain a broad range of particle sizes, magnetic properties and magnetization values, by which to control the properties of the synthesized SPIONs, while NPs under simple, environmentally friendly conditions.

The previous research on chemical fabrication of magnetic NPs accumulated knowledge, experience and understanding on SPIONs synthesis procedures. Taking into consideration all of the studies and different aspects of SPIONs synthesis mentioned above, the fabrication of these NPs with an expected size distribution and stability is no longer the biggest challenge for researchers. Each of the synthesis methods can be controllable in a way to obtain SPIONs with required parameters and properties. Nowadays, the crucial factor for *in vivo* bioapplications is to modify their surface in a way to achieve the aim of stealth of SPIONs in the bloodstream and target them to the required area in the body.

1.1.2. Superparamagnetic Iron Oxide Nanoparticles surface modification

A major limitation of nanoparticle-based biodevices for *in vivo* applications (including drug delivery and imaging) is their nonspecific biodistribution. In the absence of any surface coating, SPIONs have hydrophobic surfaces with a large surface area to volume ratio. When NPs are administered intravenously, they tend to agglomerate through van der Waals attractions [Talelli *et al.*2009], adsorb plasma proteins, and consequently, form large clusters. These aggregates are rapidly cleared from the bloodstream by macrophages, namely in the lungs, liver, and spleen (organs of the reticuloendothelial system (RES)) [Ujiie *et al.*2011], before reaching their target. Several studies have already revealed that the *in vivo* behavior of NPs depends greatly on their morphology and surface properties [Hseih, Huang, and Lue 2002]. Therefore, certain modifications are required for biomedical applications of SPIONs to stabilize them under physiological conditions [Sun *et al.*2010].

Surface modifications of SPIONs can be achieved using different approaches and could be modified e.g. through the creation of few atomic layers of inorganic metallic (e.g. gold) or oxide surfaces (e.g. silica) suitable for further functionalization by the attachment of various bioactive molecules or using functional groups of polymers [Chomoucka *et al.*2010]. With proper surface coating, SPIONs can be dispersed into suitable solvents, forming homogenous suspensions, called ferrofluids. Such a suspension can interact with an external magnetic field and be positioned to a required site, facilitating MRI for medical diagnosis and magnetic field-assisted cancer therapy. A numerous efforts have been put to conjugate targeting and therapeutic agents

onto SPIONs surfaces. They include covalent linkage strategies (direct nanoparticle conjugation, click chemistry, covalent linker chemistry) and physical interactions (electrostatic, hydrophilic/hydrophobic, affinity interactions). The chemical properties and functional groups present on the SPIONs coating determine the choice of conjugate method to be used. The main aim is to bind the targeting and therapeutic agents without compromising its functionality once attached. Functionality in such assemblies is dictated by the nature of the ligand and the manner in which it is attached. For example, if an antibody is bonded to the NP such that its recognition site is shielded, it may lose its ability to bind a target. A diverse range of materials have been used for coating including both inorganic and polymeric materials. Metallic core shell types of iron oxide NPs have been investigated by several researchers. These NPs have inner iron oxide core with an outer metallic shell of inorganic materials e.g. gold [M. Chen *et al.*2003; Carpenter 2001], silica [Tartaj and Gonzμlez-carreæo 2001] or gadolinium [Morawski *et al.*2004]. These coatings give not only the stability to the NPs in solution, but also provides a good surface for subsequent functionalization with chemical or biological agents for various biomedical applications (Lin *et al.*2001). Polymeric materials can be divided into natural and synthetic. Natural polymers includes coatings like dextran [Dutz *et al.*2007], chitosan [Unsoy *et al.*2012] or gelatin [Gaihre *et al.*2009], among others. Polymers based on poly(ethyleneglycol) (PEG) [Mojica Pisciotti *et al.*2014], poly(lactic-co-glycolic acid) (PLGA) [Wassel *et al.*2007; Zhao, Saatchi, and Häfeli 2009] or poly(vinyl alcohol) (PVA) [Petri-Fink *et al.*2005] are typical synthetic nanocoatings and offer a high potential in several areas of applications. PEG and PEG-containing copolymers have been widely investigated for bio-applications [Nagasaki 2008; Yoshitomi, Miyamoto, and Nagasaki 2009]. PEG is a hydrophilic, uncharged and non-immunogenic polymer [Allard-Vannier *et al.*2012] commonly used in commercial products. It can be grafted onto NPs surface to form a hydrophilic outer layer that reduces protein adsorption as well as minimizes potential aggregation between particles. A very high requirement of coating density is desirable for the effective suppression of nonspecific interactions between NPs with biological components. Once the PEG density increases, the space between each polymer and its degree of freedom is reduced. The formation of the polymer molecule is then switched from a "mushroom" to a "brush" configuration (Figure 3). In the first one, the surface of the particle is still accessible, in the second one, the density and length of the polymer force the PEG-chains to be closely and regularly aligned, which reduces access to the NPs surface and in consequence reduces opsonization. NPs in the "mushroom" configuration are exposed to increased uptake by RES and those with "brush" configuration remain in the blood for prolonged periods of time [Dufort, Sancey, and Coll 2012; Lai *et al.*2010].
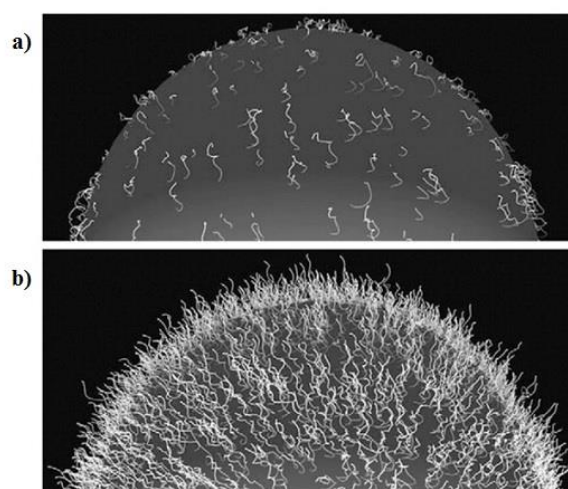
Figure 3. Different polymer conformations on a polymeric nanoparticle, (a) represents the 'mushroom' configuration, (b) represents the 'brush' configuration [Pirollo and Chang 2008].

Ujiie *et al.*[Ujiie *et al.*2011], highly improved PEG-chain density (PEG derivative with "brush" configuration) and obtained its high surface immobilization density, as well as its binding stability to the NPs surface, so that the PEGylated NPs remained intact in harsh biological environments over a long period. Most of NPs injected *in vivo* have some sort of coating that serves to avoid premature clearance, render the NPs water-soluble, protect particle surface from oxidation and improves biocompatibility. However, coatings can also provide chemical entrance points for conjugation of imaging, targeting and other functional modalities. Various biological molecules such as antibodies, proteins, targeting ligands, etc., may be bound to the polymer surfaces onto the NPs by chemically coupling *via* amide or ester bonds to make the particles target specific. The possibilities of targeting protein coatings are numerous. Targeting ligand such as transferrin is widely applied in the active targeting of anticancer agents, proteins and genes to primary proliferating cells *via* transferrin receptors [Catherine C Berry *et al.*2004]. Folic acid preferentially targets cancer cells, is poorly immunogenic and folate receptor facilitates internalization of NPs [Y. Zhang, Kohler, and Zhang 2002]. There is another important role of surfactants on SPIONs. When SPIONs are injected as MRI contrast agent, they must locate the targeting area accurately and rapidly. Appropriate surfactant or functional attachment of surfactant could achieve such objective. Some experiments *in vitro* already approved folate-mediated NPs composed of PEG/poly ε-caprolactone have potential of tumor cell-selective targeting [Gee *et al.*2003]. Optimization of

coating procedure for SPIONs biomedical use raises demands for nano-engineers. It allows dispersal into solvents to form ferrofluids, which can interact with an external magnetic field. The nature of the coating, charge state, and functionalization determine particle biocompatibility, stability, biodistribution, opsonization, metabolism, and clearance *in vivo*. Important advantages of prolonged circulation of drug carriers and drugs themselves in the bloodstream include the possibility of maintaining a required concentration of an active drug or drug carrier in the blood for a long time after a single administration; the ability to utilize the EPR effect for the accumulation of drugs in the areas with leaky vasculature and the possibility of enhancing ligand-mediated targeting of drug carriers into the areas with a limited blood supply, where an extended time is required to allow for a sufficient quantity of a drug in the target zone.

1.1.3. Characteristics of Superparamagnetic Iron Oxide Nanoparticles for *in vivo* applications

Systemic application of SPIONs, proves more difficult due to their rapid clearance from the blood by the RES and therefore, reducing the concentration of SPIONs reaching the target organ. To improve the systemic application of SPIONs, coating and functionalization with a targeting moiety is advantageous. SPIONs designed for biomedical applications are required to form a non-toxic aqueous dispersions with a narrow size distribution [Patel *et al.*2008], good colloidal stability under physiological conditions and prolonged circulation in the bloodstream. SPIONs for *in vivo* administration should be biodegradable and biocompatible. In order to improve the blood circulation behavior as well as the *in vivo* distribution of NPs, their sizes have to be controlled within the range 10–50 nm. Furthermore, NPs surface should be engineered to maximally reduce the nonspecific interactions with plasma proteins, since the RES-mediated rapid clearance of NPs is triggered by the adsorption of these proteins on their surface.

1.1.3.1. Colloidal stability

The dispersion stability of SPIONs under physiological conditions is crucial for their systemic administration. SPIONs are generally well tolerated *in vivo*, however appropriate surface modification or core-ligand composition play major role in physiological responses [Viali *et al.*2013]. In general, the stability of SPIONs is controlled by three types of interactions:

hydrophobic–hydrophilic, magnetic and van der Waals. NPs aggregate in suspension due to van der Waals forces in order to minimize the total surface or interfacial energy. Consequently, such aggregation impedes the efficacy of SPIONs in drug delivery (less drug loading) due to their low surface area and larger sizes. For that reason, the SPIONs surface is modified or coated with biocompatible functional molecules or polymers, which improves their colloidal stability in physiological media, reduces toxicity and significantly increases the blood circulation lifetime by minimizing the protein absorption onto NP surface. The ideal molecules used for stabilization of SPIONs should be biocompatible and biodegradable and surface modification can be carried out during synthesis or in a post-synthesis process.

1.1.3.2. Size and size distribution

The size distribution of SPIONs is the first parameter describing the quality of SPIONs related to their biological applications. The hydrodynamic diameter of NPs in hydrophilic ferrofluid after surface coating plays the vital role at *in vivo* application. Biomedical applications of SPIONs, including drug delivery, MRI, hyperthermia, and magnetic cell separation, depend on the magnetic properties of these particles, which in turn are largely dependent upon size. Only small enough NPs would display superparamagnetism and be stable in suspension with suitable surfactant coating. The magnetic properties of SPIONs are size dependent. The saturation magnetization and their sizes are linearly correlated as the surface curvature changes with size [Varanda *et al.*2002]. The smaller the particles, the longer their circulation time in blood vessel. Gupta *et al.*[A. K. Gupta and Gupta 2005] reported that the sizes between 10 and 100 nm are most effective for drug delivery purposes because they can evade the RES. They should remain in the circulation after injection and be capable of passing through the capillary systems of organs and tissues avoiding vessel embolism. In addition, it has been reported that particles which exceed 200 nm, tend to eliminate immediately by one of the organs from monoclear phagocytic system regardless of being polymer coated or not. Similarly, the small hydrodynamic size is important for achieving EPR effect and can make it tumor-specific accumulation feasible. Another main advantage of using particles of sizes smaller than 100 nm is their higher effective surface areas (easier attachment of ligands), lower sedimentation rates (i.e. high stability in suspension) and improved tissular diffusion. However, SPIONs with a particle size smaller than 2 nm may not be suitable for medical use[Wahajuddin 2012]. This is due to the increased potential of particles in this size range to diffuse through cell

membranes, damaging intracellular organelles and thus exhibiting potentially toxic effects. Therefore, control of particle size during preparation of SPIONs is an important concern.

1.1.3.3. Toxicity

The nanoscale properties of NPs facilitate their novel bio-applications, however at the same time they can induce cytotoxicity by impairing major components of the cell (mitochondria, DNA and nucleus) [Brunner *et al.*2006; Nel *et al.*2006]. It can lead to significant toxic effects such as inflammation, generation of reactive oxygen species or chromosome condensation [Veranth *et al.*2007; Stroh *et al.*2004]. Since applications of SPIONs involve *in vivo* use, it is a vital factor to study their toxicity in appropriate model. Acute side effects should be avoided by testing *in vitro* cytotoxicity of NPs before injection. Uncoated SPIONs have very low solubility that can lead to precipitation after intravenous administration. Due to that fact their surface is appropriately modified, nevertheless the stability of these coatings and the consequences of their breakdown *in vitro* or *in vivo* have not been yet completely evaluated. Many of the clinically approved MRI contrast agents such as Ferridex, Resovist or Supravist, nowadays commercially available, are coated with dextran and its derivatives [Wang, Hussain, and Krestin 2001]. Numerous studies have reported that these NPs are biocompatible and lack cytotoxicity [Singh *et al.*2010]. Although, the results of recent studies indicates that these coatings are not strongly bound to the NPs surface and therefore there is a potential risk of detachment leading to aggregation and precipitation [McCarthy and Weissleder 2008], there is still insufficient information on the effect of these coatings on cytotoxicity associated with DNA damage and oxidative stress. The cytotoxicity of SPIONs coated with different polymers, with different shapes and morphologies has been comprehensively examined by Mahmoudi research group [M Mahmoudi *et al.*2009; Morteza Mahmoudi, Shokrgozar, *et al.*2009]. According to their results, SPIONs showed no or little toxicity. *In vivo* tests [Weissleder *et al.*1989] on animals showed that even with a large dosage of 3000 µmol Fe of the iron based NPs per kg body weight, the histology and serologic blood tests have indicated that no side effects occurred after 7 days treatment. It has to be considered that in view of the *in vivo* applications, SPIONs suspension requires hydrophilic solvents such as physiological saline and be controlled at near neutral pH value about 7.4. Another *in vivo* investigations performed in humans found that a dextran-coated SPIONs - Ferumoxtran-10 - only induced mild and short in duration side effects such as urticaria, diarrhea and nausea [Anzai *et al.*2003]. It was concluded that they can be degraded and cleared from the bloodstream by the endogenous iron metabolic pathways. Iron

released from SPIONs is metabolized in the liver and then used in the formation of red blood cells or removed through renal clearance [Anzai *et al.*2003]. Use of SPIONs is increasing not only because their superparamagnetic properties, but also because their use is associated with low toxicity in human body [Karlsson *et al.*2009; Jeng and Swanson 2006].

Understanding the potential risks associated with exposure to SPIONs and the influence of their coatings is crucial for their *in vivo* applications and every novel product for *in vivo* applications should be examined carefully. It is crucial to design functionalized SPIONs that can not only be sufficiently and effectively internalized, but also have appropriate saturation magnetization without compromising on cellular toxicity. Improved understanding of biological impacts will lead to fabrication of more biodegradable and biocompatible nanostructures that are well fit for their function [Singh *et al.*2010].

1.1.3.4. Surface charge and protein adsorption

When the drug-loaded NPs are injected systemically into the bloodstream, the size, morphology and surface charge are the three important parameters for their behavior. In general, particles with the same electronic charged surface are more stable in dispersion due to the homo-charged surface [Neuberger *et al.*2005]. The zeta potential can be qualitatively evaluated in NPs suspension in the presence of an electrolyte at a certain pH, as an electrical potential in the interfacial double layer on the surface of NPs. Surface charge of SPIONs can affect their cellular interaction, especially during endocytosis and phagocytosis [Coey and Wiesendanger 1993]. It was previously reported that polystyrene microparticles with a primary amine at the surface determined higher phagocytosis as compared to microparticles having sulfate, hydroxyl, phosphorous or carboxyl groups. Thus, it was found that for positively charged NPs *in vivo* phagocytosis the non-specific internalization process occurs faster as compared to neutral or negatively charged formulations. NPs carrying a positively charged surface are also expected to have a high nonspecific internalization rate and short blood circulation half-life. In conclusion, it was established that NPs are better to be neutral or slightly negatively charged on surface to have a reduced plasma protein adsorption and low rate of nonspecific cellular uptake [Link *et al.*2015].

When NPs are administered into bloodstream, they are rapidly bound by plasma components including plasma proteins (opsonins). They can be easily adsorbed on the surface of NPs depending on their sizes, surface charge and morphology. Prolonging the circulation time in blood vessels is examining the capability of protein adsorption of the coating. Resistance

to their non-specific adsorption could prevent magnetic NPs from attachment of opsonin proteins and recognition by phagocytic cells in a certain time [Owens and Peppas 2006]. However, for the active targeting purpose, specific protein adsorption in the particle surface is allowed for functionalization of the NPs [Torchilin 2000]. Moghimi *et al.*[Moghimi, Hunter, and Murray 2001] performed an extensive research of the opsonisation process based on the NPs' surface charge, size and hydrophilicity/hydrophobicity. The results of this study showed that the smaller the size and the higher the hydrophilicity of the NPs, the less efficient the opsonisation process is. In this context, PEG and folic acid coating have been found to be efficient for inhibiting the protein adsorption *in vivo*[Y. Zhang, Kohler, and Zhang 2002].

With the requirements mentioned above, protein adsorption capability of the particles need to be under control that is not only resisting to the non-specific protein adsorption, but also adsorbing the specific functional proteins for targeting.

1.1.4. Magnetic properties of iron oxide NPs

Magnetic properties of iron oxide NPs are determined by a variety of factors including their composition, microstructure, size and shape, therefore their optimization is very important factor. The size and crystal structure of magnetic NPs determine their unique properties which make them useful as e.g. MR contrast agents or drug delivery systems. Materials like iron possess valence orbitals with unpaired electrons, thus exhibit paramagnetic properties. In general, magnetic materials are divided by several groups, i.e. diamagnetic, paramagnetic, ferromagnetic, ferrimagnetic and antiferromagnetic. The characteristic feature of diamagnetic materials (e.g. water, DNA, gold) is that their magnetic moments tend to align opposite to the external magnetic field (B_0) and in consequence are repelled by the applied magnetic field. The opposite situation occurs in case of paramagnetic materials (e.g. gadolinium), which are attracted by the applied B_0, and their magnetic moments tend to align parallel to B_0 (Figure 4).
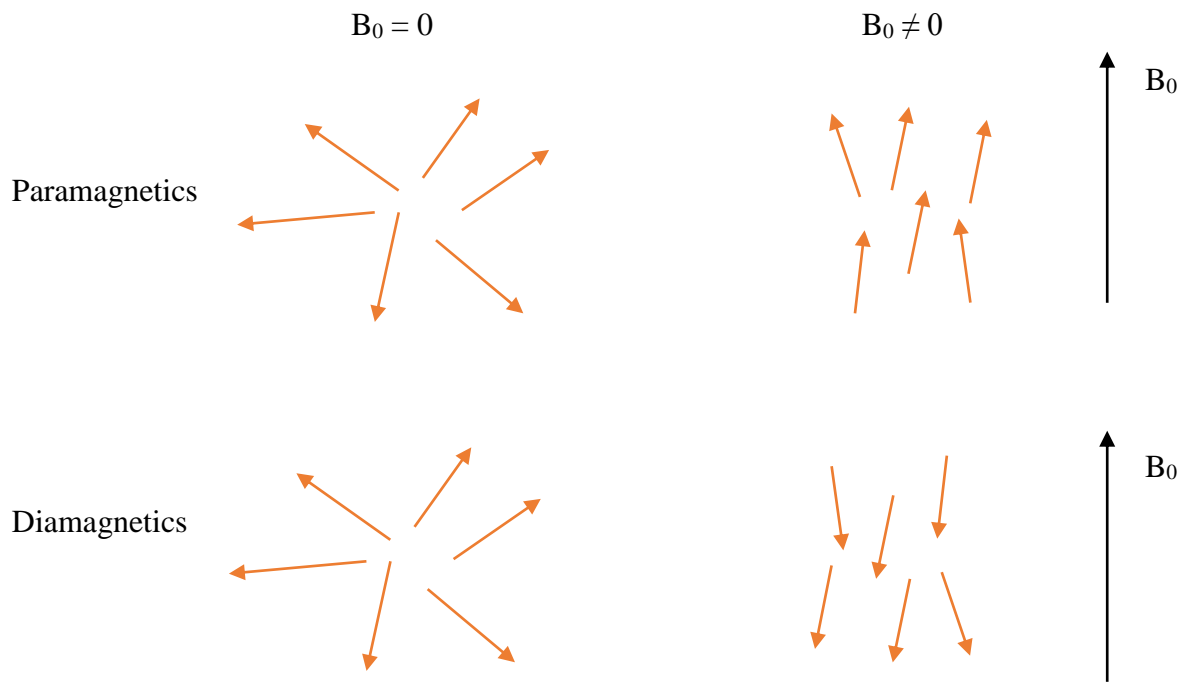
Figure 4. Alignment of individual magnetic magnetic moments in para- and diamagnetic materials.

Materials, which characteristic feature is the creation of magnetic domains by absorbing and storing the (magnetic) energy, remain magnetic even after removal of B_0 and are defined as ferromagnetic or ferrimagnetic (Figure 5).
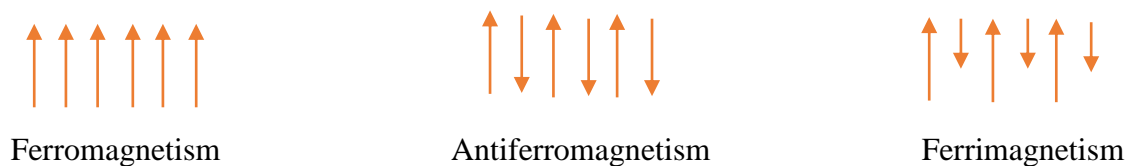

Figure 5. Alignment of individual magnetic moments within different types of materials.

Ferromagnetics (e.g. iron, cobalt) contain only magnetic moments with the same value, going in the same direction. On the other side, ferrimagnetics (magnetite, maghemite) include two types of atoms with magnetic moments of different strengths that are arranged in an antiparallel arrangement [Teja and Koh 2009]. If the antiparallel magnetic moments are of the same magnitude, then the crystal is antiferromagnetic (hematite, chromium) and possesses no net magnetic moment. Another important type of magnetic behavior is superparamagnetism. It occurs in materials with specific size, shape and chemical composition. These parameters allow to obtain a single domain ferri- or ferromagnetic system with paramagnetic behavior possessing

28

a large magnetic moment. To evaluate their magnetic properties, the magnetization (M) vs. the external magnetic field alteration (H) characteristic can be performed (Figure 6). One of the parameters that can be obtained from these measurement is so called coercivity, i.e. the energy which is required to demagnetize material to its initial stage. It is commonly known that coercivity of magnetic materials alters with their size. The variation of coercivity with NPs size is presented in Figure 6a. A single magnetic domain material has zero coercivity and is said to be superparamagnetic, but just until a particular size, then the coercivity increases as the particle size increases, and becomes a single- or multidomain ferri- or ferromagnetic system. The hysteresis loop differs for extremely small SPIONs (or single paramagnetic ions), SPIONs and ferromagnetic NPs (Figure 6b, 6c, 6d). Due to very a small magnetic moment, extremely small SPIONs exhibit almost a linear relationship between magnetization and magnetic field, and the saturation magnetization appears at very high magnetic field (Figure 6b). SPIONs do not exhibit coercivity due to fluctuations of magnetic moments (Figure 6c) and ferromagnetic NPs exhibit coercivity (Figure 6d).
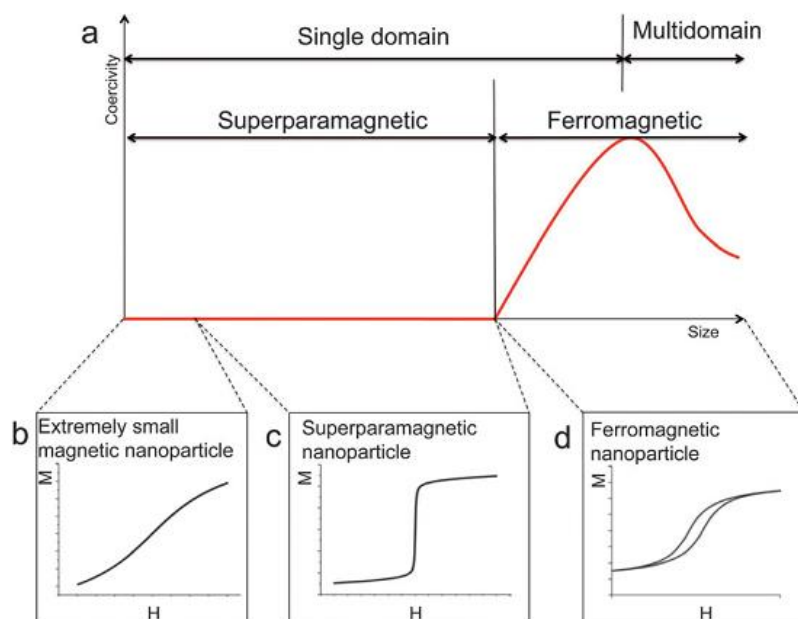

Figure 6. The magnetization (M) vs. the external magnetic field alteration (H) in different types of NPs [N. Lee and Hyeon 2012].

One of the methods which allow to examine the properties of the NPs, especially paramagnetic materials is Electron Paramagnetic Resonance (EPR). EPR is a spectroscopic technique that allows the direct and non-invasive detection of paramagnetic species consisting

of one or more unpaired electrons in complex and non-transparent samples [Kempe, Metz, and Mäder 2010]. This method enables to examine short living, stable free radicals or transition metal ions, such as Mn^{2+}, Fe^{3+} or Cu^{2+}. Electron paramagnetic resonance (EPR) of the ferromagnetic particles, also known as FMR, is performed like any other EPR experiment, except that the samples contain approximately spherical aggregates of ferro or ferrimagnetic monodomains of the order of a few nanometers [Gamarra et al. 2009]. EPR is a technique based on the absorption of electromagnetic radiation, which is usually in the microwave frequency region, by a paramagnetic sample placed in an external magnetic field. The absorption takes place only for definite frequencies and magnetic field combinations, depending on the sample characteristics. EPR is based on interaction of the external magnetic field with magnetic moments of unpaired electrons in a sample, which leads to the splitting of the electron energy levels [Dobosz *et al.*2014]. This effect is called the Zeeman effect (Figure 7).
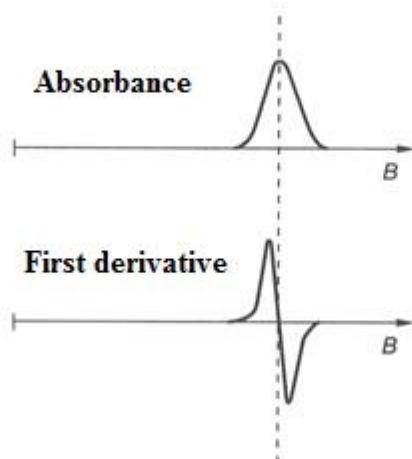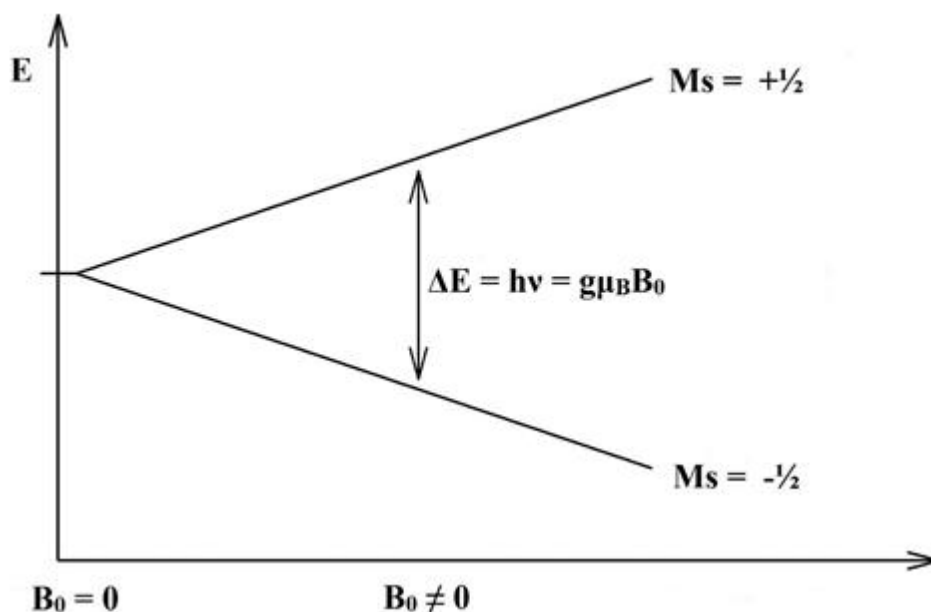
Figure 7. Energy levels for an electron spin ($M_S = \pm 1/2$) in an applied magnetic field B_0.

Every electron has a magnetic moment and a single unpaired electron has only two allowed energy states. In the presence of an external magnetic field B_0, the electron's magnetic moment aligns itself either parallel $M_s = -\frac{1}{2}$ (then it has a state of lower energy) or antiparallel $M_s = +\frac{1}{2}$ (higher energy state) to the B_0 field. An EPR signal is observed when the quantum of the electromagnetic wave energy $h\nu$ is equal to the energy difference between the neighboring energy levels [Kabacińska *et al.*2012], which is described by the resonance condition:

$$\Delta E = h\nu = g\mu_B B_0$$

where g is the spectroscopic splitting factor and gives information about the kind of paramagnetic center, μ_B is the Bohr magneton and B_0 is the induction of external magnetic field [Kempe, Metz, and Mäder 2010]. An unpaired electron can move between the two energy levels by either absorbing or emitting a photon of energy hv, such that the resonance condition, $hv = \Delta E$, is obeyed. EPR spectrometers measure the absorption of electromagnetic radiation. In a conventional X-band EPR experiments, the microwave frequency is chosen in the X-band, i.e. around 9.5 GHz. This frequency is kept fixed while the absorption of microwaves is monitored as a function of the varying external magnetic field. When the resonance condition is fulfilled, absorption of microwaves will be detected [Van Doorslaer et al. 2009] and a simple absorption spectra will appear (Figure 7). However, in EPR spectrometers, a phase-sensitive detector is used, which converts the normal absorption signal to its first derivative. This results in the absorption signal being presented as its first derivative in the spectrum (Figure 7). Therefore, the absorption maximum corresponds to the point where the spectrum passes through zero. This is the point that is used to determine the center of the signal. In order to fully evaluate the magnetic properties of examined SPIONs by EPR, the typical spectroscopic parameters: resonance magnetic field (H_r), g-spectroscopic splitting factor value, peak-to-peak line width (ΔH_{pp}) are determined for collected spectra. These parameters are characteristics for particular types of magnetic nanomaterials and can provide number of important information regarding examined sample, like e.g. superparamagnetic properties. In order to understand the superparamagnetic features exhibited by the SPIONs under investigation, the temperature dependence of the parameters such as H_r and the individual ΔH are examined. And so, at elevated temperatures a superparamagnetic narrowing of the resonance spectra occurs, quoted as the superparamagnetic resonance (SPR). Temperature dependence of the individual ΔH_{pp} is another cause of the temperature dependence of the SPR spectra, the broadening and shift to lower magnetic fields of the magnetic resonance spectra with the decrease of temperature is typical of superparamagnetic nanoparticles and has been recently observed in a number of systems [Berger Bissey, Kliava, and Estourn 2001]. The g-factor is characteristic of the local environment around the electron and the value depends on the orientation of the molecule with respect to the magnetic field [Van Doorslaer et al. 2009]. In order to examine the magnetic ordering of SPIONs, sample is cooled in the presence of the external magnetic field (field cooling, FC) the spin moments of NPs are then oriented approximately in parallel to the external magnetic field. The sample shows non-zero magnetization even if the field decreases to zero after freezing the sample. When the sample is cooled at a zero field (ZFC) the spin moments of

different domains are totally disordered and the sample shows zero magnetization when the field is zero [Dobosz *et al.*2014].

1.2. Superparamagnetic Iron Oxide Nanoparticles as drug delivery systems

Drug delivery in cancer treatment has developed over the last several decades to become more accurate and efficacious. A few notable achievements in that field include: special pills coatings, which have resulted in formulations of sustained release of the drug substance (e.g. Lynparza® - Olaparib capsules, the first monotherapy for patients with deleterious or suspected deleterious germline BRCA-mutated (gBRCAm) advanced ovarian cancer); development of drug patches (e.g. Sancuso® - Granisetron Transdermal System, indicated for the prevention of nausea and vomiting in patients receiving moderately and/or highly emetogenic chemotherapy) with extended release of active ingredient that can penetrate through the skin to reach the bloodstream or development of nanoparticulate carriers to entrap and deliver anticancer drugs to disease locations (e.g. Doxil®, a liposomal carrier of doxorubicin hydrochloride). Nevertheless, even with the present achievements, more breakthroughs are still requested to further improve the efficacy of existing drugs, thus anticancer therapy. To reach these aims, it is important to understand the goals for drug delivery. For the purposes of its improvement, the goals are all similar and include: 1) protecting drugs from degradation during formulation or dosage preparation and after administration into the bloodstream; 2) controllable release period to achieve required concentration in the specific site for prolonged period of time or increased dosing intervals; 3) enhanced targeting of drug molecules to disease sites; 4) reducing overall adverse effects.

Two major issues related to present cancer treatments are suboptimal efficacy and toxicity. No drug is free from side effects, and these ones usually arise from nonspecific drug action. In the case of anticancer therapy, adverse effects, such as bone marrow depression or reduced immunity, can be so severe that may lead to termination of therapy. In targeted drug delivery, the drug is released only within a targeted area of the body. Therefore the therapeutic effect in diseased cells and/or tissues is maximized while side effects of normal tissues are minimized. Furthermore, because of their large surface area and diverse surface chemistry, NPs can distinct drugs simultaneously to a diseased tissue. Targeting ligands can also be conjugated to the NPs surface to facilitate selective and efficient delivery of drugs [Torchilin 2000; Veiseh, Gunn, and Zhang 2010].

SPIONs hold a great promise as carriers for site-specific drug delivery [Mody *et al.*2013]. In these nanosystems, the drugs are bound to the NPs surface (especially for NPs) or entrapped in magnetic liposomes and nano/microspheres. SPIONs-assisted drug delivery systems have been engineered to deliver peptides, DNA molecules, chemotherapeutic, radioactive and hyperthermic drugs [Leader, Baca, and Golan 2008; Antosova *et al.*2009; Scherer 2002]. The combination of appropriately modified SPIONs surface (e.g. with targeting ligand/ molecules attached to their surfaces) together with application of the external magnetic field is surface engineered SPIONs is nowadays considered as a desirable technology to target active substance from carrier to the required location where the drug is slowly released. Such a system has the potential to minimize the side effects and the needed dosage of the drugs [Rudge *et al.*2001; Neuberger *et al.*2005; a S. Lübbe, Alexiou, and Bergemann 2001]. As mentioned previously there are few important considerations for SPIONs in drug delivery applications. The surface engineered magnetic iron oxide NPs are required to have superparamagnetic properties together with a specific size, which should be suitable for their delivery and a very narrow size distribution in order to have uniform biophysicochemical properties. The charge and surface chemistry are particularly crucial and strongly affect both the blood circulation time as well as bioavailability of the particles within the body. In addition, the magnetic properties are strongly related to impurity content or structural imperfections of the particles.

The primary requirement of NPs for drug delivery is that the therapeutic molecules should be loaded in such a manner that its functionality is not compromised. Furthermore, these drug-loaded NPs should release the active substance at the desired rate and desirable location. Drug loading can be achieved either by conjugating the active substance on the surface or by co-encapsulating drug molecules along with magnetic particles within the coating material envelope [Wahajuddin 2012]. Conjugation of therapeutic agents or targeting ligands on the surface of NPs can be grouped under two categories, i.e. by means of physical interactions or conjugation by means of cleavable covalent linkages. In the first strategy, physical interactions such as electrostatic interactions or hydrophobic/hydrophilic interactions, can lead to coupling of the therapeutic agents or targeting molecules on the surfaces of SPIONs. For example, SPIONs coated with polyethylenimine, a cationic polymer, interact electrostatically with negatively charged DNA, demonstrating their applicability as transfection agents [Steitz *et al.*2007]. Similarly, dextran-coated SPIONs functionalized with negatively charged functional groups can couple with peptide oligomers *via* electrostatic interactions [Hildebrandt *et al.*2007]. Because of hydrophobic interactions, lipophilic drugs can easily be attached to SPIONs covered with hydrophobic polymers, from where the drug can be released when the

coating degrades. The second strategy involves linkage of the active substance directly with e.g. amino or hydroxyl functional groups present on the surface of polymer-coated SPIONs. This methods leads to enhanced loading capacity, but also results in more specific linkages, protecting the drug's functionality and thus efficacy. Low entrapment efficiency is one of the major drawbacks of delivering the drug by conjugating the drug onto the surface coating the surface, because only a limited amount of drug can be conjugated in this way. Other disadvantages include highly stable linkages as a result of covalent bonding between drug molecules and the surface of SPIONs, leading to failure to release the drug molecule at the target site. Once SPIONs accumulate inside the required tissue, they should be able to release their drug payload at an optimal rate. However, in most cases upon injection into the *in vivo* environment the burst effect is observed, thus a majority of the drug substance is quickly released. As a consequence, inadequate amounts of the active substance reach the desired location. In order to reduce the burst effect, many research groups tried to modify SPIONs surface and so, Mahmoudi *et al.*[Morteza Mahmoudi, Simchi, *et al.*2009] synthesized SPIONs with a crosslinked poly (ethylene glycol)-co-fumarate coating. To evaluate the effectiveness of the coating, tamoxifen (i.e. an anti-oestrogen drug used to treat breast cancer) was loaded onto the surface of coated NPs. The results confirmed that the cross-linked polymer coating reduced the burst release by 21% in comparison with the non-cross-linked tamoxifen loaded particles. In another studies [Guo *et al.*2009; Hałupka-Bryl *et al.*2014], the surface of monodisperse SPIONs were appropriately modified to obtain required DOX release from NPs surface. The DOX release studies indicated that these SPIONs had a high drug loading capacity and favorable release kinetics for this drug.

There is an increasing amount of new SPIONs formulations for targeted drug delivery nowadays. However, there is still lack of their biodistribution studies in *in vivo* experiments on animal models, moreover available studies show that still more than 95% of the NPs, are distributed to entire body in a non-specific manner after systemic administration [Hałupka-Bryl *et al.*2014], therefore less than 5% of administered NPs can reach the tumor site [Mok and Zhang 2013]. Thus recently, the main goal is not only to minimize toxicity of these nanosystems, but to significantly increase their bioavailability. It is also worth noting that the magnetic drug delivery systems follow similar rules as other pharmaceutical drug delivery strategies. More particularly, SPIONs magnetically brought to the required location, should release chemotherapeutic in order to extinguish the tumor, but should also undergo the same firm rules with respect to sterility, non-immunogenicity, and non-toxicity as any other developing drug delivery systems.

1.3. Enhanced permeability and retention effect

The critical factor for application of NPs in biomedicine, such as diagnostic imaging and targeted therapies is their specifity for selected tissues [Misra 2008; Leuschner *et al.*2006]. In order to limit nonspecific cell binding, which may place healthy tissue at risk, NPs have been appropriately engineered to have an affinity for targeting tissues through passive, active, and magnetic targeting approaches. Passive targeting uses the predetermined properties of NPs to specifically locate in a given tissue region. Such selective targeting is not possible with low-molecular-weight substances (many of the drugs being used today for chemotherapy), because small molecules do not distinguish tumor tissue from normal tissue. Therefore, common pharmaceutical agents reach most normal tissues and organs as well as tumor tissues by free diffusion-dependent equilibrium. Clearance of macromolecules from the interstitial space of normal and inflammatory tissues follows rapidly and steadily *via* the lymphatic system, even in the inflammatory state after extravasation from blood vessels. However, unlike in normal tissues, clearance of macromolecules from tumor is so impaired that they stay in the tumor interstitium for a long time [Hiroshi Maeda 1991]. This phenomenon has been characterized and termed the tumor-selective enhanced permeability and retention (EPR) effect [H. Maeda 2001]. The EPR effect permits macromolecules, such as SPIONs, in the bloodstream to enter tumors more easily than healthy tissues. This phenomenon is primarily due to a combination of the fenestrated endothelium (vascular permeability) and the inefficient lymphatic drainage of the tumor, which generates the retention effect. The EPR effect is based on the principle that tumor cells, in order to grow rapidly, highly stimulate production of new blood vessels (rapid angiogenesis) that are poorly developed, thus the vasculature of tumor is leaky and damaged [Brannon-Peppas and Blanchette 2012; H Maeda *et al.*2000]. This process enables extravasation of NPs and other small macromolecules out of the vascular bed and accumulation in the tumor's interstitial space [R.K. Jain 2001]. Small molecules (less than 40 kDa) are rapidly cleared by diffusion, and large molecules and NPs (up to 500 nm size) are retained in the interstitial space due to the absence of drainage, leading to selective accumulation for a prolonged period of time of these agents resulting in increased contrast between the tumor and the surrounding healthy tissue [Thorek et al. 2006; Mcneil 2005]. In other words, high permeability of the tumor vasculature permits macromolecules and NPs to enter the tumor interstitial space, while the lymphatic filtration allows them to stay there. Unlike macromolecules, low-molecular-weight substances are not retained in tumors because of their ability to return to the circulation by diffusion [Hiroshi Maeda, Sawa, and Konno 2001]. EPR-

mediated drug delivery is currently seen as an effective way to bring drugs to and into tumors, especially macromolecular drugs and drug-loaded pharmaceutical nanocarriers. Clearly, EPR-based type of tumor targeting can function only if the macromolecules or NPs remains available in the bloodstream long enough, in order to provide a sufficient level of accumulation in the target. According to the EPR concept, biocompatible macromolecules accumulate at much higher concentrations in tumor tissues than in normal tissues or organs, even higher than those in plasma. Studies performed with a rat gliosarcoma model showed that cancerous tissues had a 10-fold higher uptake of dextran-coated SPIONs compared to healthy brain tissues [Moore *et al.* 2000]. As mentioned above, the most usual way to keep drug carriers in the blood long enough is to "mask" them by modifying their surface e.g. with certain water-soluble polymers such as PEG [Klibanov *et al.*1990]. Previous research shows that it takes at least 6 hours for drugs in circulation to exert the EPR effect [H. Maeda 2001]. This means that any candidate pharmaceutical agent must have a molecular size above the renal clearance threshold, to circulate for a prolonged time. Also, polymeric drugs should not be cationic but either neutral or anionic, because the luminal surface of blood vessels is highly negatively charged and thus cationic polymer drugs are adsorbed on the vascular surface and are expected to have a short *in vivo* half-life. If a transported drug presents good cell permeability, a NPs that will release its content in the tumor interstitium is required. With the EPR effect, the intratumoral concentration of a drug is increased 10–100-fold compared with what is obtained when the drug is given conventionally. Moreover, the slow release of active substances from a carrier results in sustained, high intratumoral drug levels and lower plasma concentrations [Dosio *et al.*2011]. In this case, a biodegradable stealth nanoparticle is preferred that will accumulate by the EPR effect and be progressively degraded in the extracellular matrix.

2. Experimental methods

2.1. Materials

All chemicals were used without further purification. Iron (II) chloride tetrahydrate (99.9%), acetic acid (99.0%), dimethyl sulfoxide, sodium chloride, sodium acetate, and Dulbecco's phosphate-buffered saline (PBS) were purchased from WAKO (Wako Pure Chemical Industries, Ltd., Osaka, Japan). Iron (III) chloride hexahydrate and ammonia solution were obtained from Kanto Chemicals (Tokyo, Japan). Doxorubicin hydrochloride (>99.9%, MW 579.98) was received from LC Laboratories (Woburn, MA, USA) and acetonitrile (99.99%) was provided by Honeywell (Muskegon, MI, USA). Dialysis membranes (MWCO 12-14 KDa) were purchased from SPECTRUMLABS (Ritto, Japan). Amicon Ultra centrifugal devices (MWCO 10 KDa) were obtained from Millipore, Toyonaka, Japan. PEG-*b*-PVBP was synthesized using the two-step side-chain conversion of the PEG-*poly*(4-chloromethylstyrene) block copolymer. To synthesize this polymer the following reagents were used: α-Methoxy-ω-mercapto-poly(ethylene glycol) (MeOPEG-SH, M_n =5000 g mol^{-1}) was purchased from NOF Corporation (Tokyo, Japan), 4-Chloromethylstyrene (CMS) was provided by Seimi Chemical Co. Ltd., (Kanagawa, Japan), 2,2'-Azobisisobutyronitrile (AIBN; Kanto Chemicals Co. Ltd., Tokyo, Japan) was purified by recrystallization from methanol. Tetrahydrofuran (THF; Kanto Chemicals) was passed through purification columns (Glass Contour Solvent Dispensing System, HANSEN & Co., Ltd.) before use. Diethyl phosphite, diethyl 2-bromoethylphosphonate, trimethylsilyl bromide (TMSBr) were purchased from Tokyo Chemical Industry, Co., Ltd, Japan, sodium hydride (NaH; 55% oil dispersion), sodium iodide (NaI), benzene and dichloromethane from Kanto Chemicals. Dialysis membranes (MWCO 3,5 KDa) were purchased from SPECTRUMLABS (Ritto, Japan). In cell culture and *iv vivo* experiments were used as follows: penicillin, streptomycin, and neomycin (PSN), fetal bovine serum (FBS), trypsin-EDTA, and trypan blue stain (from Gibco, USA). Hoechst 33258 solution was obtained from Dojindo (Kumamoto, Japan) and cell proliferation Kit I (MTT) from Roche (Tokyo, Japan). Dulbecco's modified Eagle's medium (DMEM) was received from Sigma, USA. Murine colon adenocarcinoma 26 (C26) cells were provided by RIKEN BioResource Centre. Male BALB/c mice (age, 5-6 weeks and weight, 20-24 g) were purchased from Charles River Japan Inc. Deionized water was used throughout the experiments.

2.2. Synthesis of Poly(ethylene glycol)-*block*-poly(4-vinylbenzylphosphonate) block copolymer

PEG-*b*-PVBP was synthesized by the two-step side-chain conversion of the PEG-poly (4-chloromethylstyrene) block copolymer (PEG-*b*-PCMS) [Kamimura *et al.* 2011] (Figure 8).
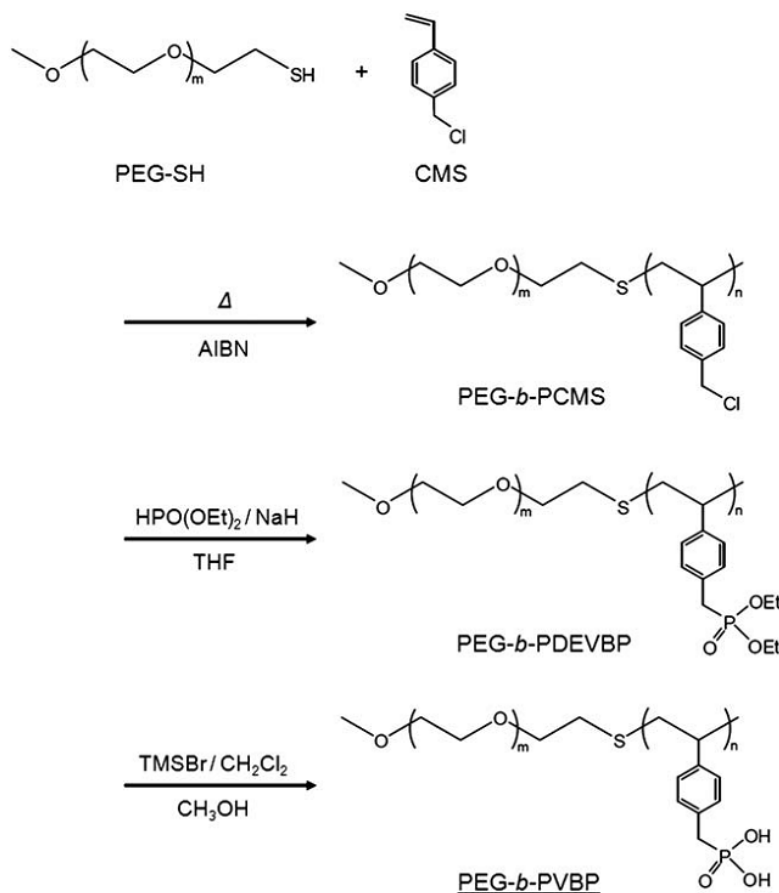

Figure 8. Scheme of PEG-*b*-PVBP synthesis [(Kamimura *et al.* 2011)].

At first, PEG-*b*-PCMS was synthesized by the radical telomerization of CMS using PEG-SH as a telogen [Yoshitomi, Miyamoto, and Nagasaki 2009]. Briefly, PEG-SH (1.0 g, 0.2 mmol), CMS (1.38 g, 10.0 mmol) and AIBN (16.5 mg, 0.1 mmol) were weighed into flask and dissolved in 10 mL of toluene. The obtained solution was then degassed through three freeze–thaw–evacuate cycles. Polymerization was conducted for 24 h at 60ºC under the nitrogen atmosphere. Subsequently, the received polymer was purified by repeating precipitation into *n*-hexane and diethyl ether and freeze-dried with benzene to obtain PEG-*b*-PCMS. The side chains

of the PCMS segment were converted to diethylphosphonate (PEG-*b*-poly(diethyl-4 vinylbenzylphosphonate) (PEG-*b*-PDEVBP)) by the following reaction [(Boutevin *et al.*2002)]. NaH (126 mg, 5.25 mmol) and NaI (ca.40 mg) were weighted into a flask and dissolved in THF (5 mL). After cooling to 0ºC with magnetic stirring, diethyl phosphite (0.35 mL, 3eq., 2.63 mmol) was added over 5 min, and the reaction mixture was further stirred for 20 min. A solution of PEG-*b*-PCMS (500 mg) in 5 mL of THF was slowly added to the mixture at 0ºC, and the mixture was heated to room temperature and stirred for 12 h. Afterward, the solvent was removed by evaporation and the polymer was purified by dialysis (Spectra/Por 6, MWCO 3,500, SPECTRUM) for 2 days against excess methanol (2 L), which was changed after 3, 6, 9, 18, and 32 h. The final solution was concentrated under reduced pressure, followed by freeze-drying with benzene. The diethyl phosphonate moiety of the obtained PEG-*b*-PDEVBP was hydrolyzed to the corresponding by treatment with TMSBr followed by methanolic hydrolysis. In brief, 450 mg of PEG-*b*-PDEVBP was weighted into a flask, solution of TMSBr (0.46 mL, 5eq., 3.55 mmol) in dichloromethane (5 mL) was added and the solution was mixed for 2 h at 45ºC. After the solvent was evaporated, 20 mL of methanol was added, and the mixture was stirred at room temperature for 15 h. After stirring, the solvent was removed by evaporation. The obtained polymer was purified by dialysis (Spectra/Por 6, MWCO 3,500, SPECTRUM) for 2 days against excess methanol (2 L), which was changed after 3, 6, 9, 18, and 32 h. The final product was concentrated under reduced pressure, followed by freeze-drying with benzene to obtain PEG-*b*-PVBP.

2.3. Synthesis of PEG-PIONs/DOX

PEG-PIONs/DOX were prepared by optimized co-precipitation method. The initial iron oxide NPs precipitated upon addition of ammonium hydroxide to an aqueous mixture of iron (II) and iron (III) chlorides containing PEG-*b*-PVBP solution. Briefly, $FeCl_2 \cdot 4H_2O$ and $FeCl_3 \cdot 6H_2O$ in the ratio of 1:2 were weighted into a flask and dissolved in MilliQ water. PEG-*b*-PVBP solution was added to this solution in the feed-weight ratio between polymer and iron salts 1:1 and the resulting mixture was vigorously stirred for 3 minutes. NH_4OH (28% (v/v) in water) was added to this solution in ultrasonic bath. After the addition of ammonia, the dispersion was immediately put on vortex to vigorously stir for 3 minutes and then, the reaction mixture was allowed to stir at 1300 rpm at room temperature for 3 hours. Afterwards, the obtained mixture was dialyzed (MWCO 20,000) against 2L of water. The dialysate water was changed after 3, 6 and 15h.

The water-soluble anticancer drug DOX was chosen as a model drug after dialysis. The DOX loading was carried out by adding water-soluble drug substance (at final DOX concentration of 1mg/ 1 mL PEG-PIONs suspension) to 7.2 mg of PEG-PIONs in 1 mL aqueous dispersion (based on magnetic NPs dry weight), mixed and ultrasonicated for 2 minutes. The reaction mixture was shaken on a rotary shaker at 1300 rpm in the dark at room temperature for 20 hours to facilitate DOX uptake. To optimize PEG-PIONs/DOX preparation, the unbound DOX was removed at fixed time intervals by ultrafiltration using an Amicon Ultra centrifugal devices (MWCO 10 KDa) pretreated with DOX. Then, the optical density of residual DOX in the supernatant was measured at 481 nm by using an ultraviolet-visible (UV-Vis) spectrophotometer (VarioSkan Flash plate reader; Thermo Fisher Scientific Inc., UK). After the measurement, the PEG-PIONs/DOX were redispersed for further DOX adsorption. Beyond a certain adsorption time, there were no further changes in the concentration of DOX since the loading capacity of the particles had reached saturation. The drug encapsulation efficiency (EE, refers to the percentage of drug encapsulated into the PEG-PIONs/DOX relating to the total drug added) and drug loading capacity (LC), refers to the drug content in the PEG-PIONs/DOX) of the NPs were calculated according to the following formulae:

$$EE\,(\%) = (W_D - W_S)/W_D \times 100\%$$
$$LC\,(\%) = (W_D - W_S)/W_{PPD} \times 100\%$$

where, W_D refers to the weight of DOX added initially to system, W_S refers to the DOX content in the supernatant, and W_{PPD} refers to the weight of PEG-PIONs/DOX.

The resulting PEG-PIONs/DOX were then dispersed in an appropriate medium and were stored at 4 °C before use [Kamimura *et al.* 2012; Kayal and Ramanujan 2010]. The proposed objective of the synthesis has been schematically illustrated in Fig. 9.
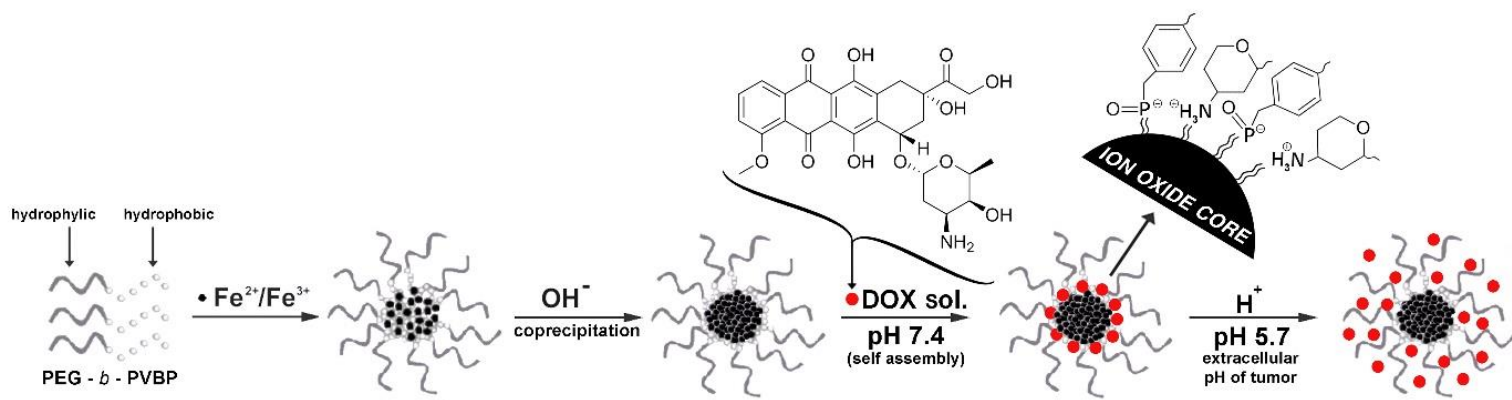
Figure 9. Synthesis of PEG-PIONs/DOX.

2.4. Physicochemical characterization of PEG-PIONs/DOX

2.4.1. Particle size and morphology determination

The morphology and core size of PEG-PIONs/DOX were observed by High-Resolution Transmission Electron Microscope (HRTEM) with a Jeol model ARM 200F operating at 200kV. For sample preparation, a drop of PEG-PIONs/DOX aqueous dilute dispersion was deposited on cooper grid covered with a formal-carbon membrane.

2.4.2. Stability studies

The hydrodynamic size of the particles were measured by using Dynamic Light Scattering (DLS) technique with ZetaSizer Nano ZS (Malvern Instruments, Ltd., UK). Samples were prepared by dispersing PEG-PIONs/DOX in physiological saline, Phosphate Buffered Saline (PBS) and in PBS containing 10% Fetal Bovine Serum (FBS) and were stored over a period more than one moth at room temperature. Each measurement was performed at room temperature in triplicates.

2.4.3. Study of complex formation (gel filtration chromatography)

The gel filtration chromatography using PD-10 test column was used to confirm the complex formation between synthesized PEG-PIONs and DOX. For sample preparation, PEG-PIONs/DOX suspension (1 mg DOX/1 mL PEG-PIONs) and free DOX solution (1 mg/mL) were loaded onto the top of a PD-10 column (Sephadex G25 medium; GE healthcare) and passed through a filtration column pre-rinsed with MilliQ water and PBS pH 7.5. Afterward,

the column was eluted with PBS pH 7.5 and fractions (0.5 mL/fraction) were retrieved. 32 obtained fractions were collected and analyzed using UV-Vis spectroscopy (481 nm). Each measurement was performed in triplicates.

2.4.4. Superconducting quantum interference experiments

A superconducting quantum interference device (SQUID) was used to study the specific magnetic properties of synthesized PEG-PIONs/DOX. The field dependence of magnetization was recorded at room temperature in powder form. The magnetic field range in the magnetometer is $\pm 7T$ and, sensitivity $<6 \cdot 10^{-7}$ emu.

2.4.5. Analysis of crystalline structure

The crystalline structure of PEG-PIONs/DOX was studied by an X-ray diffraction (XRD) technique on Empyrean (PANalytical) diffractometer operated with Cu Kα radiation (1.54 Å), reflection-transmission spinner (sample stage) and PIXcel 3D detector, operating in the Bragg–Brentano geometry. The 2 Theta scans were recorded at room temperature (300 K) in angles ranging from 20 to 80 (°2Theta) with a step size of 0.003 (°2Th.) and continuous scan mode. The identification of PEG-PIONs/DOX was carried out by comparing the diffraction pattern of the sample with library data in powder diffraction files using ICDD PDF- 4+ 2012 database.

2.4.6. Electron paramagnetic resonance analysis

The Electron Paramagnetic Resonance (EPR) measurements were carried out to study the magnetic properties of synthetized NPs using a conventional X-band Bruker EMX −10 spectrometer with a magnetic field second modulation frequency of 100 kHz. Low temperatures were maintained by a Bruker temperature controller ER 4131VT. EPR analysis was carried out in the range of 77K − 290 K in a magnetic field sweep width of 6500 G. The typical spectroscopic parameters such as resonance field (H_r), g-spectroscopic splitting factor value, peak-to-peak line width (ΔH) were determined for all collected spectra.

In order to examine the magnetic ordering of PEG-PIONs/DOX, sample of synthesized NPs was left for 5 minutes in the external magnetic field of 5000 Gs and then cooled to 120 K. When the sample is cooled in the presence of magnetic field (field cooling, FC) the spin moments of NPs are oriented approximately in parallel to the external magnetic field. The sample shows non-zero magnetization even if the field decreases to zero after freezing the sample. When the

sample is cooled at a zero field (ZFC) the spin moments of different domains are totally disordered and the sample shows zero magnetization when the field is zero [Dobosz *et al.*2014].

2.5. *In vitro* studies

2.5.1. DOX release profile

DOX release experiments were performed at least in triplicate using dialysis method (membrane MWCO 12-14 KDa). Analysis of DOX released from PEG-PIONs/DOX was performed in acetate buffer saline (ABS; pH, 5.7 and NaCl, 145 mM) and PBS (pH, 7.4 and NaCl, 145 mM) placed in an orbital shaker bath which was maintained at 37 °C in dark, and shaken horizontally at 120 rpm. At the particular range of time intervals (from 0.5 h to 96 h), 200 µL of a sample of dialysate solution was withdrawn and replaced with an equal volume of fresh buffer. The DOX concentration was determined in dialysate samples from the intensity of the drug fluorescence at 481 nm by using VarioSkan Flash plate reader (Thermo Fisher Scientific Inc) using a calibration curve. The amount of DOX released from PEG-PIONs was expressed as a percentage of total DOX and plotted as a function of time. The solution obtained from a dialysis test performed using unloaded PEG-PIONs was used as a control.

2.5.2. Cell culture and *in vitro* cytotoxicity assay

C-26 colon cancer cells were cultured in Dulbecco's Modified Eagle's Medium (DMEM) supplemented with 10% FBS and 1% penicillin- streptomycin at 37 °C in a humidified 5% CO_2 atmosphere. The medium was replenished every other day and the cells were collected by trypsinization using 0.25% of Trypsin-EDTA solution followed to subculture. The cytotoxic effect of DOX on C-26 cells was evaluated by a standard MTT assay as described in the literature [Munnier *et al.*2010]. MTT analysis is a non-radioactive, colorimetric assay [Morteza Mahmoudi *et al.*2010] frequently used to determine the antiproliferative effect on cells. The assay is based on the conversion of the yellow tetrazolium salt MTT to purple formazan crystals by metabolic active cells (Figure 10). The formazan crystals formed are solubilized and the resulting colored solution is quantified using a scanning multiwell spectrophotometer. The reduction takes place only when reductase enzymes are active, therefore the conversion is often used as a measure of cell viability.

Briefly, 2500 cells were seeded in each well of a flat-bottomed 96-well culture plate and allowed to grow for 24 h before desired treatment. Afterward, the cells were treated with series of suspensions of PEG-PIONs/DOX or free DOX at various concentrations and incubated for 24 and 72 h. The culture medium without any drug formulations, only with PBS, were performed as a control. Then, the cells were incubated with MTT (5µL/ well) for 2-3 h at 37 °C in the dark. Subsequently, the resulting formazan was solubilized using solubilization agent (50 µL/ well) and, after overnight incubation at 37 °C in the dark, the absorbance was read using the VarioSkan Flash plate reader (Thermo Fisher Scientific Inc) at 572 nm. The half-maximal inhibitory concentration (IC_{50}) was determined as the drug concentration that resulted in a 50% reduction in cell viability. The results were expressed as a percentage relative to the control. All measurements were recorded in triplicates.
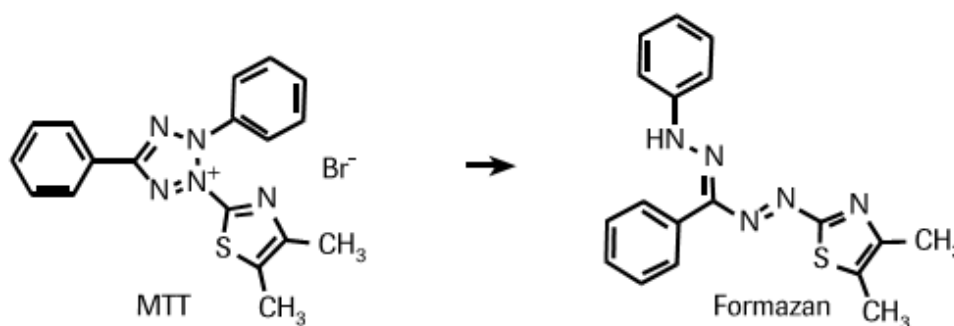
Figure 10. Scheme of conversion of MTT to formazan salt by viable cells.

2.5.3. DOX subcellular distribution (Fluorescence imaging)

To observe the drug substance distribution in C-26 cells the confocal fluorescence imaging was used. The C-26 cells were seeded in a 6-well plate at a density of 65,000 cells per well in 1 mL of DMEM medium supplemented with 10% FBS and 1% penicillin-streptomycin and incubated for 24 h at 37 °C in a humidified 5% CO2 atmosphere to allow cells to attach. Afterward, the medium was replaced by free DOX solution of PEG-PIONs/DOX in the culture medium at a concentration of 25 µM of DOX. After 24 h at 37 °C/5% CO2, cells were washed thrice with PBS and fixed with ethanol for 5 min. Subsequently, 4 µg/mL of Hoechst solution was added for 30 min to stain the nuclei. Finally, cells were washed thrice with PBS (pH 7.5), covered with PBS, and directly observed under a confocal laser scanning microscope (CLSM).

The CLSM images were obtained using a Zeiss Laser Scanning microscope LSM 700 (Carl Zeiss, Inc., USA) at excitation/emission filter wavelengths of 488 nm/505-605 nm for DOX and 405 nm/430-470 nm for Hoechst 33258.

2.6. *In vivo* studies

2.6.1. Biodistribution of PEG-PIONs/DOX

All procedures involving animal care were approved by the Animal Ethics Committee of the University of Tsukuba and were conducted according to the Guidelines for Animal Experimentation of the University of Tsukuba. The *in vivo* distribution of the drug substance from PEG-PIONs/DOX or free DOX solution was examined in tumor-bearing male BALB/c mice (5-6-week-old; 20-24 g, n = 3-4 for each group). Tumors were induced in the mice by subcutaneous injection of C-26 cells into the right femur (1.0×10^6 cells/mouse) [Sumitani *et al.*2012]. When the tumor reached 100 mm^3, BALB/c mice were administered intravenously with various DOX formulations, including: PEG-PIONs/DOX dispersion and free DOX solution, or saline (as a control group) *via* the tail vein at a single dose of DOX 10 or 20 mg/kg (10-12 mg Fe kg^{-1}) [Chertok *et al.*2008]. Tumor volume was calculated using the following formula: $(L \times W^2)/2$, where L is the longest, and W is the shortest tumor diameter (mm), as measured by a caliper. At different time points i.e. 24 and 36 h post-injection blood samples were collected in a heparinized tubes by intracardiac puncture and then the major organs were harvested from the mice under sodium pentobarbital (40 mg/kg) anesthesia. The samples were frozen and stored at -80 °C until the further use. A simplified, rapid extraction procedure method was designed and appropriately modified to identify and quantify DOX in tissue extracts. To extract the drug from the organs, tissue samples were further optimized and processed to measure DOX content by using Liquid Chromatography – Mass Specroscopy (LC-MS; LC Elite La Chrome Hitachi UV Detector L-2400U; MS AB Sciex API 2000 LC/MS/MS system, Tokyo, Japan) as follows. For analysis, frozen tissue samples (liver, heart, spleen and tumor) were removed from the freezer, and a 50-100 mg sample was quickly cut and transferred into a fresh, tared tube. A sufficient volume of mobile phase was added to achieve a final concentration of 12.5 – 25 % (w/v) tissue to solvent. The tissue homogenates were prepared using an ultra-sonic homogenizer (UH-50; SMT Company, Tokyo, Japan). All samples were homogenized briefly on ice (2 minutes), incubated on ice for 10 minutes and centrifuged for 13 minutes at approximately 15,000 x g at 4°C. The supernatant was recovered and analyzed

immediately. The composition of the mobile phase was optimized empirically to maximize sensitivity and minimize analytical time. The optimum extraction solvent consisted of 70% of acetonitrile, 30% of deionized water and 5% of acetic acid. Standard and quality control samples were prepared by extracting tissues obtained from untreated mice (from control group).

2.6.2. Serum toxicity analysis

At 24 h after the injection of PEG-PIONs/DOX dispersion, free DOX solution, or saline (as a control group) dosage, after the mice were anesthetized, blood samples were collected by intracardiac puncture using a heparinized syringe. Afterward, the blood was separated by centrifugation (6,200 rpm, 2000 g, for 10 min) and plasma was isolated for the analysis. Serum chemistry studies included evaluation of levels of aspartate aminotransferase (AST), blood urea nitrogen (BUN) (hepatic and renal function panels, respectively), and markers of cardiotoxicity such as creatine kinase (CK) and lactate dehydrogenase (LDH) were measured by a Fuji Dri-chem 3500 (Fuji-Film, Tokyo, Japan).

2.7. Statistics

All values are expressed along with respective means ± standard deviation (SEM). All values are expressed as SEM. Differences between groups were compared using one-way analysis of variance. All ANOVA were performed with ANOVA tests followed by Tukey's test. Differences with a value of $P < 0.05$ were considered statistically significant.

3. Results and discussion

3.1. Characterization of Poly(ethylene glycol)-*block*-poly(4-vinylbenzylphosphonate) block copolymer

PEG-*b*-PVBP was synthesized by the two-step side-chain conversion of the PEG-poly (4-chloromethylstyrene) block copolymer (PEG-*b*-PCMS). The polymerization degree of PCMS segment (n) was determined as n = 14 by ^{1}HNMR analysis (Figure 11), assuming the number-averaged molecular weight (M_n) of the PEG segment to be 5000 g mol^{-1}. The quantitative conversion of the chloromethyl side chains into phosphoric acid groups was confirmed by both ^{1}H- and ^{31}P-NMR spectroscopy (Figure 11, Figure 12). The number-averaged molecular weight (M_n) of the PEG segment was 5000 g mol^{-1}, and the degree of polymerization of the PVBP segment (n) was 14.
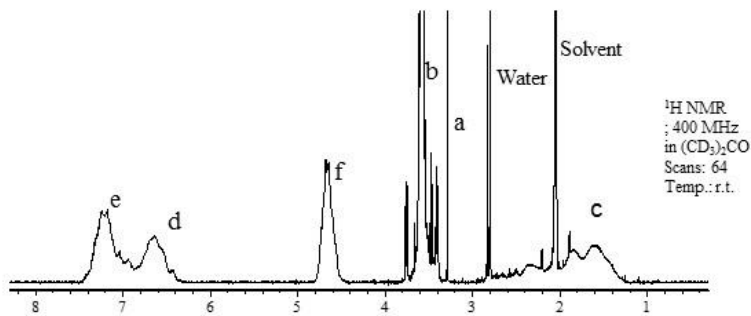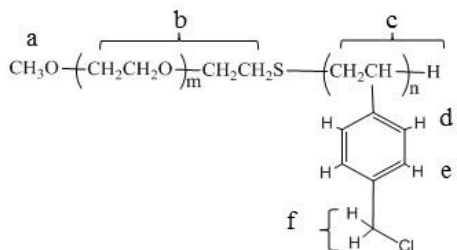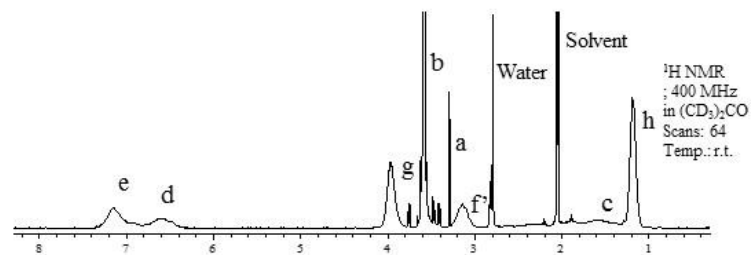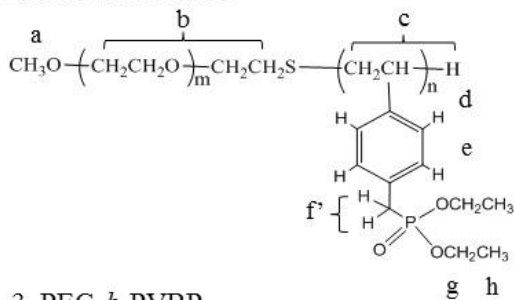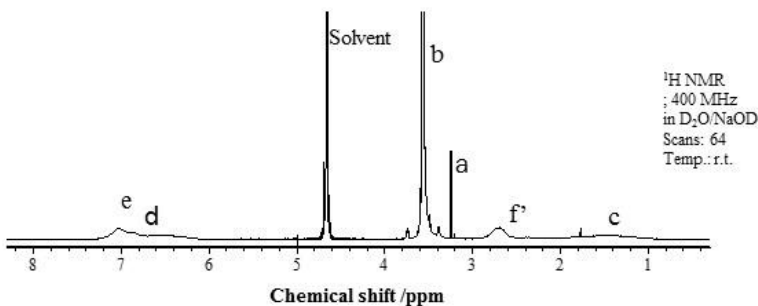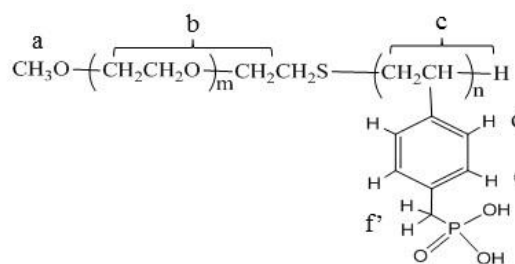
Figure 11. ^{1}H-NMR spectra of PEG-*b*-PCMS, PEG-*b*-PDEVBP (400 MHz, acetone-d$_6$, room temperature) and PEG-*b*-PVBP (400 MHz, deuterium oxide/sodium deuteroxide, room temperature).
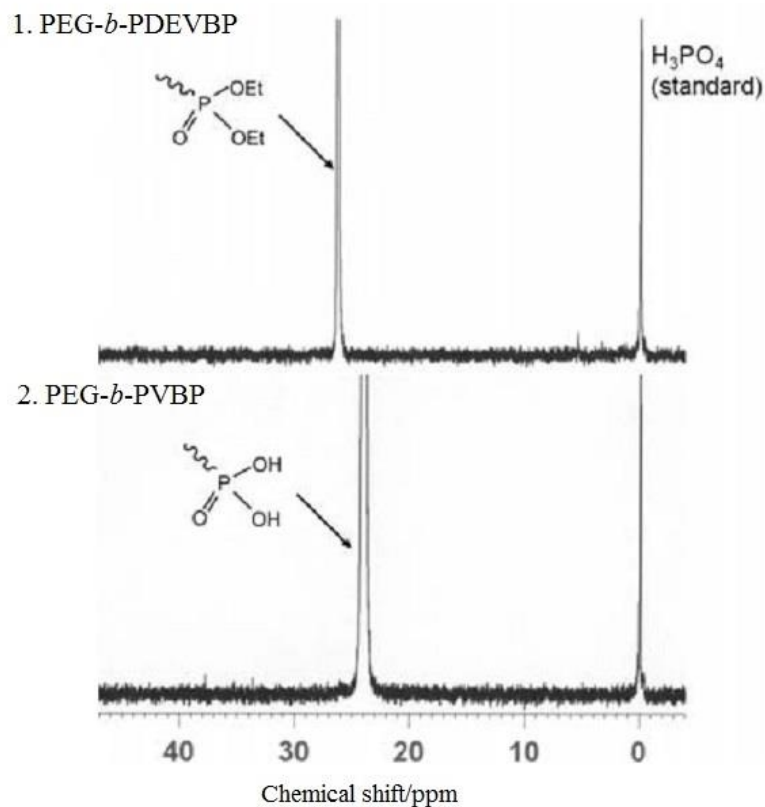
Figure 12. ^{31}P-NMR spectra of PEG-*b*-PDEVBP and PEG-*b*-PVBP (600 MHz, methanol-d$_4$, room temperature).

3.2. Physicochemical characterization of PEG-PIONs/DOX

A number of different methodologies have been reported to synthesize SPIONs, however commonly used co-precipitation method of iron salts under alkali conditions seems to be one of the best choices, due to its ease of operation and amenable scale-up. One of the major challenges related to SPIONs preparation is their surface modification, in order to avoid NPs aggregation. The coating procedure, and synthesis of NPs itself, used in my study has been optimized to prevent such aggregation and subsequently, the PEG-PIONs/DOX could be easily dispersed in appropriate medium and remain stable even at high ionic strength. PEG-PIONs/DOX were prepared by the alkali co-precipitation of iron salts in the presence of PEG-*b*-PVBP block copolymer. Synthesis of iron oxides NPs in a liquid phase containing stabilizer has been proved to be useful for controlling the particle size and preventing from their aggregation [Lutz *et al.*2006; Ishii *et al.*2004; Gu *et al.*2008; Papaphilippou *et al.*2009]. Aqueous dispersion of iron salts containing PEG-*b*-PVBP was prepared and NH$_4$OH solution was then added to the mixture. The color of the solution changed immediately from yellow to

black after the addition of ammonia solution, indicating the generation of iron oxide NPs. In my study, DOX, an anthracycline antibiotic, was used as a model drug. DOX is one of the most widely used chemotherapeutic anticancer agents with a broad spectrum and high antitumor activity. It is usually used in the treatment of leukemia and various solid tumors and it has significant activity against tumor of the ovaries, lung, testis, prostate and bladder [Li *et al.*2011]. DOX inhibits DNA and proteins synthesis, and different mechanisms of action have been proposed to explain its' effect. It exerts antitumor activity through inhibition of topoisomerase II, and therefore prevents chain unfolding and separation in DNA replication; in addition, it forms complexes with DNA by intercalation between base pairs and subsequent inhibition of DNA synthesis [Burden and Osheroff 1998; Sartiano, Lynch, and Bullington 1979]. However, systemic administration of DOX itself demonstrates severe side effects, including dose-dependent cardiac toxicity and congestive heart failure, due to the lack of ability to target cancer cells [Chang *et al.*2011] and limits its clinical application. DOX is the drug model used in numerous published studies on delivery nanosystems. It possess the central anthracycline group, responsible for the intrinsic fluorescence of its molecule [Gautier *et al.*2013] (Figure 13). Thus, its biodistribution in cells can be visualized using fluorescence-based microscopy and imaging. Modifying its biodistribution and clearance by using SPIONs as a carrier can more effectively target them to tumor tissues, thus prevent the adverse effects and increase the efficacy of the drug [Munnier *et al.*2008; Aljarrah *et al.*2012].

After the PEG-PIONs synthesis, DOX was loaded onto their surface using the adsorption technique. The pKa of DOX is 8.6, which provides positive charge to the drug in the neutral pH [(Gaihre *et al.*2009)] (pH of PEG-PIONs/DOX synthesis). The pKa value of PEG-*b*-PVBP is both 2.1 and 7.2; thus, at neutral conditions, about 25% of phosphonate groups are protonated, which imparts a negative charge to the polymer. Hence, the electrostatic interaction between the polymer and DOX and hydrophobic interaction between fused rings of DOX and the aromatic group of styrene from PEG-*b*-PVBP and IONs is the basis for the drug binding. Drug loading efficacy plays an important role in formulation of the drug delivery system and affects its therapeutic effect. The DOX encapsulation efficiency (EE) and DOX loading capacity (LC) into PEG-PIONs/DOX were estimated using UV-Vis spectroscopy. The results showed high efficacy of DOX loading, EE was 96.3% ± 0.8 and LC was 11.7% ± 0.5, which indicated relatively high efficiency of drug loading compared to that reported previously [Nigam, Barick, and Bahadur 2011; Rahimi *et al.*2010]. This high drug loading efficiency is critical to minimize the amount of NPs required to deliver cytotoxic drugs.
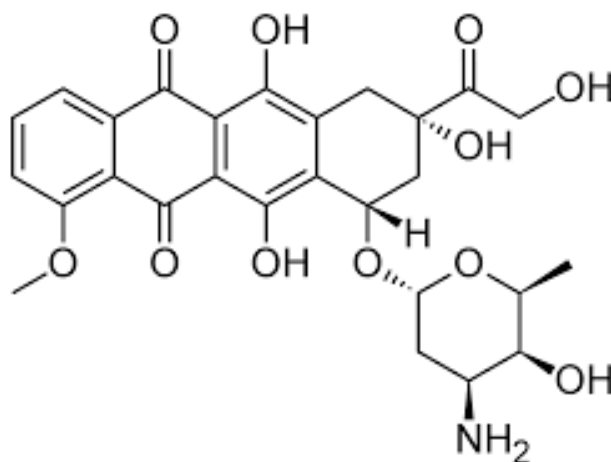
Figure 13. Doxorubicin structure.

The physicochemical properties of nanostructures designed for biomedical applications are the crucial parameters describing their quality [Hałupka-Bryl et al. 2015]. Therefore number of them like, the core size, morphology, hydrodynamic diameter and ζ-potential after synthesis, stability in different media, crystalline structure, complex formation between DOX and NPs as well as magnetic properties of these particles were evaluated using different methods.

The core size of PEG-PIONs/DOX was visually confirmed by HRTEM measurements. Figure 14 shows a typical HRTEM image of PEG-PIONs/DOX. The number-averaged diameters of the PEG-PIONs/DOX were determined by HRTEM image analyses. The images demonstrated a nearly spherical iron oxide core shape and uniform size distribution with the narrow range of 8 – 12 nm. In the context of drug delivery, a narrow particle size range such as that obtained is useful since uniform size particles offer equal probability of magnetic capture of drug loaded nanoparticles and similar drug content.
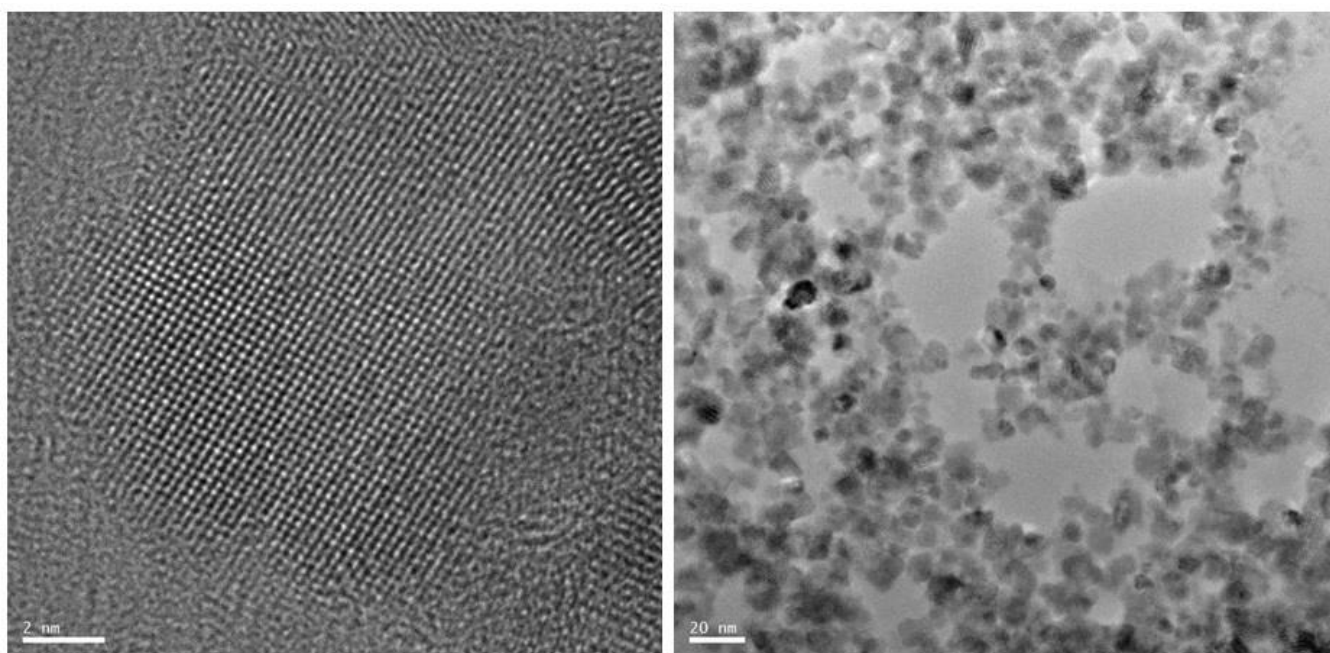
Figure 14. HRTEM images of PEG-PIONs/DOX

NPs designed for *in vivo* usage should be in the range of 10-100 nm to prevent elimination by the kidneys (<10 nm) and recognition by RES (>100 nm), therefore, PEG-PIONs/DOX are supposed to penetrate the tumor by the EPR effect, and neutral or slightly negative surface charge cause a reduced plasma protein adsorption and low rate of nonspecific cellular uptake. DLS was processed to determine a hydrodynamic size of synthesized NPs – these values are more significant than HRTEM data due to the fact that NPs will be used as a dispersions in appropriate medium and they provide information about actual size of whole core-shell nanosystem. The values of mean hydrodynamic diameter and ζ-potential of PEG-PIONs/DOX post-synthesis are in accordance with the statement above and are presented in Table 1. Prepared PEG-PIONs/DOX had particle size in the range of ~ 28 – 36 nm, and the electrokinetic potential was slightly negative, most likely resulting from the presence of numerous anionic phosphonate groups of PEG-*b*-PVBP polymer in the surface layer of the particles. A polydispersity index (PDI) describes the distribution in size measured by DLS. The value of PDI below 0.1 confirmed monodispersity of synthesized NPs.

Table 1. Size and ζ-potential of synthesized PEG-PIONs/DOX

Sample ≥ 10	Hydrodynamic diameter [nm]	ζ-potential [mV]	Polydispersity index (PDI)
PEG-PIONs/DOX	31.7 ± 4.3	- 3.9 ± 1.3	0.098

As it was mentioned before, dispersion stability of nanosized drug delivery systems plays crucial role in introducing them to *in vivo* biomedical applications. They should prevent aggregation and development of an embolism. PEG-PIONs/DOX showed excellent stability and good mono-dispersity in saline, PBS, and PBS containing 10% FBS over a period more than one month at room temperature (Figure 15). Phosphate salts from PBS are known to bind to the metal oxides surface and/or displace with the chemisorbed stabilizer, resulting in decrease in the dispersion stability [Goff *et al.*2009]. PEG-PIONs/DOX dispersed stably into PBS and showed no significant changes in their hydrodynamic diameter, which indicated that they are not prone to formation of aggregates under physiological conditions. The stability of the NPs in high ionic strength solution could be attributed to the steric repulsion, thus preventing the iron oxides cores from aggregating. It should be noted that the hydrodynamic diameter of PEG-PIONs/DOX in saline and PBS was very similar to that in FBS. Therefore, good stability of PEG-PIONs/DOX was also confirmed in the serum-containing medium, which may suggest that synthesized NPs possess desired anti-biofouling surface properties, and this can be anticipated to increase their half-life in the bloodstream.
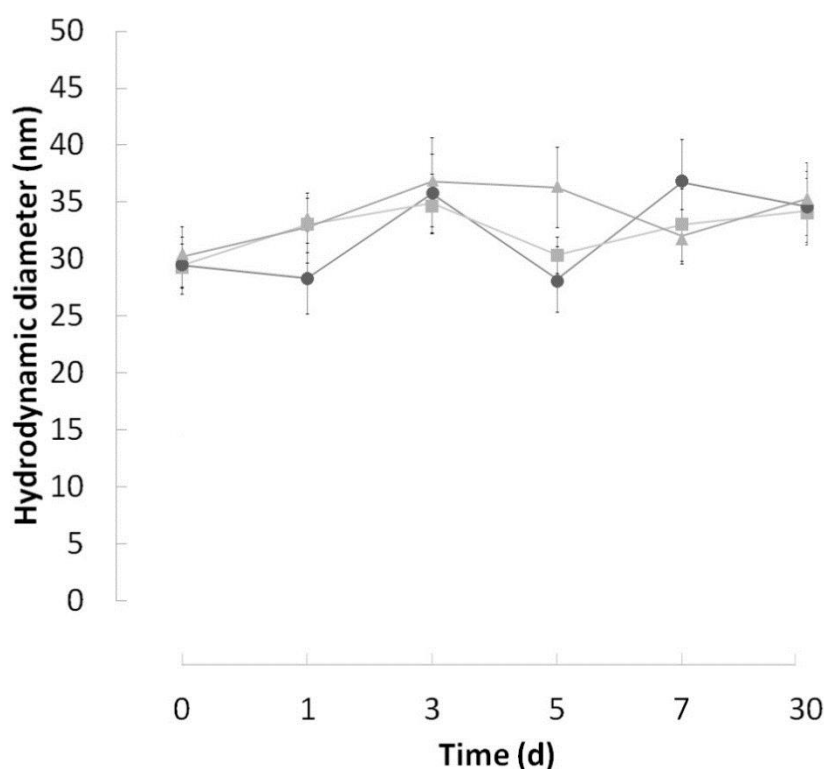

Figure 15. Stability of PEG-PIONs/DOX.

The formation of a complex between PEG-PIONs and DOX was confirmed by size exclusion chromatography (SEC) on a PD-10 column (Figure 16). In the SEC method, compounds with a high molecular weight (PEG-PIONs/DOX) are excluded from Sephadex matrix and eluted first, while the compounds with a low molecular weight (free DOX) penetrate the pores to a varying extent and are eluted after large molecules. In our study, PEG- PIONs/DOX were eluted from 3-5 mL and elution of free DOX was observed from 7-16 mL. The results of UV-Vis measurements of obtained fractions indicated the formation of a complex between PEG-PIONs and the drug.
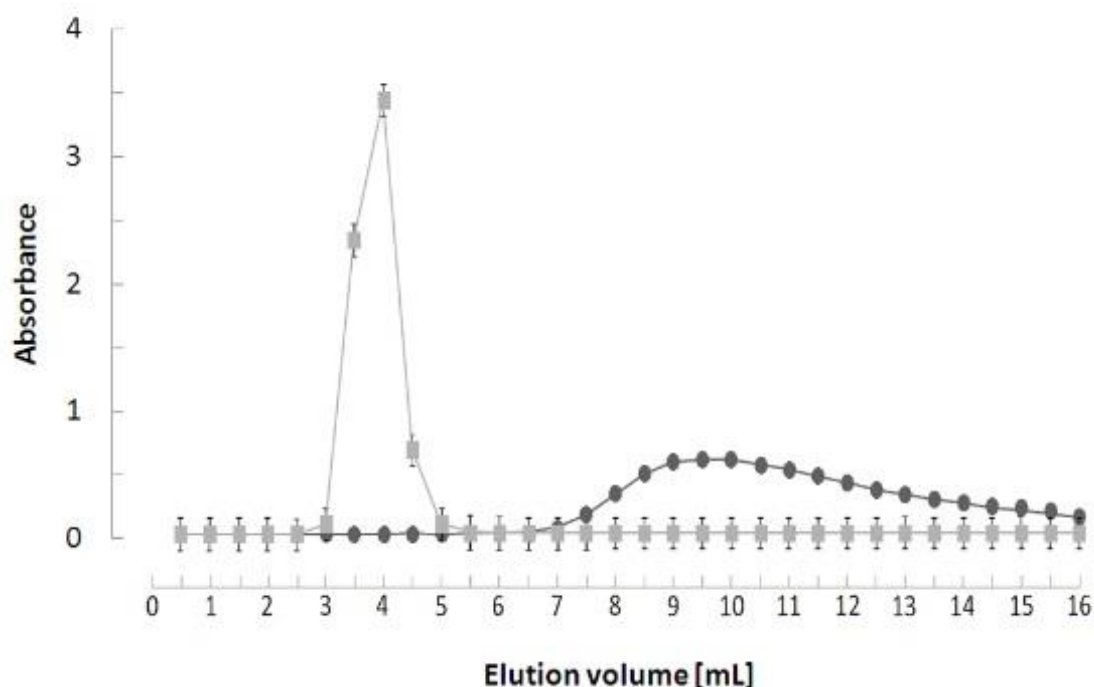

Figure 16. Confirmation of complex formation.

XRD was performed to confirm the crystalline properties of the PEG-PIONs/DOX and confirmed the presence of pure phase of magnetite. Representative powder XRD patterns of PEG-PIONs/DOX are presented in Figure 17. The presence of sharp and intense peaks confirmed the formation of highly crystalline nanoparticles. The obtained results showed characteristic diffraction peaks ($2\theta = 30.2°$, $35.5°$, $43.2°$, $53.6°$, $57.2°$ and $62.8°$) similar to those of magnetite (Fe_3O_4) [Gaihre *et al.*2009; Nigam, Barick, and Bahadur 2011]. The peaks corresponding to reflection planes are indexed. There often appears small contribution of

maghemite NPs in magnetite nanosystem, and these peaks also may occur in XRD examination. However, the absence of (210) and (300) peaks in the obtained XRD pattern, can indicate that separate maghemite was not present in the samples [Kayal and Ramanujan 2010].
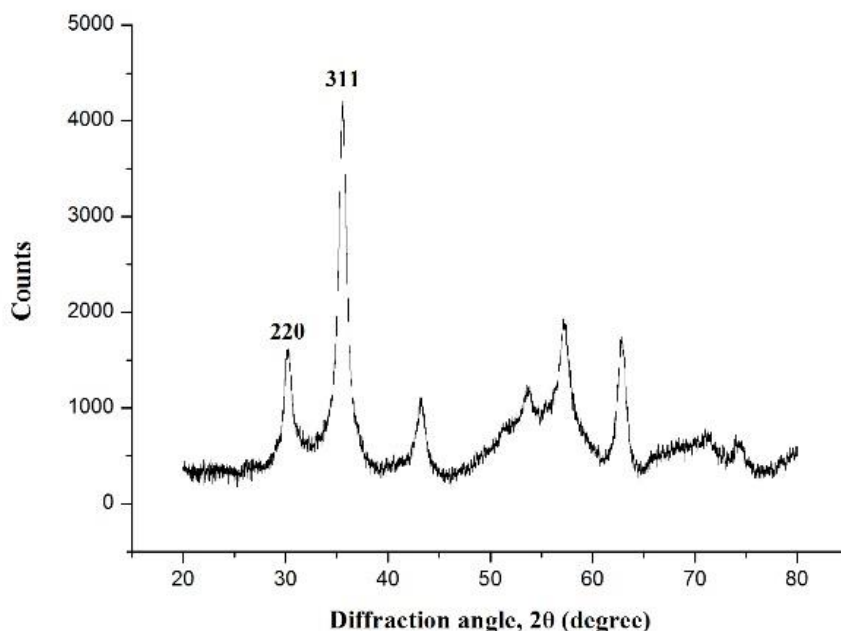

Figure 17. Crystalline structure of PEG-PIONs/DOX.

Magnetic properties of NPs depend on various factors such as their composition, size, thickness and type of surface coating. In order to study these crucial properties of prepared NPs we used SQUID. The hysteresis loop presented in Figure 18 demonstrates the magnetic behavior of PEG-PIONs/DOX. It shows the room temperature magnetization curve of PEG-PIONs/DOX where the magnetization curve demonstrates superparamagnetic behavior of these particles due to zero coercivity [Ling *et al.*2011]. Usually, particles exhibit such properties when the core size is sufficiently small (around 15 nm) [A. K. Gupta and Gupta 2005]. The small size is useful in drug delivery, as they do not retain magnetization before and after exposure to an external magnetic field, reducing the probability of particle aggregation in the smallest capillaries due to their magnetic dipole attraction. PEG-PIONs/DOX exhibited relatively high saturation magnetization values at high fields (around 30 emu/g at 40 kOe), where they approach to the saturation value and comparable to those previously reported [Maver *et al.*2009; Kayal and Ramanujan 2010].
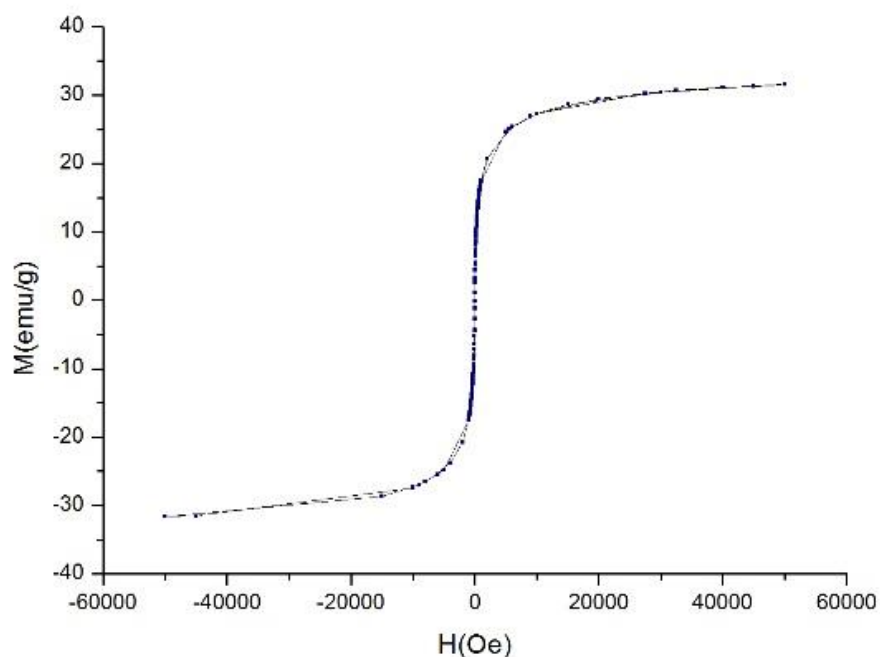
Figure 18. Magnetic properties of PEG-PIONs/DOX

The other very useful, simple and accurate method to examine magnetic properties of SPIONs is EPR technique. The EPR spectra of PEG-PIONs and PEG-PIONs/DOX recorded at different temperatures and angles are shown in **Figures 19 – 26.** Typical EPR spectrum of these NPs is represented by a broad line assigned to the magnetite. As the temperature decreased the linewidth become broadened and its position shifted towards lower magnetic fields. This observed behavior is typical for superparamagnetic materials [Finotelli *et al.*2004; Goikolea *et al.*2007].
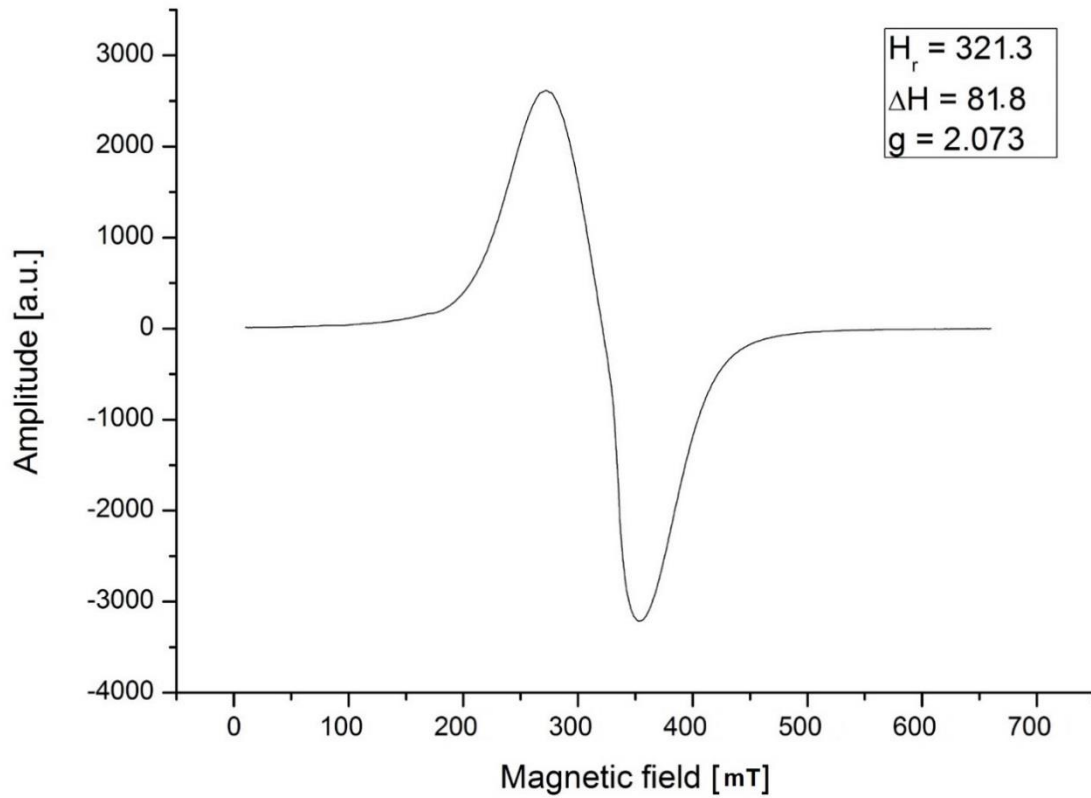
57

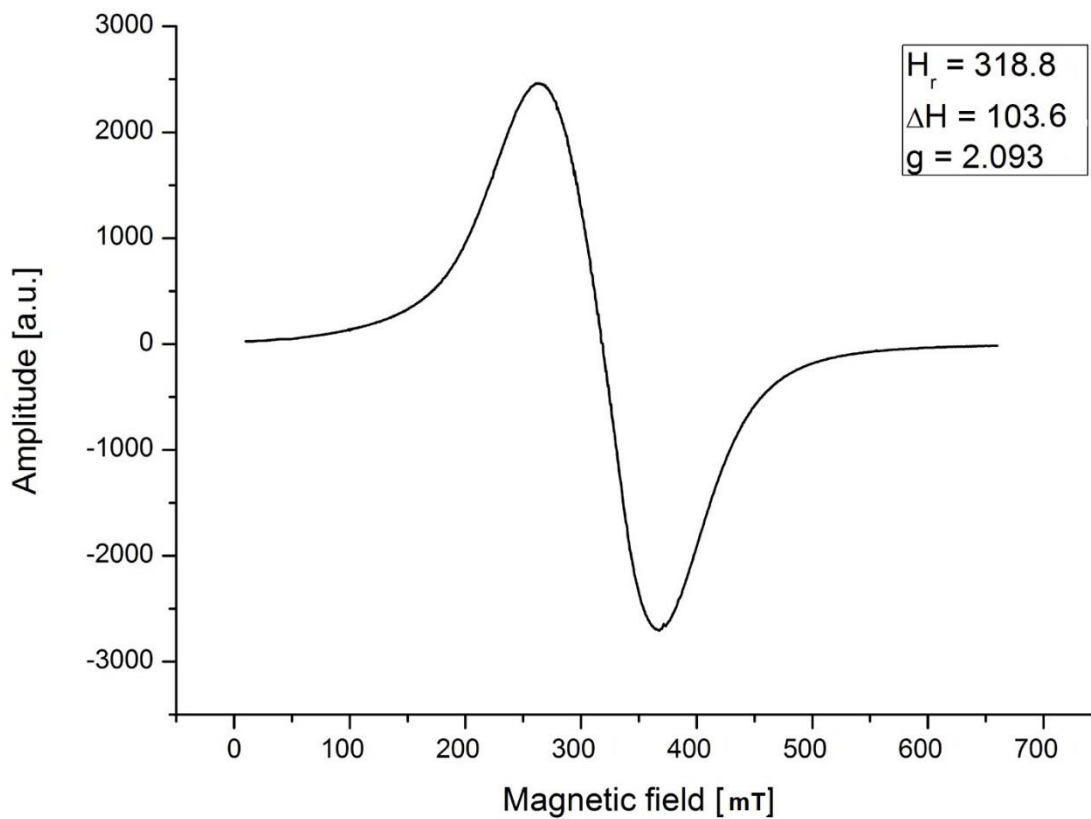Figure 19. EPR spectra of PEG-PIONs/DOX recorded at 130 K and at 0º angle.

Figure 20. EPR spectra of PEG-PIONs/DOX recorded at 130 K and at 90º angle.

Figure 21. EPR spectra of PEG-PIONs/DOX recorded at 250 K and at 0º angle.

Figure 22. EPR spectra of PEG-PIONs/DOX recorded at 250 K and at 90º angle.

Figure 23. EPR spectra of PEG-PIONs recorded at 130 K and at 0º angle.

Figure 24. EPR spectra of PEG-PIONs recorded at 130 K and at 90º angle.
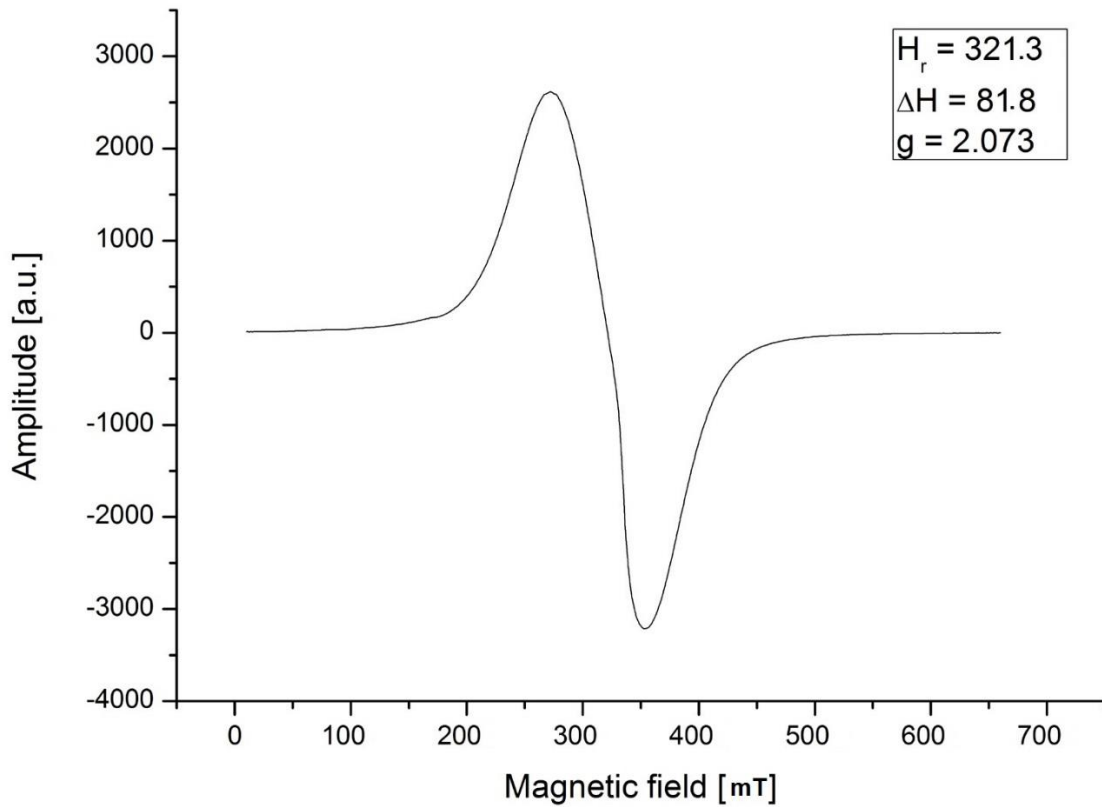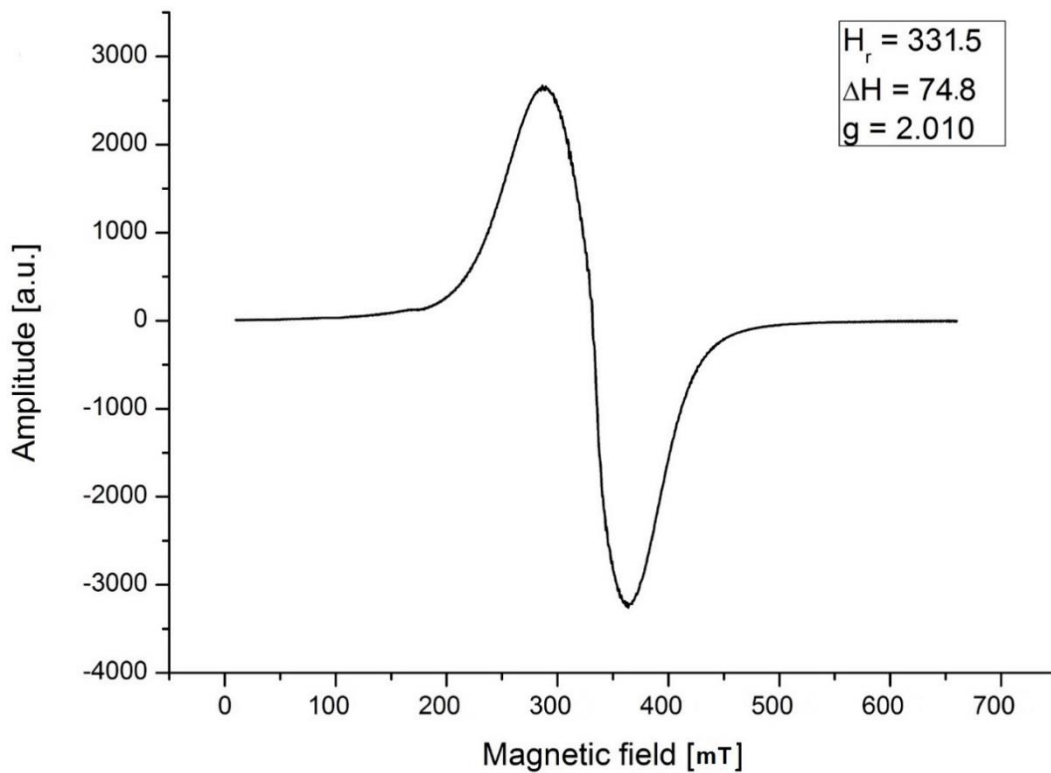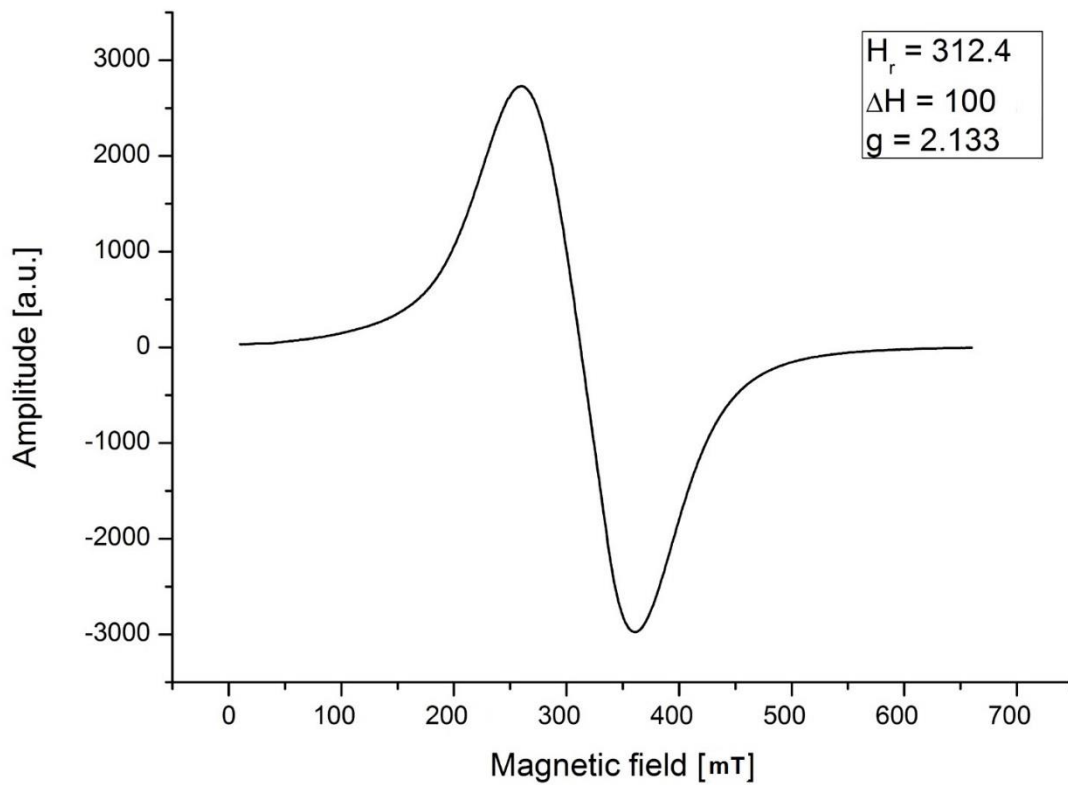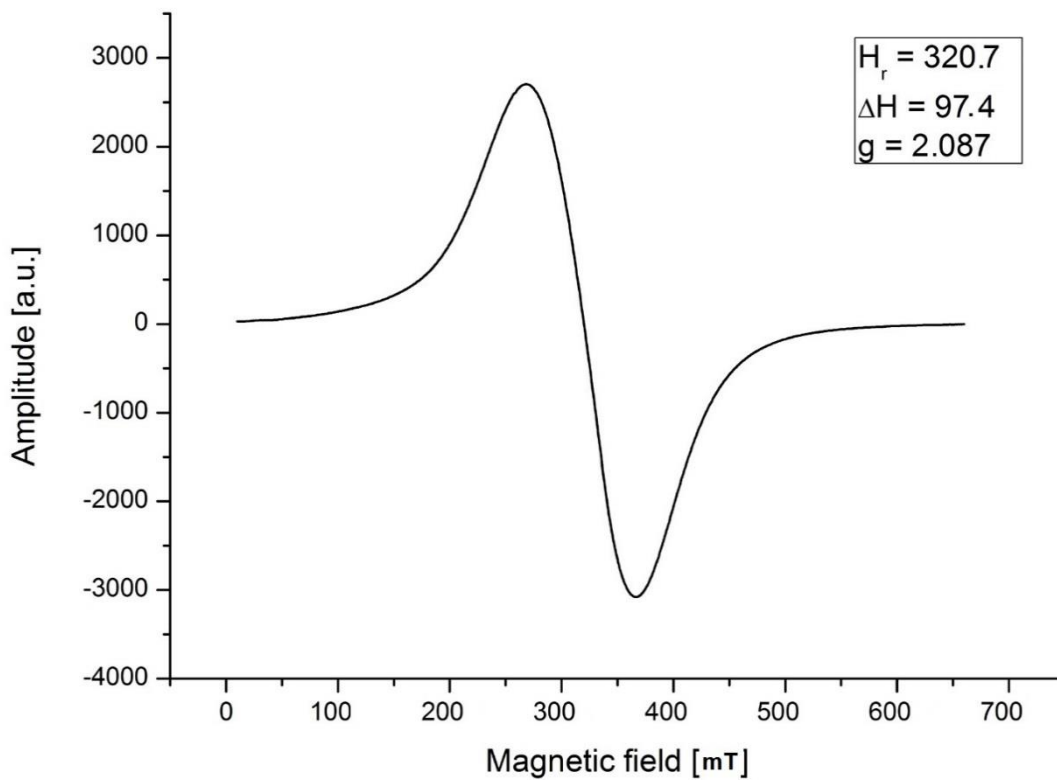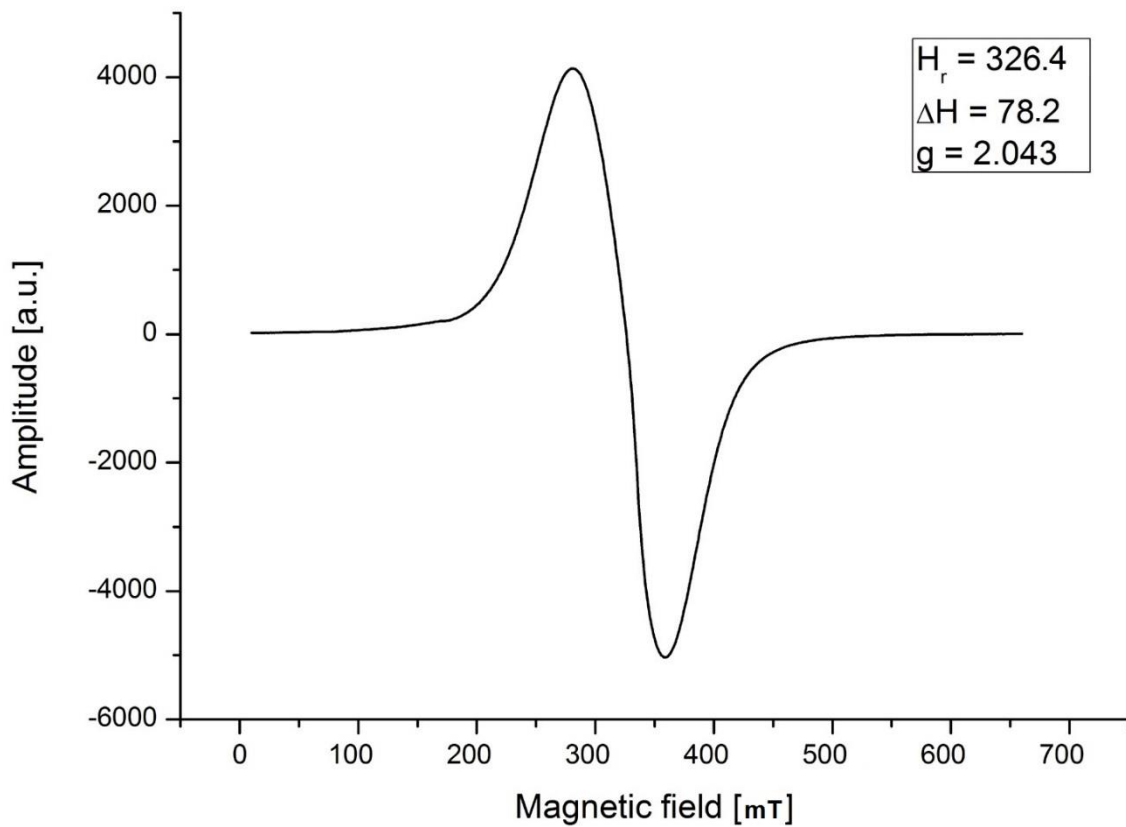
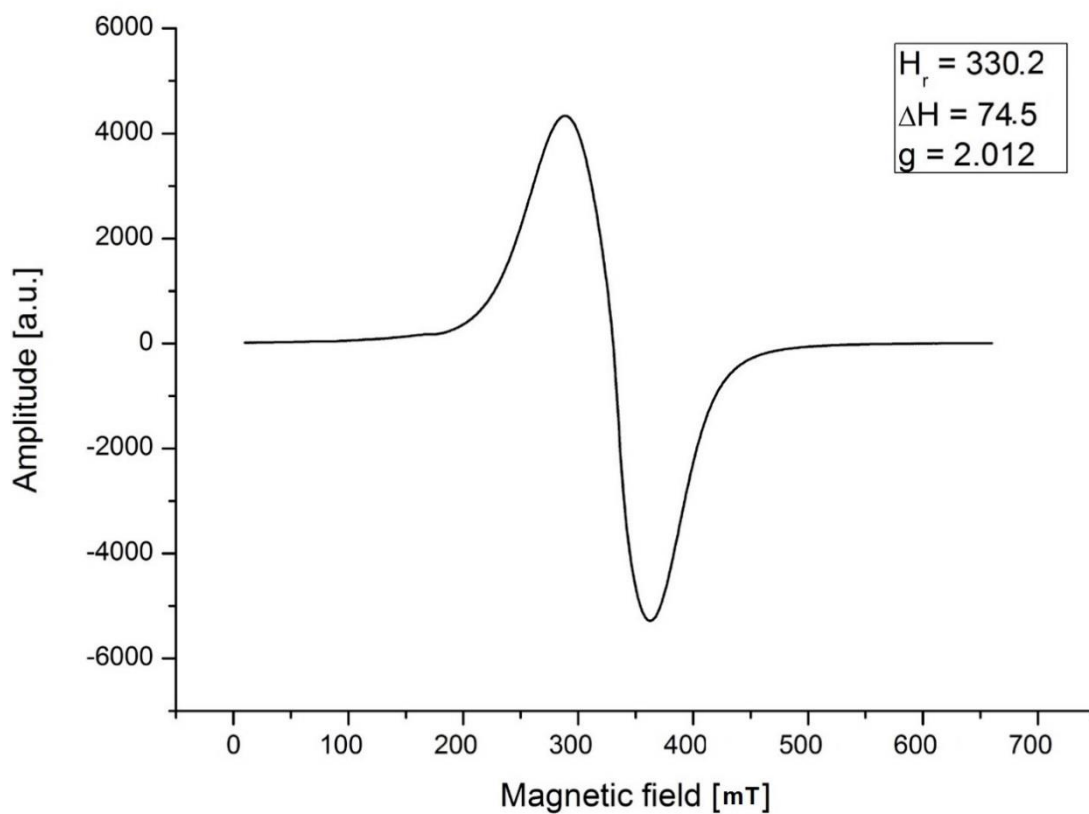Figure 25. EPR spectra of PEG-PIONs recorded at 250 K and at 0º angle.

Figure 26. EPR spectra of PEG-PIONs recorded at 250 K and at 90º angle.

Characteristic spectroscopic parameters such as resonance field (H_r), g-factor value and peak-to-peak line width (ΔH) were determined for the EPR spectra recorded at different temperatures, under both 0º and 90º angles. The measurement uncertainty were respectively $\pm$ 1.2 mT for H_r, $\pm$ 0.003 for g-factor and $\pm$ 0.6 mT for ΔH. Figures 27 - 29 shows the temperature and angular changes of those parameters. With increasing temperature the wide line was shifted towards higher values of the resonance field (H_r) (Fig. 27). The opposite temperature dependence was observed for g-factor (Fig. 28). The peak-to-peak line width (ΔH) decreased with increasing temperature (Fig. 29), which is typical for superparamagnetic NPs [Berger Bissey, Kliava, and Estourn 2001]. The particular difference between PEG-PIONs and PEG-PIONs/DOX sample for angle 0º was observed (Table 2). Smaller changes of resonance field for PEG-PIONs than for PEG-PIONs/DOX were caused by the rotation of the sample at an angle of 0º and it testified that DOX incorporation onto NPs surface causes easier ordering of the sample in the external magnetic field. Higher value of g-factor for PEG-PIONs/DOX in comparison to PEG-PIONs indicates increased anisotropic field and higher effective anisotropy field coefficient for PEG-PIONs/DOX [Figueiredo *et al.*2008]. Similarly, there is higher difference in H_r values for 0º and 90º for PEG-PIONs/DOX than PEG-PIONs [Fig. 26, Table 2] which testifies increased anisotropic field and higher effective anisotropy field coefficient for PEG-PIONs/DOX. Taking into consideration the above results, and the fact that concentration and size distribution of NPs in both samples are very similar, it can be hypothesized that the alterations in EPR parameters may be due to some minor changes in the subsurface area of NPs (e.g. slight oxidation process in subsurface area of PEG-PIONs, which are not additionally stabilized by DOX molecules).

Table 2. The EPR data for PEG-PIONs *vs*. PEG-PIONs/DOX recorded at 250 K at 0º and 90º angle.

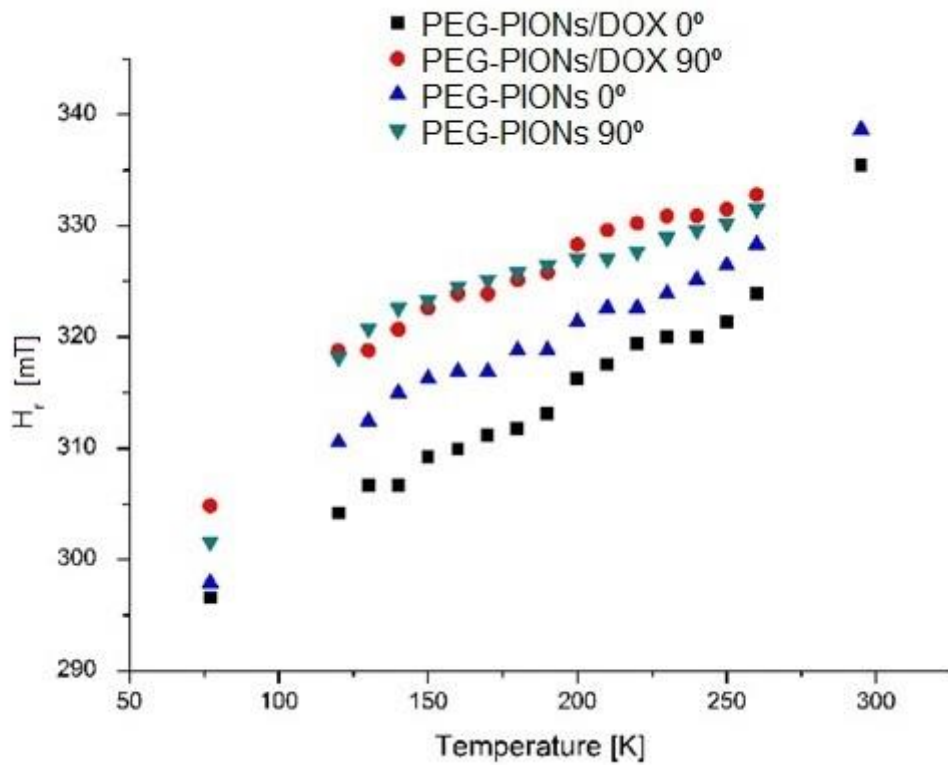|	Angle 0º PEG-PIONs/DOX	Angle 90º PEG-PIONs/DOX	Angle 0º PEG-PIONs	Angle 90º PEG-PIONs
H_r [mT]	321.3	331.5	326.4	330.2
ΔH [mT]	81.8	74.8	78.2	74.5

Figure 27. Changes of resonance field (H_r) versus angle and temperature for PEG-PIONs and PEG-PIONs/DOX.
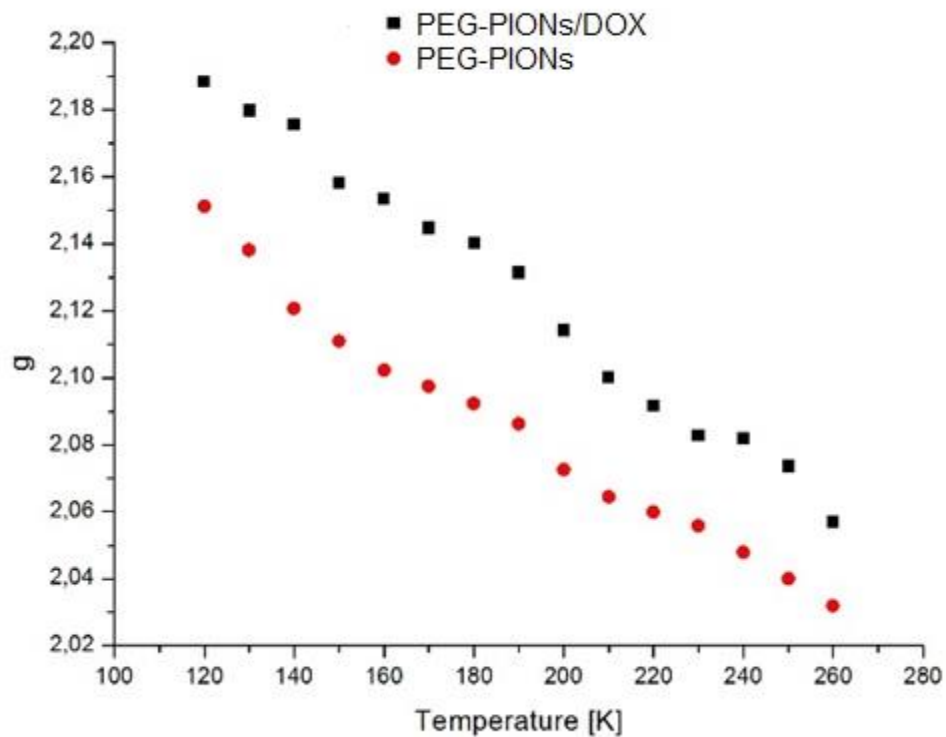

Figure 28. Changes of g-factor versus temperature for PEG-PIONs and PEG-PIONs/DOX.
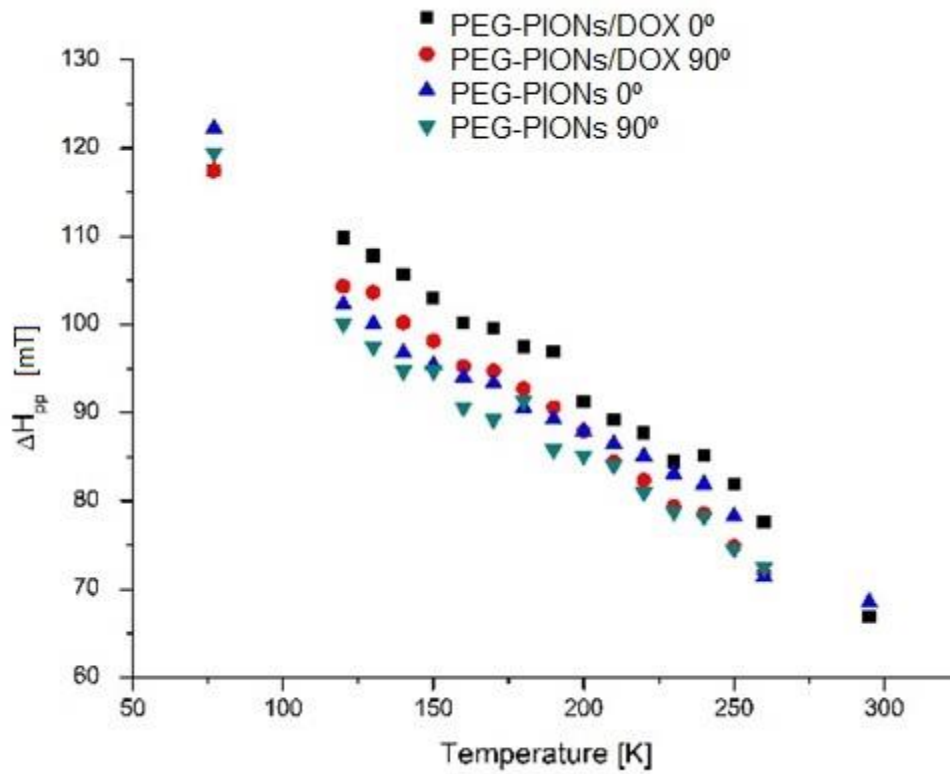
Figure 29. Changes of peak-to-peak line width (ΔH) versus angle and temperature for PEG-PIONs and PEG-PIONs/DOX.

From the line shape analysis it was possible to determine the magnetocrystalline anisotropic constant of first order K_1, following a method described in the literature [Gamarra et al. 2009]. This value is related to structure and size of NPs, and their modifications including functionalization can influence its value. K_1 was determined by using the relations $K_1 = H_a \times M_S / 2$, where $H_a = 3/5\Delta H$. M_S is the saturation magnetization of PEG-PIONs/DOX at 40kOe ($\sim$ 30 emu/g) obtained from SQUID studies and the H_a value was obtained from the field separation between the wing positions of H_{max} and H_{min}, as shown in figures 30 - 33. For K_1 of PEG-PIONs calculation, M_S for PEG-PIONs/DOX was taken. The K_1 value for PEG-PIONs/DOX at 140K was $K_1 = 9.5 \times 10^3$ erg cm^{-3} and at room temperature was $K_1 = 7.1 \times 10^3$ erg cm^{-3}. The K_1 value for PEG-PIONs at 140K was $K_1 = 8.7 \times 10^3$ erg cm^{-3} and at room temperature was $K_1 = 6.3 \times 10^3$ erg cm^{-3}. The determined magnetocrystalline anisotropic constant increased with decrease of temperature and was higher for PEG-PIONs/DOX, which can indicate some minor changes in the subsurface area of NPs related to their functionalization.

Figure 30. EPR spectrum of PEG-PIONs/DOX at 140K.

Figure 31. EPR spectrum of PEG-PIONs/DOX at room temperature.

Figure 32. EPR spectrum of PEG-PIONs at 140K.

Figure 33. EPR spectrum of PEG-PIONs at room temperature.
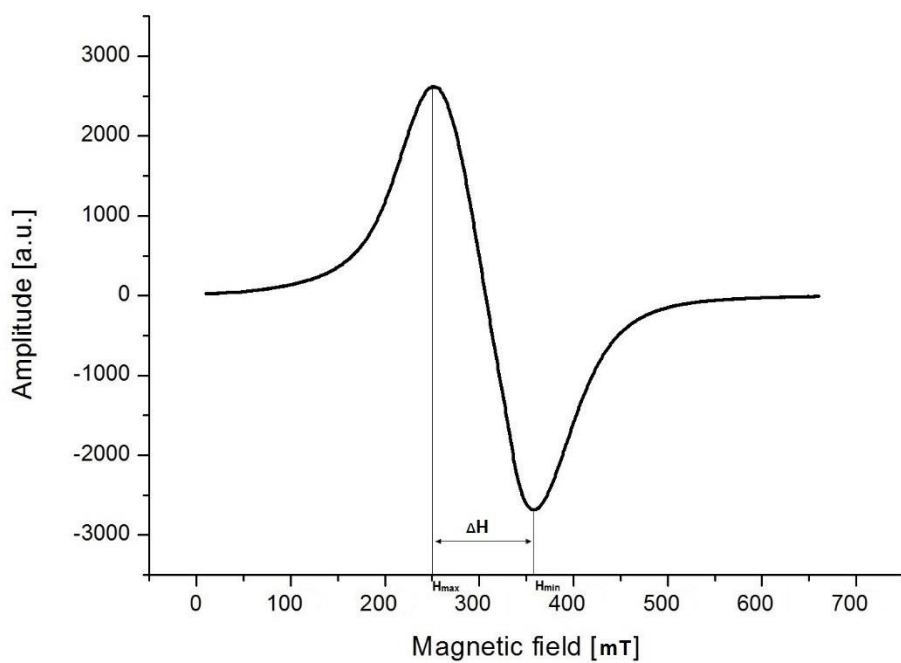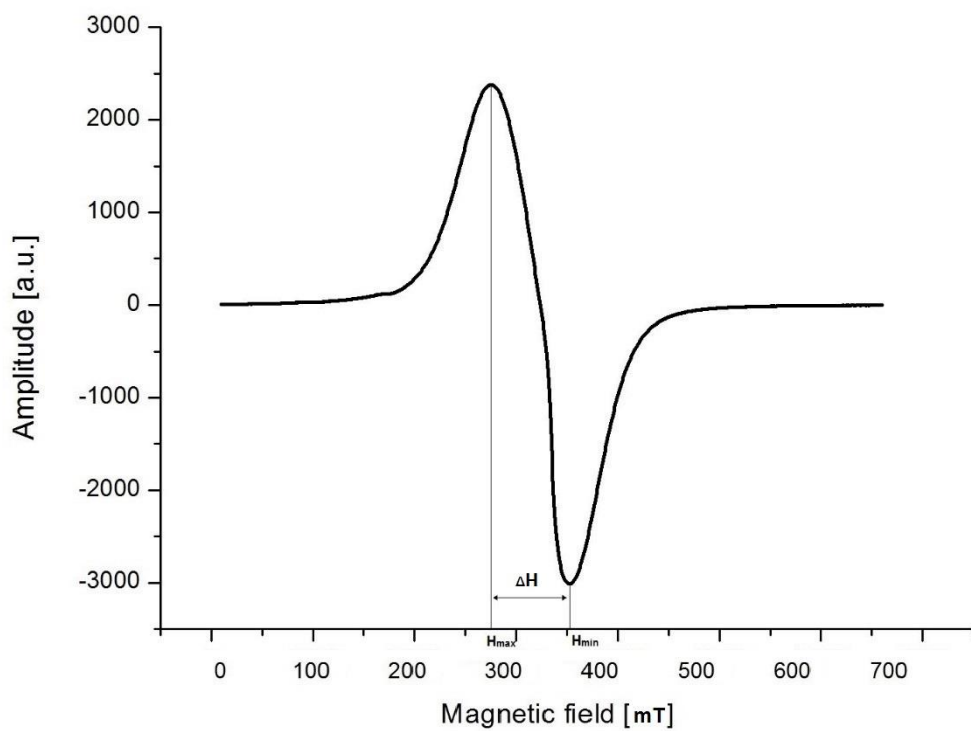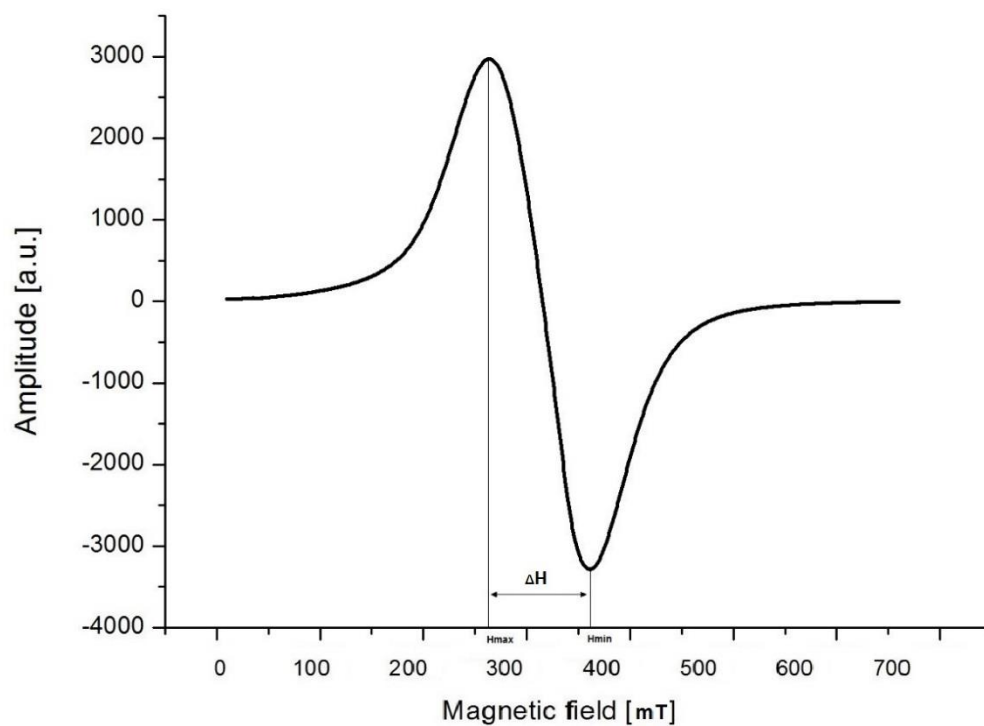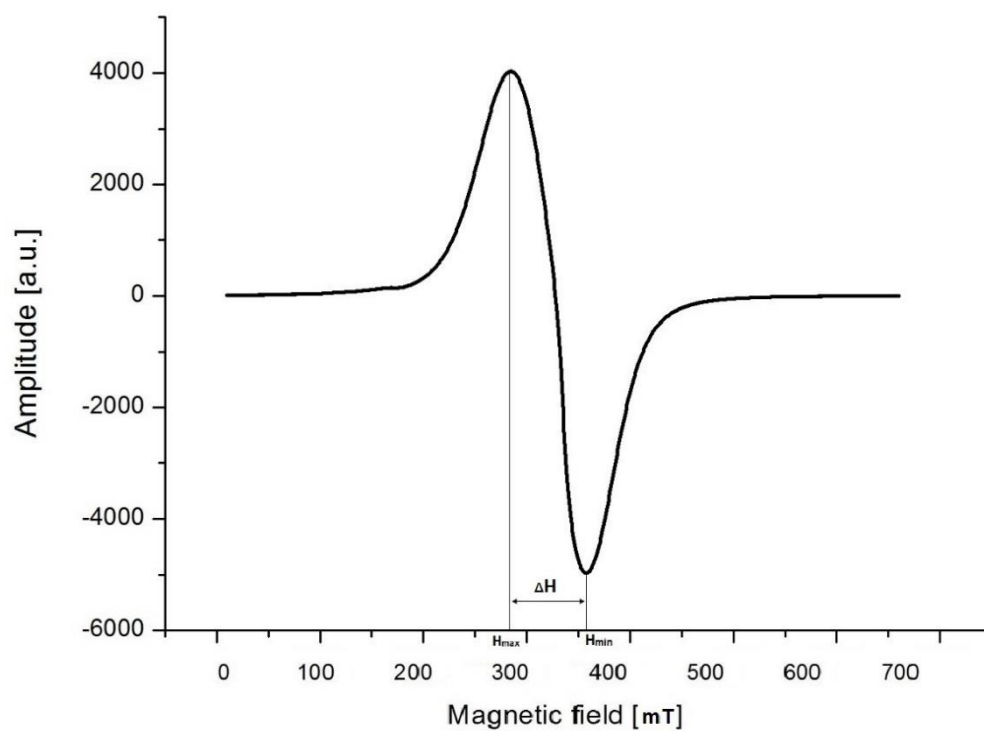
3.3. In vitro studies

3.3.1. DOX release profile

NPs designed for *in vivo* applications are coated by different surface agents such as e.g. polymers, which release the drug molecules by controlled diffusion or erosion from the core surface across the polymeric membrane or matrix. The membrane coating acts as a barrier to release, thus the diffusivity and solubility of the active substance in polymer coating becomes crucial in drug release. Release profile can be also affected by ionic interaction between the drug and additional ingredients. When drug interacts with some auxiliary molecules to form a less soluble complex in water, then its drug release profile can be very slow without burst effect [Y. Chen, Mcculloch, and Gray 1994]. It was reported previously that pH of tumor microenvironment is shifted to acidic region [Kievit *et al.*2011; Yang *et al.*2011]. PEG-PIONs/DOX were incubated at different pH media to examine drug release under conditions likely encountered following NPs tumor uptake and intracellular sequestration. The pH levels chosen replicated that found in the blood (pH 7.4), as well as the acidity characteristic of the tumor microenvironment (pH 5.7). DOX release behavior was examined in dark at a temperature of 37 °C to mimic the conditions of body fluids. It was assumed that DOX release would be faster at mildly acidic pH values than at neutral pH as a consequence of weakened binding between drug substance and the partially neutralized phosphonate groups in block copolymer coating. At both pH conditions, no burst effect was observed. As expected, the release rate of DOX (Figure 34) was higher at pH 5.7 than at pH 7.4 (approximately 20% and 10%, respectively). The shape of the release profile indicated that the complete release of the drug reached plateau only at neutral condition and DOX molecules were released slowly over a period of 96 h at lower pH. It can be noted that free DOX solution (taken as a control) was immediately released from dialysis membrane at both pH. These data imply that the physically bound drug molecules could be faster and continuously released in the mild acidic environments than at physiologically neutral pH of blood in the vascular compartment. This phenomenon could be explained by the fact that at a lower pH, the release of drug molecules was controlled by diffusion of the DOX through the PEG-*b*-PVBP polymer. The release of the active substance could be attributed to the weakening of the electrostatic interactions between the drug and the partially neutralized phosphonate groups of the polymer, because at acidic conditions, ~45-55% of phosphonate groups of PVBP chains in the PEG-PIONs/DOX are protonated [Kamimura *et al.* 2012]. However, weakening of the electrostatic interactions is a slow process, which leads

to the continuous release of DOX over a period of 96 h. Slower release in the tumor site may continue the chemotherapeutic effect and therefore increase the efficacy of anticancer therapy. This accelerated release of DOX at pH 5.7 will be particularly of benefit to anticancer therapy because of more acidic environment in tumor tissues. NPs tend to accumulate in tumor region gradually *via* the EPR effect and achieve a maximum concentration after several hours. These results indicate that the DOX could be released in substantial amounts in the acidic tumor region. Slow DOX release rate from PEG-PIONs/DOX can reflect its better stability and strong interaction between nanocarrier and drug molecules.
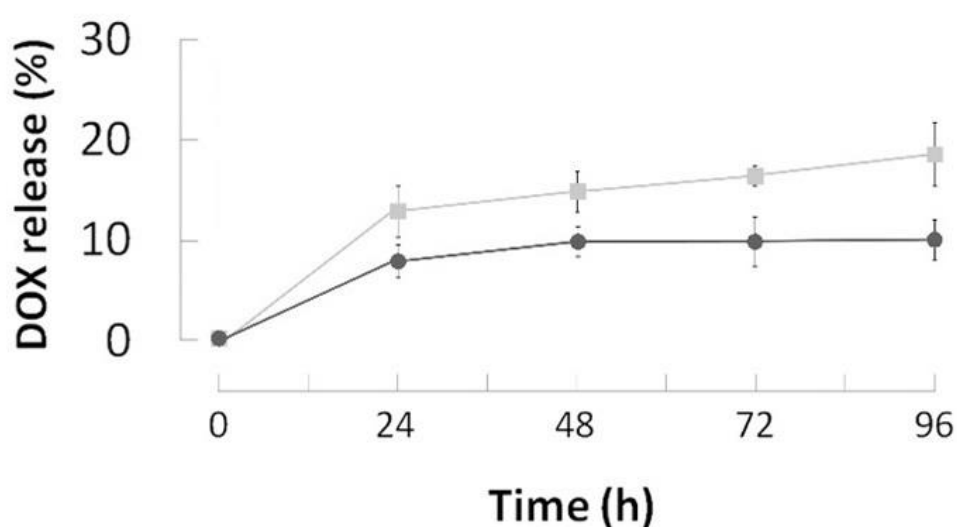
Figure 34. DOX release profile from PEG-PIONs/DOX at pH 5.7 (solid square ■) and pH 7.4 (solid circle ●) buffer solution at 37 °C.

3.3.2. Cell culture and *in vitro* cytotoxicity assay

The *in vitro* antiproliferative effect on cancer cells (C-26 cell line) of the PEG-PIONs/DOX in comparison to free DOX solution was evaluated using the MTT assay. Cells were incubated in the presence of different drug formulations at DOX concentrations from 1 to 50 μM for 24 h and 72 h. These doses for cytotoxic effect were confirmed on the basis of previous studies with DOX on cancer cell lines [S. Park *et al.*2012]. The cytotoxicity of PEG-PIONs/DOX and free DOX solutions (taken at the same drug concentration) was compared. PEG-PIONs (at Fe concentration of typical ion-based drug delivery systems for mice (1-15 mg

Fe mL^{-1})) showed minimal toxicity: cell viability was 98.1 % ± 1.3 and 97. 2 % ± 2.2 after 24 h and 72 h, respectively. The antiproliferative profiles, i.e., the cell viability after treatment for 24 and 72 h versus drug concentration are shown in Figure 35. Compared to free DOX solution, DOX-incorporated PEG-PIONs showed lower cytotoxicity. The IC$_{50}$ values were determined to be 33.06 μM and 23.14 μM after 24 h and 25.3 μM and 14.1 μM after 72 h of incubation with PEG-PIONs/DOX and free DOX solution, respectively. It can be assumed that not all DOX was released from the PEG-PIONs/DOX because of electrostatic and hydrophobic interactions. Similar to that reported previously [Shkilnyy *et al.*2010; Gautier *et al.*2012; Yang *et al.*2011], the results of cytotoxicity assay showed that the cell viability decreased with an increase in the concentration of DOX nano-formulation. Nevertheless, DOX incorporated into PEG-PIONs surface showed lower toxicity against C-26 cancer cells than free DOX solution, which may suggest high stability of the PEG-PIONs/DOX complex even in cell cultivation media and thus may improve its accumulation tendency in the tumor *in vivo*.

	IC$_{50}$
PEG-PIONs/DOX	33,06
DOX	23,14

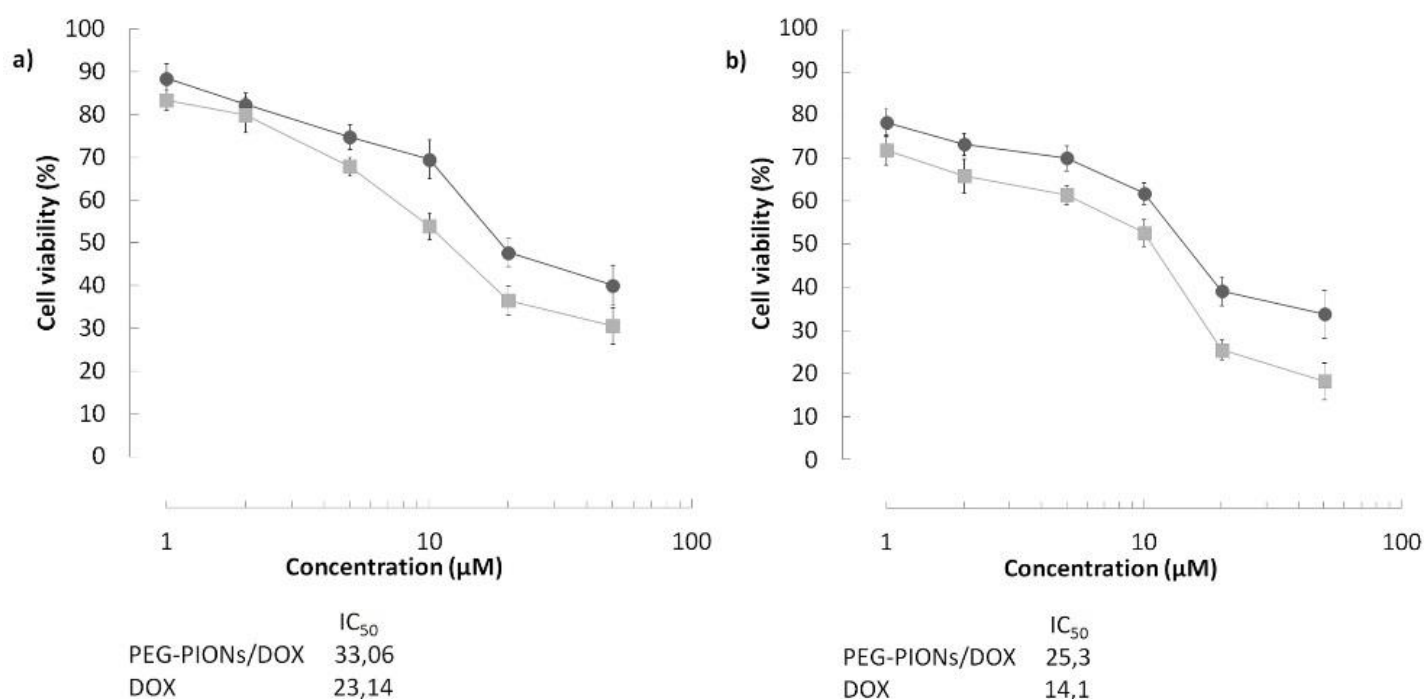|	IC$_{50}$
PEG-PIONs/DOX	25,3
DOX	14,1

Figure 35. Cell viability of C-26 cells incubated with various concentrations of PEG-PIONs/DOX (solid circle ●) and free DOX (solid square ▪) measured by MTT assay after 24 h (a) and 72 h (b) of incubation.

3.3.3. DOX subcellular distribution (Fluorescence imaging)

The magnetic NPs can be targeted to tumor tissue by the EPR effect, appropriate surface modification (targeting ligands attached) and external magnetic field. The internalization ability of magnetic nanocarriers into cancer cells is a crucial factor to reach optimal curative effect of drug, due to the fact that DOX exerts its effect in the nucleus [Ying *et al.*2011]. If the drug is covalently attached to NPs it could need specific enzymes in lysosomes to trigger its release and the whole particle has to enter the cell. However, in the case of physical interaction, simple diffusion through the polymer can be sufficient to desorb drug from the particle [Douziech-Eyrolles *et al.*2007]. The cellular uptake ability of synthesized NPs was examined using CLSM. In this study, the fluorescence signal from PEG-PIONs/DOX allowed us to follow the intracellular DOX release in C-26 cell line used as a model tumor cell. As anticipated, after 24 h of incubation (Figure 36) with free DOX, the drug was primarily present in the nucleus and in the cytoplasm, with small regions of punctuated accumulation in cellular compartments. In contrast, after 24 h of incubation with DOX conjugated to PEG-PIONs/DOX, the active substance was mainly localized in subcellular vesicles or organelles within the cytoplasm and only small amounts were present in the nucleus. However, after 72 h (Figure 37) of incubation with PEG-PIONs/DOX dispersion, the amount of released DOX very slightly increased, which is consistent with the drug release profile, but the drug molecules shifted into the nucleus in significant amount, where DOX can exhibit its mechanism of action. These results may indicate that free and conjugated DOX use different uptake mechanisms, suggesting that the conjugated DOX was taken up by endocytosis [Laurent et al. 2008; Singh et al. 2010]. The above results may also indicate that the active substance is released from PEG-PIONs/DOX in the endocytic compartments at a slower and continuous rate than free DOX.
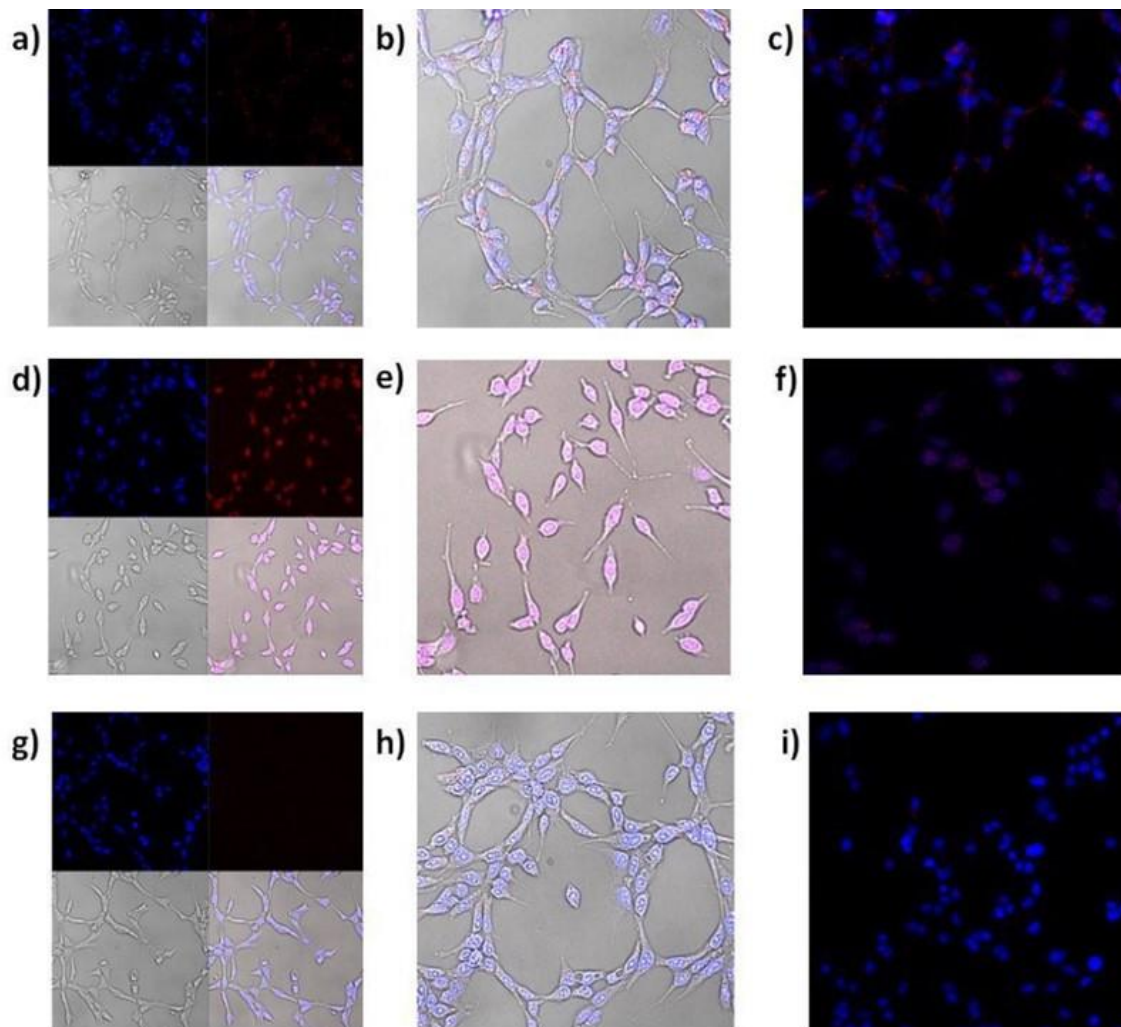
Figure 36. Fluorescent images of cells incubated with 25 μM DOX formulations (free cells as a control) for 24 h (a, b, c - PEG- PIONs/DOX; d, e, f - free DOX solution, g, h, i – cells in PBS). Nuclei are stained in Hoechst solution (blue), red is DOX distribution.
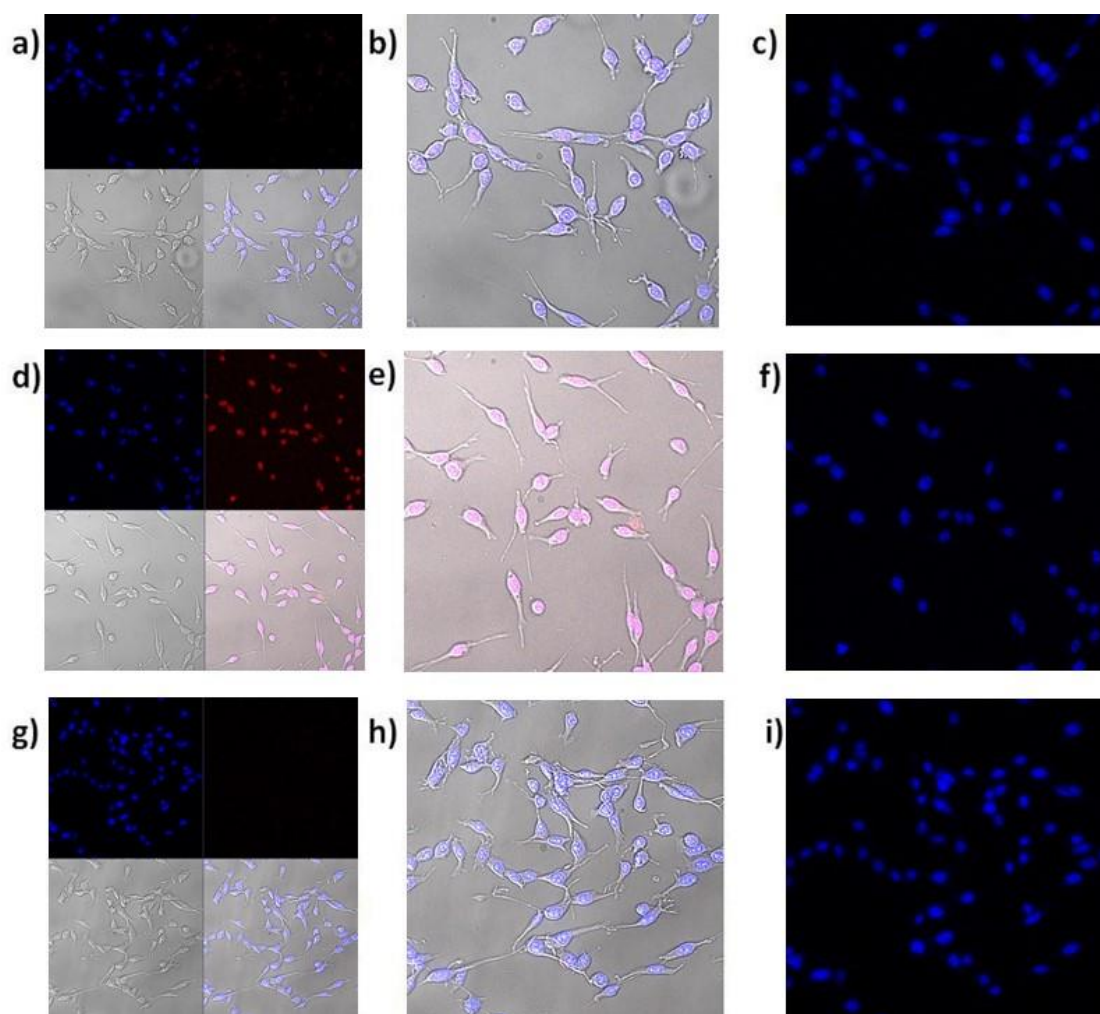
Figure 37. Fluorescent images of cells incubated with 25 μM DOX formulations (free cells as a control) for 72 h (a, b, c - PEG- PIONs/DOX; d, e, f - free DOX solution, g, h, i − cells in PBS). Nuclei are stained in Hoechst solution (blue), red is DOX distribution.

3.4. *In vivo* studies

The biodistribution of drug substance from nanocarrier was evaluated in animal mice model in comparison with free drug solution. Free DOX solution and PEG-PIONs/DOX dispersion at the equivalent DOX dose of 10 or 20 mg/kg body weight, as well as saline as a control group were intravenously administered to tumor-bearing BALB/c mice. The major organs were collected and extracted for the DOX measurements after 24 h and 36 h. A simplified rapid extraction procedure was developed and optimized to identify and quantify DOX levels in the tissue extracts using LC-MS method. Compared to the free drug, PEG-PIONs/DOX significantly increased drug accumulation into the tumor region (Figure 38). The

preferential uptake of DOX formulation is likely due to the prolonged circulation and EPR effect [Rosen *et al.*2012; Hiroshi Maeda 2001]. Drug delivery nanocarriers increase the intratumoral drug concentration mainly because of their nanometer size. The leaky fenestrations of the neovasculature system in the tumor damaged tumor vasculature, poorly developed and inefficient lymphatic drainage enable extravasation and accumulation of such small objects. This results in accumulation of NPs for a prolonged period of time. Our biodistribution studies showed preferential accumulation of PEG-PIONs/DOX in the tumor tissue. Furthermore, it was noted that DOX nanoparticulate formulation reduced significant amounts of drug distribution into the heart compared with free DOX solution, which may lower DOX-associated cardiotoxicity. In addition, the toxicity in all mice was monitored by serum chemistry examinations (Figure 39, 40), including hepatic and renal panels as well as cardiac enzymes (AST, BUN, LDH, and CK). The hepatic and renal function tests indicated that AST and BUN levels did not change significantly in all groups compared to those in the control group. Serum CK and LDH levels are two well-characterized markers for cellular damage in a variety of cardiac disease models. Importantly, encapsulation of DOX onto PEG-PIONs/DOX nanocarrier was found to decrease the cardiotoxicity compared with free drug. The induction of CK and LDH enzymes in the serum of mice treated with free DOX solution was significantly increased, compared with untreated mice. However, when mice were treated with PEG-PIONs/DOX, both serum CK and LDH levels were not significantly different from saline control group. The decreased cardiotoxicity of PEG-PIONs/DOX formulations can be attributed to the reduced uptake in the heart as demonstrated in the above *in vivo* biodistribution studies. These results may indicate that PEG-PIONs/DOX have the potential for their application in targeted delivery of antitumor drugs.
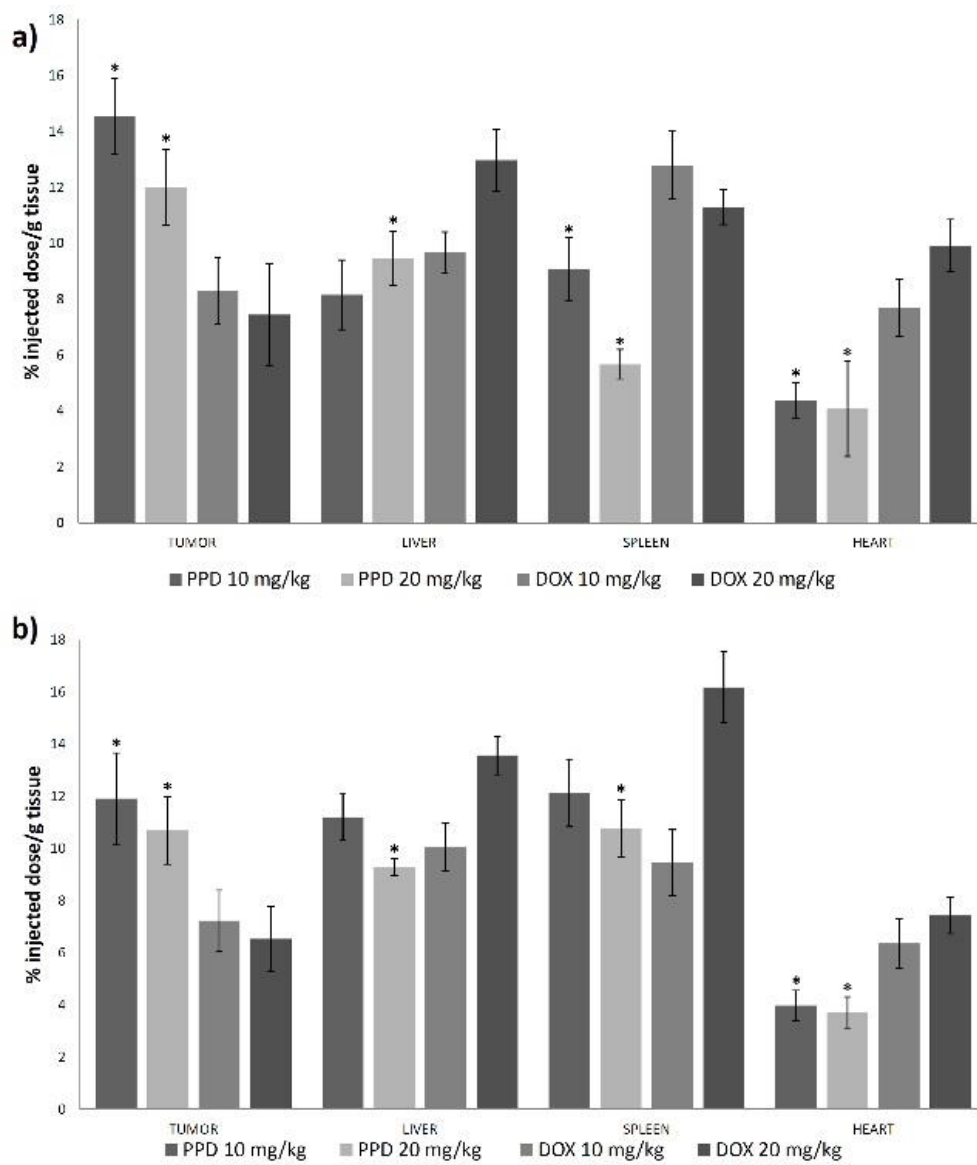
Figure 38. The biodistribution data of PEG-PIONs/DOX (PPD) and free DOX solution (DOX) at the dose of 10 and 20 mg/kg mice after 24 h (a) and 36 h (b) of intravenous injection compared to saline (control group). Values are expressed as ± SEM. * $P < 0.05$ as compared PEG-PIONs/DOX with free DOX solution (10 and 20 mg/kg respectively).
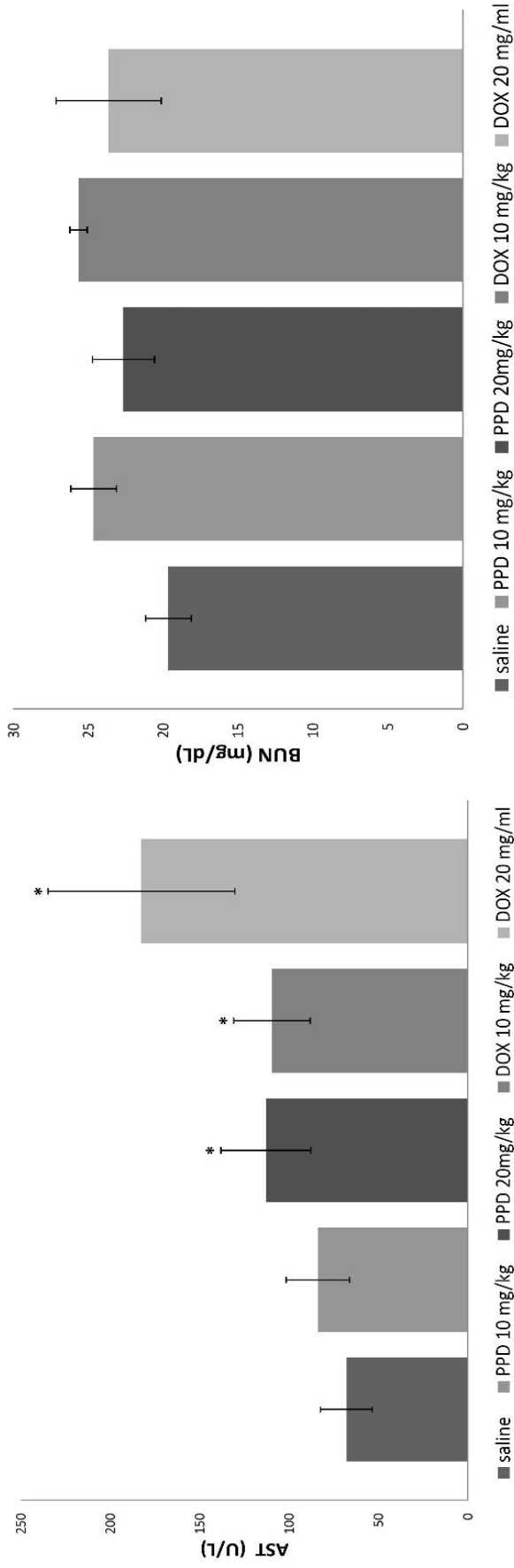
Figure 39. Aspartate aminotransferase (AST) and blood urea nitrogen (BUN) after 24 h of different DOX formulations intravenous injection (saline, PEG-PIONs/DOX (PPD) and free DOX solution (DOX)). Values are expressed as $\pm$ SEM. * $P < 0.05$ as compared to saline.
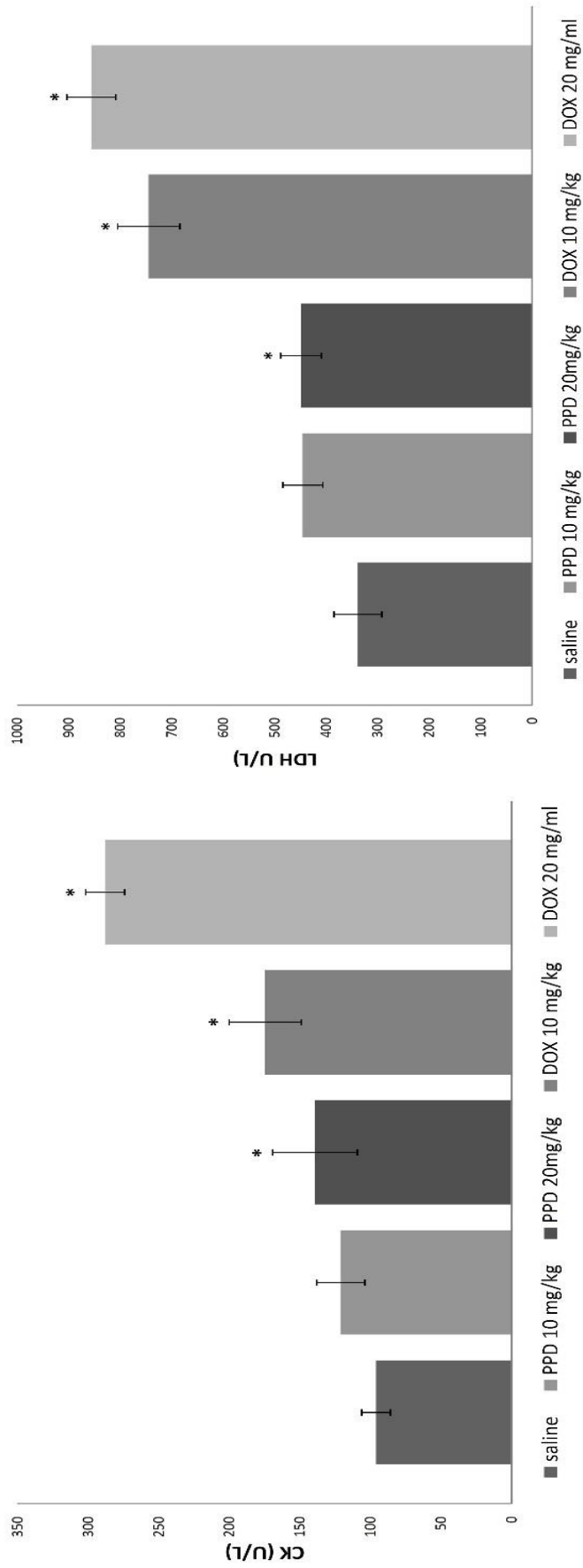
Figure 40. Serum creatine kinase (CK) and lactate dehydrogenase (LDH) after 24 h of different DOX formulations intravenous injection (saline, PEG-PIONs/DOX (PPD) and free DOX solution (DOX)). Values are expressed as ± SEM. * $P < 0.05$ as compared to saline.

4. Conclusions

The main objective of this work was to design a stable, biocompatible and injectable nanocarrier with antiproliferative effect on cancer cells and high drug encapsulation efficiency. The synthesis, functionalization of prepared nanosystem and detailed characterization of PEG-PIONs/DOX enabled to prove the usefulness of the nanocarrier as a potential targeted drug delivery system. Hereafter, several most important conclusions are highlighted.

1. PEG-PIONs/DOX were successfully synthesized by appropriately optimized alkali co-precipitation method with original polymer PEG-derivative and the anticancer agent. Several techniques were used to test the quality of as-synthesized NPs.

2. PEG-PIONs/DOX showed nearly spherical shape and uniform size distribution with the narrow range of 8 – 12 nm.

3. Synthesized NPs showed very high efficacy of DOX loading, relatively higher compared to that previously reported.

4. The magnetic properties of obtained material was tested by several methods. SQUID magnetization curve demonstrated superparamagnetic behavior of PEG-PIONs/DOX. The presence of sharp and intense peaks obtained by XRD studies confirmed the formation of highly crystalline Fe_3O_4 NPs.

5. The EPR temperature measurements demonstrated the superparamagnetic nature of PEG-PIONs/DOX and magnetite structure of their cores. The alterations in magnetocrystalline anisotropic coefficient (K_1) may indicate the surface changes of synthesized PEG-PIONs/DOX related to their functionalization and modification. The higher value of K_1 indicates that the lower thickness of canted surface spins in the case of PEG-PIONs/DOX.

6. Prepared nanocarriers demonstrated excellent stability in dispersions mimicking physiological conditions with hydrodynamic diameter in the range of ~ 28 – 36 nm.

7. The studies using size exclusion chromatography confirmed the formation of a complex between PEG-PIONs and DOX.

8. The *in vitro* studies of DOX release rate showed sustained and continuous drug release, which was higher at pH 5.7 than at pH 7.4. This accelerated release of DOX at pH 5.7 would be particularly of benefit to anticancer therapy because of more acidic environment in tumor tissues.

9. Fluorescence imaging studies showed that PEG-PIONs/DOX have been successfully used for the efficient delivery of an anticancer drug into the tumor region.

10. The *in vitro* cytotoxicity studies demonstrated the antiproliferative effect of PEG-PIONs/DOX on cancer cells, as a result of slowly released drug from synthesized nanosystem. DOX incorporated into PEG-PIONs showed lower toxicity against cancer cells than free DOX solution.

11. The performed *in vivo* biodistribution studies showed that the uptake of PEG-PIONs/DOX in the tumor tissue was greater than that of an equivalent dose of DOX in BALB/c tumor-bearing mice. The serum chemistry examinations were also monitored and proved that the DOX-associated cardiotoxicity was significantly reduced.

Based on the obtained results, it can be concluded that PEG-PIONs/DOX are promising magnetic drug carriers to be used in biomedical applications. Taking into consideration that even without external magnetic field PEG-PIONs/DOX easily accumulate in tumor region, one may predict its high efficacy in future therapy, avoiding side effects of low-molecular weight anticancer drugs like DOX, which frequently causes severe cardiotoxicity. The developed material may be used in the future as a potential drug delivery system of anticancer agents in targeted antitumor therapy.

5. References

Aljarrah, Khaled, Nizar M Mhaidat, M-Ali H Al-Akhras, Ahmad N Aldaher, Ba Albiss, Khaled Aledealat, and Fawzi M Alsheyab. 2012. "Magnetic Nanoparticles Sensitize MCF-7 Breast Cancer Cells to Doxorubicin-Induced Apoptosis." *World Journal of Surgical Oncology* 10: 62. http://www.pubmedcentral.nih.gov/articlerender.fcgi?artid=3407771&tool=pmcentrez&rendertype=abstract.

Allard-Vannier, E, S Cohen-Jonathan, J Gautier, K Hervé-Aubert, E Munnier, M Soucé, P Legras, C Passirani, and I Chourpa. 2012. "Pegylated Magnetic Nanocarriers for Doxorubicin Delivery: A Quantitative Determination of Stealthiness in Vitro and in Vivo." *European Journal of Pharmaceutics and Biopharmaceutics : Official Journal of Arbeitsgemeinschaft Für Pharmazeutische Verfahrenstechnik e.V* 81 (3). Elsevier B.V.: 498–505. doi:10.1016/j.ejpb.2012.04.002.

Amara, Daniel, Israel Felner, Israel Nowik, and Shlomo Margel. 2009. "Synthesis and Characterization of Fe and Fe3O4 Nanoparticles by Thermal Decomposition of Triiron Dodecacarbonyl." *Colloids and Surfaces A: Physicochemical and Engineering Aspects* 339 (1-3): 106–10. doi:10.1016/j.colsurfa.2009.02.003.

Antosova, Zuzana, Martina Mackova, Vladimir Kral, and Tomas Macek. 2009. "Therapeutic Application of Peptides and Proteins: Parenteral Forever?" *Trends in Biotechnology* 27 (11): 628–35. doi:10.1016/j.tibtech.2009.07.009.

Anzai, Yoshimi, Catherine W Piccoli, Eric K Outwater, William Stanford, David A Bluemke, Pamela Nurenberg, Sanjay Saini, et al. 2003. "Radiology For the Group Evaluation of Neck and Body Metastases to Nodes with Ferumoxtran 10 – Enhanced MR Imaging : Phase III Safety and Efficacy Study 1," 5–10.

Arnold, Matthew M, Eric M Gorman, Loren J Schieber, Eric J Munson, and Cory Berkland. 2007. "NanoCipro Encapsulation in Monodisperse Large Porous PLGA Microparticles." *Journal of Controlled Release : Official Journal of the Controlled Release Society* 121 (1-2): 100–109. doi:10.1016/j.jconrel.2007.05.039.

Arya, Geetanjali, Mallaredy Vandana, Sarbari Acharya, and Sanjeeb K Sahoo. 2011. "Enhanced Antiproliferative Activity of Herceptin (HER2)-Conjugated Gemcitabine-Loaded Chitosan Nanoparticle in Pancreatic Cancer Therapy." *Nanomedicine : Nanotechnology, Biology, and Medicine* 7 (6). Elsevier Inc.: 859–70. doi:10.1016/j.nano.2011.03.009.

Berger Bissey, Jean-claude, Janis Kliava, and Claude Estourn. 2001. "Temperature Dependence of Superparamagnetic Resonance of Iron Oxide Nanoparticles." *Journal of Magnetism and Magnetic Materials* 234: 535–44.

Berry, Catherine C, Stuart Charles, Stephen Wells, Matthew J Dalby, and Adam S.G Curtis. 2004. "The Influence of Transferrin Stabilised Magnetic Nanoparticles on Human Dermal Fibroblasts in Culture." *International Journal of Pharmaceutics* 269 (1): 211–25. doi:10.1016/j.ijpharm.2003.09.042.

Berry, Catherine C., Stephen Wells, Stuart Charles, and Adam S.G. Curtis. 2003. "Dextran and Albumin Derivatised Iron Oxide Nanoparticles: Influence on Fibroblasts in Vitro." *Biomaterials* 24 (25): 4551–57. doi:10.1016/S0142-9612(03)00237-0.

Berry, Catherine Cecilia, Stephen Wells, Stuart Charles, Gregor Aitchison, and Adam S G Curtis. 2004. "Cell Response to Dextran-Derivatised Iron Oxide Nanoparticles Post Internalisation." *Biomaterials* 25 (23): 5405–13. doi:10.1016/j.biomaterials.2003.12.046.

Boutevin, Bernard, Yves Hervaud, Ahmed Boulahna, and El Mestafa El Hadrami. 2002. "Synthesis of Phosphonated Styrenic Copolymers and Their Chemical Modifications." *Polymer International* 51 (5): 450–57. doi:10.1002/pi.890.

Brannon-Peppas, Lisa, and James O. Blanchette. 2012. "Nanoparticle and Targeted Systems for Cancer Therapy." *Advanced Drug Delivery Reviews* 64 (December). Elsevier B.V.: 206–12. doi:10.1016/j.addr.2012.09.033.

Brunner, Tobias J., Peter Wick, Pius Manser, Philipp Spohn, Robert N. Grass, Ludwig K. Limbach, Arie Bruinink, and Wendelin J. Stark. 2006. "In Vitro Cytotoxicity of Oxide Nanoparticles: Comparison to Asbestos, Silica, and the Effect of Particle Solubility †." *Environmental Science & Technology* 40 (14): 4374–81. doi:10.1021/es052069i.

Bulte, Jeff W M, Trevor Douglas, Brian Witwer, Su-chun Zhang, Erica Strable, Bobbi K Lewis, Holly Zywicke, et al. 2001. "Magnetodendrimers Allow Endosomal Magnetic Labeling and in Vivo Tracking of Stem Cells." *Nature Biotechnology* 19 (December): 1141–47.

Burda, Clemens, Xiaobo Chen, Radha Narayanan, and Mostafa a El-Sayed. 2005. *Chemistry and Properties of Nanocrystals of Different Shapes. Chemical Reviews*. Vol. 105. doi:10.1021/cr030063a.

Burden, D. Andrew, and Neil Osheroff. 1998. "Mechanism of Action of Eukaryotic Topoisomerase II and Drugs Targeted to the Enzyme." *Biochimica et Biophysica Acta - Gene Structure and Expression* 1400: 139–54. doi:10.1016/S0167-4781(98)00132-8.

Butoescu, Nicoleta, Christian a Seemayer, Michelangelo Foti, Olivier Jordan, and Eric Doelker. 2009. "Dexamethasone-Containing PLGA Superparamagnetic Microparticles as Carriers for the Local Treatment of Arthritis." *Biomaterials* 30 (9). Elsevier Ltd: 1772–80. doi:10.1016/j.biomaterials.2008.12.017.

Cao, Haining, Jiang He, Li Deng, and Xiaoqing Gao. 2009. "Fabrication of Cyclodextrin-Functionalized Superparamagnetic Fe3O4/amino-Silane Core–shell Nanoparticles via Layer-by-Layer Method." *Applied Surface Science* 255 (18): 7974–80. doi:10.1016/j.apsusc.2009.04.199.

Carpenter, Everett E. 2001. "Iron Nanoparticles as Potential Magnetic Carriers." *Journal of Magnetism and Magnetic Materials* 225 (1-2): 17–20. doi:10.1016/S0304-8853(00)01222-1.

Chakravarthi, Sudhir S, and Dennis H Robinson. 2011. "Enhanced Cellular Association of Paclitaxel Delivered in Chitosan-PLGA Particles." *International Journal of Pharmaceutics* 409 (1-2). Elsevier B.V.: 111–20. doi:10.1016/j.ijpharm.2011.02.034.

Chang, Yulei, Xinlei Meng, Yili Zhao, Kun Li, Bao Zhao, Ming Zhu, Yapeng Li, Xuesi Chen, and Jingyuan Wang. 2011. "Novel Water-Soluble and pH-Responsive Anticancer Drug Nanocarriers: Doxorubicin-PAMAM Dendrimer Conjugates Attached to Superparamagnetic Iron Oxide Nanoparticles (IONPs)." *Journal of Colloid and Interface Science* 363 (1). Elsevier Inc.: 403–9. doi:10.1016/j.jcis.2011.06.086.

Chen, Min, Saeki Yamamuro, Dorothy Farrell, and Sara a. Majetich. 2003. "Gold-Coated Iron Nanoparticles for Biomedical Applications." *Journal of Applied Physics* 93 (10): 7551. doi:10.1063/1.1555312.

Chen, Y, R Mcculloch, and B Gray. 1994. "Synthesis of Albumin-Dextran Sulfate Microspheres Possessing Favourable Loading and Release Characteristics for the Anticancer Drug Doxorubicin☆." *Journal of Controlled Release* 31: 49–54. doi:10.1016/0168-3659(94)90250-X.

Cheng, Ziyong, Yunlu Dai, Xiaojiao Kang, Chunxia Li, Shanshan Huang, Hongzhou Lian, Zhiyao Hou, Pingan Ma, and Jun Lin. 2014. "Gelatin-Encapsulated Iron Oxide Nanoparticles for Platinum (IV) Prodrug Delivery, Enzyme-Stimulated Release and MRI." *Biomaterials* 35 (24). Elsevier Ltd: 6359–68. doi:10.1016/j.biomaterials.2014.04.029.

Cheong, Su-Jin, Chang-Moon Lee, Se-Lim Kim, Hwan-Jeong Jeong, Eun-Mi Kim, Eun-Hye Park, Dong Wook Kim, Seok Tae Lim, and Myung-Hee Sohn. 2009. "Superparamagnetic Iron Oxide Nanoparticles-Loaded Chitosan-Linoleic Acid Nanoparticles as an Effective Hepatocyte-Targeted Gene Delivery System." *International Journal of Pharmaceutics* 372 (1-2): 169–76. doi:10.1016/j.ijpharm.2009.01.009.

Chertok, Beata, Bradford a Moffat, Allan E David, Faquan Yu, Christian Bergemann, Brian D Ross, and Victor C Yang. 2008. "Iron Oxide Nanoparticles as a Drug Delivery Vehicle for MRI Monitored Magnetic Targeting of Brain Tumors." *Biomaterials* 29 (4): 487–96. doi:10.1016/j.biomaterials.2007.08.050.

Chomoucka, Jana, Jana Drbohlavova, Dalibor Huska, Vojtech Adam, Rene Kizek, and Jaromir Hubalek. 2010. "Magnetic Nanoparticles and Targeted Drug Delivering." *Pharmacological Research : The Official Journal of the Italian Pharmacological Society* 62 (2). Elsevier Ltd: 144–49. doi:10.1016/j.phrs.2010.01.014.

Coey, and F L Wiesendanger. 1993. "Charge Freezing and Surface Anisotropy on Magnetite (100)." *Journal of Applied Physics* 73 (10): 6742–44.

Dang, Feng, Naoya Enomoto, Junichi Hojo, and Keiji Enpuku. 2010. "Synthesis of Monodispersed Cubic Magnetite Particles through the Addition of Small Amount of Fe3+ into Fe(OH)2 Suspension." *Journal of Crystal Growth* 312 (10). Elsevier: 1736–40. doi:10.1016/j.jcrysgro.2010.02.012.

Debrassi, Aline, Cristiani Bürger, Clóvis Antonio Rodrigues, Nataliya Nedelko, Anna Ślawska-Waniewska, Piotr Dłużewski, Kamil Sobczak, and Jean-Marc Greneche. 2011. "Synthesis, Characterization and in Vitro Drug Release of Magnetic N-Benzyl-O-Carboxymethylchitosan Nanoparticles Loaded with Indomethacin." *Acta Biomaterialia* 7 (8): 3078–85. doi:10.1016/j.actbio.2011.05.001.

Dobosz, Bernadeta, Ryszard Krzyminiewski, Grzegorz Schroeder, and Joanna Kurczewska. 2014. "Electron Paramagnetic Resonance as an Effective Method for a Characterization of Functionalized Iron Oxide." *Journal of Physics and Chemistry of Solids* 75 (5). Elsevier: 594–98. doi:10.1016/j.jpcs.2014.01.013.

Dosio, Franco, Barbara Stella, Silvia Arpicco, and Luigi Cattel. 2011. "Macromolecules as Taxane Delivery Systems." *Expert Opinion on Drug Delivery* 8 (1): 33–55. doi:10.1517/17425247.2011.541437.

Douziech-Eyrolles, Laurence, Hervé Marchais, Katel Hervé, Emilie Munnier, Martin Soucé, Claude Linassier, Pierre Dubois, and Igor Chourpa. 2007. "Nanovectors for Anticancer Agents Based on Superparamagnetic Iron Oxide Nanoparticles." *International Journal of Nanomedicine* 2 (4): 541–50. http://www.pubmedcentral.nih.gov/articlerender.fcgi?artid=2676819&tool=pmcentrez&rendertype=abstract.

Dufort, Sandrine, Lucie Sancey, and Jean-Luc Coll. 2012. "Physico-Chemical Parameters That Govern Nanoparticles Fate Also Dictate Rules for Their Molecular Evolution." *Advanced Drug Delivery Reviews* 64 (2). Elsevier B.V.: 179–89. doi:10.1016/j.addr.2011.09.009.

Dutz, Silvio, Wilfried Andrä, Rudolf Hergt, Robert Müller, Christiane Oestreich, Christopher Schmidt, Jorg Töpfer, Matthias Zeisberger, and Matthias E. Bellemann. 2007. "Influence of Dextran Coating on the Magnetic Behaviour of Iron Oxide Nanoparticles." *Journal of Magnetism and Magnetic Materials* 311 (1): 51–54. doi:10.1016/j.jmmm.2006.11.168.

Elsherbini, Alsayed a M, Mahmoud Saber, Mohamed Aggag, Ahmed El-Shahawy, and Hesham a a Shokier. 2011. "Magnetic Nanoparticle-Induced Hyperthermia Treatment under Magnetic Resonance Imaging." *Magnetic Resonance Imaging* 29 (2). Elsevier Inc.: 272–80. doi:10.1016/j.mri.2010.08.010.

Figueiredo, L.C., B.M. Lacava, K. Skeff Neto, F. Pelegrini, and P.C. Morais. 2008. "Magnetic Resonance Study of Maghemite-Based Magnetic Fluid." *Journal of Magnetism and Magnetic Materials* 320 (14): e347–50. doi:10.1016/j.jmmm.2008.02.069.

Finotelli, P.V., M.a. Morales, M.H. Rocha-Leão, E.M. Baggio-Saitovitch, and a.M. Rossi. 2004. "Magnetic Studies of iron(III) Nanoparticles in Alginate Polymer for Drug Delivery Applications." *Materials Science and Engineering: C* 24 (5): 625–29. doi:10.1016/j.msec.2004.08.005.

Freeman, M. W., a. Arrott, and J. H. L. Watson. 1960. "Magnetism in Medicine." *Journal of Applied Physics* 31 (5): S404. doi:10.1063/1.1984765.

Gaihre, Babita, Myung Seob Khil, Douk Rae Lee, and Hak Yong Kim. 2009. "Gelatin-Coated Magnetic Iron Oxide Nanoparticles as Carrier System: Drug Loading and in Vitro Drug Release Study." *International Journal of Pharmaceutics* 365 (1-2): 180–89. doi:10.1016/j.ijpharm.2008.08.020.

Gamarra, L F, W M Pontuschka, J B Mamani, D R Cornejo, T R Oliveira, E D Vieira, a J Costa-Filho, and E Amaro Jr. 2009. "Magnetic Characterization by SQUID and FMR of a Biocompatible Ferrofluid Based on Fe 3 O 4." *Journal of Physics: Condensed Matter* 21: 115104. doi:10.1088/0953-8984/21/11/115104.

Gautier, J, E Munnier, a Paillard, K Hervé, L Douziech-Eyrolles, M Soucé, P Dubois, and I Chourpa. 2012. "A Pharmaceutical Study of Doxorubicin-Loaded PEGylated Nanoparticles for Magnetic Drug Targeting." *International Journal of Pharmaceutics* 423 (1). Elsevier B.V.: 16–25. doi:10.1016/j.ijpharm.2011.06.010.

Gautier, J., E. Allard-Vannier, E. Munnier, M. Soucé, and I. Chourpa. 2013. "Recent Advances in Theranostic Nanocarriers of Doxorubicin Based on Iron Oxide and Gold Nanoparticles." *Journal of Controlled Release* 169 (1-2). Elsevier B.V.: 48–61. doi:10.1016/j.jconrel.2013.03.018.

Gee, S. H., Y. K. Hong, D. W. Erickson, M. H. Park, and J. C. Sur. 2003. "Synthesis and Aging Effect of Spherical Magnetite (Fe[sub 3]O[sub 4]) Nanoparticles for Biosensor Applications." *Journal of Applied Physics* 93 (10): 7560. doi:10.1063/1.1540177.

Goff, J. D., P. P. Huffstetler, W. C. Miles, N. Pothayee, C. M. Reinholz, S. Bail, R. M. Davis, and J. S. Riffle. 2009. "Novel Phosphonate-Functional Poly(ethylene Oxide)-Magnetite Nanoparticles Form Stable Colloidal Dispersions in Phosphate-Buffered Saline." *Chemistry of Materials* 21 (7): 4784–95. doi:10.1021/cm901006g.

Goikolea, E., M. Insausti, T. Rojo, L. Lezama, and J.S. Garitaonandia. 2007. "Low-Temperature Electron Paramagnetic Resonance in Silver-Iron Oxide Nanoparticles." *Journal of Non-Crystalline Solids* 353 (8-10): 832–34. doi:10.1016/j.jnoncrysol.2006.12.051.

Gould, Paula. 2006. "Nanomagnetism Shows in Vivo Potential." *Nanotoday* 1 (4): 34–39.

Goya, G. F., T. S. Berquó, F. C. Fonseca, and M. P. Morales. 2003. "Static and Dynamic Magnetic Properties of Spherical Magnetite Nanoparticles." *Journal of Applied Physics* 94 (5): 3520. doi:10.1063/1.1599959.

Gu, Lina, Zhong Shen, Chun Feng, Yaogong Li, Guolin Lu, Xiaoyu Huang, Guowei Wang, and Junlian Huang. 2008. "Synthesis of PPEGMEA-G-PMAA Densely Grafted Double Hydrophilic Copolymer and Its Use as a Template for the Preparation of Size-Controlled Superparamagnetic Fe3O4/polymer Nano-Composites." *Journal of Materials Chemistry* 18: 4332. doi:10.1039/b805841e.

Guo, Shaojun, Dan Li, Lixue Zhang, Jing Li, and Erkang Wang. 2009. "Monodisperse Mesoporous Superparamagnetic Single-Crystal Magnetite Nanoparticles for Drug Delivery." *Biomaterials* 30 (10). Elsevier Ltd: 1881–89. doi:10.1016/j.biomaterials.2008.12.042.

Gupta, a.K., and S. Wells. 2004. "Surface-Modified Superparamagnetic Nanoparticles for Drug Delivery: Preparation, Characterization, and Cytotoxicity Studies." *IEEE Transactions on Nanobioscience* 3 (1): 66–73. doi:10.1109/TNB.2003.820277.

Gupta, Ajay Kumar, and Adam S G Curtis. 2004. "Surface Modifed Superparamagnetic Nanoparticles for Drug Delivery : Interaction Studies with Human Fibroblasts in Culture." *Journal of Material Science: Materials in Medicine* 15: 493–96.

Gupta, Ajay Kumar, and Mona Gupta. 2005. "Synthesis and Surface Engineering of Iron Oxide Nanoparticles for Biomedical Applications." *Biomaterials* 26 (18): 3995–4021. doi:10.1016/j.biomaterials.2004.10.012.

Hałupka-Bryl, Magdalena, Kei Asai, Sindhu Thangavel, Magdalena Bednarowicz, Ryszard Krzyminiewski, and Yukio Nagasaki. 2014. "Synthesis and in Vitro and in Vivo Evaluations of Poly(ethylene Glycol)-Block-poly(4-Vinylbenzylphosphonate) Magnetic Nanoparticles Containing Doxorubicin as a Potential Targeted Drug Delivery System." *Colloids and Surfaces. B, Biointerfaces* 118 (June). Elsevier B.V.: 140–47. doi:10.1016/j.colsurfb.2014.03.025.

Hałupka-Bryl, Magdalena, Magdalena Bednarowicz, Bernadeta Dobosz, Ryszard Krzyminiewski, Tomasz Zalewski, Beata Wereszczyńska, Grzegorz Nowaczyk, Marcin Jarek, and Yukio Nagasaki. 2015. "Doxorubicin Loaded PEG-B-poly(4-Vinylbenzylphosphonate) Coated Magnetic Iron Oxide Nanoparticles for Targeted Drug Delivery." *Journal of Magnetism and Magnetic Materials* 384: 320–27. doi:10.1016/j.jmmm.2015.02.078.

Harris, L. a., J. D. Goff, a. Y. Carmichael, J. S. Riffle, J. J. Harburn, T. G. St. Pierre, and M. Saunders. 2003. "Magnetite Nanoparticle Dispersions Stabilized with Triblock Copolymers." *Chemistry of Materials* 15 (6): 1367–77. doi:10.1021/cm020994n.

Hildebrandt, Nicole, Dana Hermsdorf, Ruth Signorell, and Stephan A Schmitz. 2007. "Superparamagnetic Iron Oxide Nanoparticles Functionalized with Peptides by Electrostatic Interactions" 2007 (v): 79–90.

Hong, R.Y., B. Feng, L.L. Chen, G.H. Liu, H.Z. Li, Y. Zheng, and D.G. Wei. 2008. "Synthesis, Characterization and MRI Application of Dextran-Coated Fe3O4 Magnetic Nanoparticles." *Biochemical Engineering Journal* 42 (3): 290–300. doi:10.1016/j.bej.2008.07.009.

Hradil, Jiří, Alexander Pisarev, Michal Babič, and Daniel Horák. 2007. "Dextran-Modified Iron Oxide Nanoparticles." *China Particuology* 5 (1-2): 162–68. doi:10.1016/j.cpart.2007.01.003.

Hseih, C.T, W.L Huang, and J.T Lue. 2002. "The Change from Paramagnetic Resonance to Ferromagnetic Resonance for Iron Nanoparticles Made by the Sol–gel Method." *Journal of Physics and Chemistry of Solids* 63 (5): 733–41. doi:10.1016/S0022-3697(01)00222-0.

Iida, Hironori, Kosuke Takayanagi, Takuya Nakanishi, and Tetsuya Osaka. 2007. "Synthesis of Fe3O4 Nanoparticles with Various Sizes and Magnetic Properties by Controlled

Hydrolysis." *Journal of Colloid and Interface Science* 314 (1): 274–80. doi:10.1016/j.jcis.2007.05.047.

Ishii, Takehiko, Hidenori Otsuka, Kazunori Kataoka, and Yukio Nagasaki. 2004. "Preparation of Functionally PEGylated Gold Nanoparticles with Narrow Distribution through Autoreduction of Auric Cation by ??-Biotinyl-PEG-Block-[poly(2-(N,N-Dimethylamino)ethyl Methacrylate)]." *Langmuir* 20 (8): 561–64. doi:10.1021/la035653i.

Jain, R.K. 2001. "Delivery of Molecular Medicine to Solid Tumors: Lessons from in Vivo Imaging of Gene Expression and Function." *Journal of Controlled Release* 74 (1-3): 7–25. doi:10.1016/S0168-3659(01)00306-6.

Jain, Rakesh K. 1999. "Transport of Molecules , Particles , and Cells in Solid Tumors," no. 96: 241–63.

Javid, Amaneh, Shahin Ahmadian, Ali a Saboury, Seyed M Kalantar, and Saeed Rezaei-Zarchi. 2013. "Chitosan-Coated Superparamagnetic Iron Oxide Nanoparticles for Doxorubicin Delivery: Synthesis and Anticancer Effect against Human Ovarian Cancer Cells." *Chemical Biology & Drug Design* 82 (3): 296–306. doi:10.1111/cbdd.12145.

Jeng, Hueiwang Anna, and James Swanson. 2006. "Toxicity of Metal Oxide Nanoparticles in Mammalian Cells." *Journal of Environmental Science and Health. Part A, Toxic/hazardous Substances & Environmental Engineering* 41 (12): 2699–2711. doi:10.1080/10934520600966177.

Jun, Young-wook, Jae-hyun Lee, and Jinwoo Cheon. 2007. "Nanoparticle Contrast Agents for Molecular Magnetic Resonance Imaging."

Jung, C H U W. 1995. "SURFACE PROPERTIES OF SUPERPARAMAGNETIC IRON OXIDE MR CONTRAST AGENTS: FERUMOXIDES, FERUMOXTRAN, FERUMOXSIL." *Magnetic Resonance Imaging,* 13 (5): 675–91.

Kabacińska, Zuzanna, Ryszard Krzyminiewski, Bernadeta Dobosz, and Danuta Nawrocka. 2012. "ESR Investigation of Structure and Dynamics of Paramagnetic Centres in Lime Mortars from Budinjak, Croatia." *Radiation Measurements* 47 (9): 825–29. doi:10.1016/j.radmeas.2012.03.017.

Kamimura, Masao, Naoki Kanayama, Kimikazu Tokuzen, Kohei Soga, and Yukio Nagasaki. 2011. "Near-Infrared (1550 Nm) in Vivo Bioimaging Based on Rare-Earth Doped Ceramic Nanophosphors Modified with PEG-B-poly(4-Vinylbenzylphosphonate)." *Nanoscale* 3 (9): 3705–13. http://www.ncbi.nlm.nih.gov/pubmed/21792433.

Kamimura, Masao, Jong Oh Kim, Alexander V Kabanov, Tatiana K Bronich, and Yukio Nagasaki. 2012. "Block Ionomer Complexes of PEG-Block-poly(4-Vinylbenzylphosphonate) and Cationic Surfactants as Highly Stable, pH Responsive Drug Delivery System." *Journal of Controlled Release : Official Journal of the Controlled Release Society* 160 (3). Elsevier B.V.: 486–94. doi:10.1016/j.jconrel.2012.04.027.

Karlsson, Hanna L, Johanna Gustafsson, Pontus Cronholm, and Lennart Möller. 2009. "Size-Dependent Toxicity of Metal Oxide Particles--a Comparison between Nano- and Micrometer Size." *Toxicology Letters* 188 (2): 112–18. doi:10.1016/j.toxlet.2009.03.014.

Karlsson, Hanna L, Asa Holgersson, and Lennart Möller. 2008. "Mechanisms Related to the Genotoxicity of Particles in the Subway and from Other Sources." *Chemical Research in Toxicology* 21 (3): 726–31. doi:10.1021/tx7003568.

Kayal, S., and R.V. Ramanujan. 2010. "Doxorubicin Loaded PVA Coated Iron Oxide Nanoparticles for Targeted Drug Delivery." *Materials Science and Engineering: C* 30 (3). Elsevier B.V.: 484–90. doi:10.1016/j.msec.2010.01.006.

Kempe, Sabine, Hendrik Metz, and Karsten Mäder. 2010. "Application of Electron Paramagnetic Resonance (EPR) Spectroscopy and Imaging in Drug Delivery Research - Chances and Challenges." *European Journal of Pharmaceutics and Biopharmaceutics : Official Journal of Arbeitsgemeinschaft Für Pharmazeutische Verfahrenstechnik e.V* 74 (1). Elsevier B.V.: 55–66. doi:10.1016/j.ejpb.2009.08.007.

Kievit, Forrest M, Freddy Y Wang, Chen Fang, Hyejung Mok, Kui Wang, John R Silber, Richard G Ellenbogen, and Miqin Zhang. 2011. "Doxorubicin Loaded Iron Oxide Nanoparticles Overcome Multidrug Resistance in Cancer in Vitro." *Journal of Controlled Release Official Journal of the Controlled Release Society* 152 (1). Elsevier B.V.: 76–83. doi:10.1016/j.jconrel.2011.01.024.

Kim, Jun Sung, Tae-Jong Yoon, Kyeong Nam Yu, Byung Gul Kim, Sung Jin Park, Hyun Woo Kim, Kee Ho Lee, Seung Bum Park, Jin-Kyu Lee, and Myung Haing Cho. 2006. "Toxicity and Tissue Distribution of Magnetic Nanoparticles in Mice." *Toxicological Sciences : An Official Journal of the Society of Toxicology* 89 (1): 338–47. doi:10.1093/toxsci/kfj027.

Klibanov, Alexander L, Kazuo Maruyamal, Vladimir P Torchilin, and Leaf Huangl. 1990. "Amphipathic Polyethyleneglycols Effectively Prolong the Circulation Time of Liposomes" 268 (1): 235–37.

Kodama, R H. 1999. "Magnetic Nanoparticles." *Journal of Magnetism and Magnetic Materials* 200 (January): 359–72.

Kumar, R. Vijaya, Yu Koltypin, X. N. Xu, Y. Yeshurun, a. Gedanken, and I. Felner. 2001. "Fabrication of Magnetite Nanorods by Ultrasound Irradiation." *Journal of Applied Physics* 89 (11): 6324. doi:10.1063/1.1369408.

Lai, Benjamin F L, a Louise Creagh, Johan Janzen, Charles a Haynes, Donald E Brooks, and Jayachandran N Kizhakkedathu. 2010. "The Induction of Thrombus Generation on Nanostructured Neutral Polymer Brush Surfaces." *Biomaterials* 31 (26). Elsevier Ltd: 6710–18. doi:10.1016/j.biomaterials.2010.05.052.

Laurent, Sophie, Delphine Forge, Marc Port, Alain Roch, Caroline Robic, Luce Vander Elst, and Robert N Muller. 2008. "Magnetic Iron Oxide Nanoparticles: Synthesis, Stabilization, Vectorization, Physicochemical Characterizations, and Biological Applications." *Chemical Reviews* 108 (6): 2064–2110. doi:10.1021/cr068445e.

Laurent, Sophie, and Morteza Mahmoudi. 2011. "Superparamagnetic Iron Oxide Nanoparticles : Promises for Diagnosis and Treatment of Cancer." *Int J Mol Epidemiol Genet* 2 (4): 367–90.

Leader, Benjamin, Quentin J Baca, and David E Golan. 2008. "Protein Therapeutics: A Summary and Pharmacological Classification." *Natire Reviews/Drug Discovery* 7: 21–39.

Lee, C. S., H. Lee, and R. M. Westervelt. 2001. "Microelectromagnets for the Control of Magnetic Nanoparticles." *Applied Physics Letters* 79 (20): 3308. doi:10.1063/1.1419049.

Lee, Jiwon, Tetsuhiko Isobe, and Mamoru Senna. 1996. "Magnetic Properties of Ultrafine Magnetite Particles and Their Slurries Prepared via in-Situ Precipitation." *Colloids and Surfaces A: Physicochemical and Engineering Aspects* 109 (April): 121–27. doi:10.1016/0927-7757(95)03479-X.

Lee, Nohyun, and Taeghwan Hyeon. 2012. "Designed Synthesis of Uniformly Sized Iron Oxide Nanoparticles for Efficient Magnetic Resonance Imaging Contrast Agents." *Chemical Society Reviews* 41 (7): 2575. doi:10.1039/c1cs15248c.

Lee, Y., J. Lee, C. J. Bae, J.-G. Park, H.-J. Noh, J.-H. Park, and T. Hyeon. 2005. "Large-Scale Synthesis of Uniform and Crystalline Magnetite Nanoparticles Using Reverse Micelles as Nanoreactors under Reflux Conditions." *Advanced Functional Materials* 15 (3): 503–9. doi:10.1002/adfm.200400187.

Leuschner, Carola, Challa S S R Kumar, William Hansel, Wole Soboyejo, Jikou Zhou, and Josef Hormes. 2006. "LHRH-Conjugated Magnetic Iron Oxide Nanoparticles for Detection of Breast Cancer Metastases." *Breast Cancer Research and Treatment* 99 (2): 163–76. doi:10.1007/s10549-006-9199-7.

Li, Fang, Jing Sun, Huaishi Zhu, Xuejun Wen, Chao Lin, and Donglu Shi. 2011. "Preparation and Characterization Novel Polymer-Coated Magnetic Nanoparticles as Carriers for Doxorubicin." *Colloids and Surfaces B: Biointerfaces* 88 (1). Elsevier B.V.: 58–62. doi:10.1016/j.colsurfb.2011.06.003.

Lin, Jun, Weilie Zhou, a. Kumbhar, J. Wiemann, Jiye Fang, E.E. Carpenter, and C.J. O'Connor. 2001. "Gold-Coated Iron (Fe@Au) Nanoparticles: Synthesis, Characterization, and Magnetic Field-Induced Self-Assembly." *Journal of Solid State Chemistry* 159 (1): 26–31. doi:10.1006/jssc.2001.9117.

Ling, You, Kun Wei, Yun Luo, Xin Gao, and Shizhen Zhong. 2011. "Dual Docetaxel/superparamagnetic Iron Oxide Loaded Nanoparticles for Both Targeting Magnetic Resonance Imaging and Cancer Therapy." *Biomaterials* 32 (29). Elsevier Ltd: 7139–50. doi:10.1016/j.biomaterials.2011.05.089.

Link, Citable, Frank Alexis, Eric Pridgen, and Linda K Molnar. 2015. "Reviews Factors Affecting the Clearance and Biodistribution of."

Liu, Yutao, Kai Li, Bin Liu, and Si-Shen Feng. 2010. "A Strategy for Precision Engineering of Nanoparticles of Biodegradable Copolymers for Quantitative Control of Targeted

Drug Delivery." *Biomaterials* 31 (35). Elsevier Ltd: 9145–55. doi:10.1016/j.biomaterials.2010.08.053.

Liu, Z. L., X. Wang, K. L. Yao, G. H. Du, Q. H. Lu, Z. H. Ding, J. Tao, et al. 2004. "Synthesis of Magnetite Nanoparticles in W/O Microemulsion." *Journal of Materials Science* 39 (7): 2633–36. doi:10.1023/B:JMSC.0000020046.68106.22.

Lodhia, J, G Mandarano, Nj Ferris, P Eu, and Sf Cowell. 2010. "Development and Use of Iron Oxide Nanoparticles (Part 1): Synthesis of Iron Oxide Nanoparticles for MRI." *Biomedical Imaging and Intervention Journal* 6 (2): e12. doi:10.2349/biij.6.2.e12.

Lu, An-Hui, E L Salabas, and Ferdi Schüth. 2007. "Magnetic Nanoparticles: Synthesis, Protection, Functionalization, and Application." *Angewandte Chemie (International Ed. in English)* 46 (8): 1222–44. doi:10.1002/anie.200602866.

Lübbe, a S, C Alexiou, and C Bergemann. 2001. "Clinical Applications of Magnetic Drug Targeting." *The Journal of Surgical Research* 95 (2): 200–206. doi:10.1006/jsre.2000.6030.

Lübbe, Andreas Stephan, Christian Bergemann, Winfried Huhnt, Andreas Stephan Lãbbe, Thomas Fricke, and Hanno Riess. 1996. "Preclinical Experiences with Magnetic Drug Targeting : Tolerance and Efficacy Experiences Drug Targeting : And Efficacy." *Cancer Research* 56: 4694–4701.

Lutz, Jean-François, Sabrina Stiller, Ann Hoth, Lutz Kaufner, Ulrich Pison, and Régis Cartier. 2006. "One-Pot Synthesis of Pegylated Ultrasmall Iron-Oxide Nanoparticles and Their in Vivo Evaluation as Magnetic Resonance Imaging Contrast Agents." *Biomacromolecules* 7: 3132–38. doi:10.1021/bm0607527.

Maeda, H, J Wu, T Sawa, Y Matsumura, and K Hori. 2000. "Tumor Vascular Permeability and the EPR Effect in Macromolecular Therapeutics: A Review." *Journal of Controlled Release* 65 (1-2): 271–84. doi:10.1016/S0168-3659(99)00248-5.

Maeda, H. 2001. "THE ENHANCED PERMEABILITY AND RETENTION (EPR) EFFECT IN TUMOR VASCULATURE : THE KEY ROLE OF TUMOR-SELECTIVE MACROMOLECULAR." *Advan. Enzyme Regul.* 41 (00): 189–207.

Maeda, Hiroshi. 1991. "SMANCS and Polymer-Conjugated Macromolecular Drugs: Advantages in Cancer Chemotherapy." *Advanced Drug Delivery Reviews* 6 (2): 181–202. doi:10.1016/0169-409X(91)90040-J.

Maeda, Hiroshi, Tomohiro Sawa, and Toshimitsu Konno. 2001. "Mechanism of Tumor-Targeted Delivery of Macromolecular Drugs, Including the EPR Effect in Solid Tumor and Clinical Overview of the Prototype Polymeric Drug SMANCS." *Journal of Controlled Release* 74 (1-3): 47–61. doi:10.1016/S0168-3659(01)00309-1.

Mahmoudi, By Morteza, Abdolreza Simchi, Hojatollah Vali, and Mohammad Imani. 2009. "Cytotoxicity and Cell Cycle Effects of Bare and Poly (Vinyl Alcohol) -Coated Iron Oxide Nanoparticles in Mouse Fibroblasts." *Advanced Biometarials* 11 (12): 243–50. doi:10.1002/adbi.200900004.

Mahmoudi, M, a Simchi, a S Milani, and P Stroeve. 2009. "Cell Toxicity of Superparamagnetic Iron Oxide Nanoparticles." *Journal of Colloid and Interface Science* 336 (2). Elsevier Inc.: 510–18. doi:10.1016/j.jcis.2009.04.046.

Mahmoudi, Morteza, Mohammad A Shokrgozar, Abdolreza Simchi, Mohammad Imani, Abbas S Milani, Pieter Stroeve, Hojatollah Vali, Urs O Ha, and Shahin Bonakdar. 2009. "Multiphysics Flow Modeling and in Vitro Toxicity of Iron Oxide Nanoparticles Coated with Poly (Vinyl Alcohol)." *J. Phys. Chem.* 113: 2322–31.

Mahmoudi, Morteza, Abdolreza Simchi, Mohammad Imani, and Urs O Ha. 2009. "Superparamagnetic Iron Oxide Nanoparticles with Rigid Cross-Linked Polyethylene Glycol Fumarate Coating for Application in Imaging and Drug Delivery." *J. Phys. Chem.* 113: 8124–31.

Mahmoudi, Morteza, Abdolreza Simchi, Mohammad Imani, Mohammad a Shokrgozar, Abbas S Milani, Urs O Häfeli, and Pieter Stroeve. 2010. "A New Approach for the in Vitro Identification of the Cytotoxicity of Superparamagnetic Iron Oxide Nanoparticles." *Colloids and Surfaces. B, Biointerfaces* 75 (1): 300–309. doi:10.1016/j.colsurfb.2009.08.044.

Maver, Uroš, Marjan Bele, Darko Makovec, Stanislav Čampelj, Janko Jamnik, and Miran Gaberšček. 2009. "Incorporation and Release of Drug Into/from Superparamagnetic Iron Oxide Nanoparticles." *Journal of Magnetism and Magnetic Materials* 321 (19): 3187–92. doi:10.1016/j.jmmm.2009.05.054.

McCarthy, Jason R, and Ralph Weissleder. 2008. "Multifunctional Magnetic Nanoparticles for Targeted Imaging and Therapy." *Advanced Drug Delivery Reviews* 60 (11): 1241–51. doi:10.1016/j.addr.2008.03.014.

Mcneil, Scott E. 2005. "Nanotechnology for the Biologist." *Journal of Leukocyte Biology* 78 (September): 585–94. doi:10.1189/jlb.0205074.1.

Medarova, Zdravka, Wellington Pham, Christian Farrar, Victoria Petkova, and Anna Moore. 2007. "In Vivo Imaging of siRNA Delivery and Silencing in Tumors." *Nature Medicine* 13 (3): 372–77. doi:10.1038/nm1486.

Misra, R. D. K. 2008. "Magnetic Nanoparticle Carrier for Targeted Drug Delivery: Perspective, Outlook and Design." *Materials Science and Technology* 24 (9): 1011–19. doi:10.1179/174328408X341690.

Mody, Vicky V., Arthur Cox, Samit Shah, Ajay Singh, Wesley Bevins, and Harish Parihar. 2013. "Magnetic Nanoparticle Drug Delivery Systems for Targeting Tumor." *Applied Nanoscience* 4 (4): 385–92. doi:10.1007/s13204-013-0216-y.

Moghimi, S Moein, A Christy Hunter, and J Clifford Murray. 2001. "Long-Circulating and Target-Specific Nanoparticles : Theory to Practice." *Pharmacological Reviews* 53 (2): 283–318.

Mojica Pisciotti, M L, E Lima, M Vasquez Mansilla, V E Tognoli, H E Troiani, a a Pasa, T B Creczynski-Pasa, et al. 2014. "In Vitro and in Vivo Experiments with Iron Oxide

Nanoparticles Functionalized with DEXTRAN or Polyethylene Glycol for Medical Applications: Magnetic Targeting." *Journal of Biomedical Materials Research. Part B, Applied Biomaterials* 102 (4): 860–68. doi:10.1002/jbm.b.33068.

Mok, Hyejung, and Miqin Zhang. 2013. "Superparamagnetic Iron Oxide Nanoparticle-Based Delivery Systems for Biotherapeutics." *Expert Opinion on Drug Delivery* 10 (1): 73–87. doi:10.1517/17425247.2013.747507.

Moore, Anna, Lee Josephson, Rajeev M Bhorade, James P Basilion, and Ralph Weissleder. "Gene as a Marker Gene for."

Moore, Anna, Edgardo Marecos, Alexei Bogdanov, and Ralph Weissleder. 2000. "Tumoral Distribution of Iron Oxide Nanoparticles in a Rodent Model 1." *Radiology*.

Morawski, Anne M, Patrick M Winter, Kathryn C Crowder, Shelton D Caruthers, Ralph W Fuhrhop, Michael J Scott, J David Robertson, Dana R Abendschein, Gregory M Lanza, and Samuel a Wickline. 2004. "Targeted Nanoparticles for Quantitative Imaging of Sparse Molecular Epitopes with MRI." *Magnetic Resonance in Medicine : Official Journal of the Society of Magnetic Resonance in Medicine / Society of Magnetic Resonance in Medicine* 51 (3): 480–86. doi:10.1002/mrm.20010.

Mosbach, Klaus, and Ulf Schroder. 1979. "PREPARATION AND APPLICATION OF MAGNETIC POLYMERS FOR TARGETING OF DRUGS." *FEBS Letters* 102 (1): 112–16.

Munnier, E, S Cohen-Jonathan, C Linassier, L Douziech-Eyrolles, H Marchais, M Soucé, K Hervé, P Dubois, and I Chourpa. 2008. "Novel Method of Doxorubicin-SPION Reversible Association for Magnetic Drug Targeting." *International Journal of Pharmaceutics* 363 (1-2): 170–76. doi:10.1016/j.ijpharm.2008.07.006.

Munnier, E., S. Cohen-Jonathan, K. Hervé, C. Linassier, M. Soucé, P. Dubois, and I. Chourpa. 2010. "Doxorubicin Delivered to MCF-7 Cancer Cells by Superparamagnetic Iron Oxide Nanoparticles: Effects on Subcellular Distribution and Cytotoxicity." *Journal of Nanoparticle Research* 13 (3): 959–71. doi:10.1007/s11051-010-0093-1.

Nagasaki, Yukio. 2008. "PEG-B-Polyamine Stabilized Bionanoparticles for Nanodiagnostics and Nanotherapy." *Chemistry Letters* 37 (6): 564–69. doi:10.1246/cl.2008.564.

Nel, Andre, Tian Xia, Lutz Mädler, and Ning Li. 2006. "Toxic Potential of Materials at the Nanolevel." *Science (New York, N.Y.)* 311 (5761): 622–27. doi:10.1126/science.1114397.

Neuberger, Tobias, Bernhard Schöpf, Heinrich Hofmann, Margarete Hofmann, and Brigitte von Rechenberg. 2005. "Superparamagnetic Nanoparticles for Biomedical Applications: Possibilities and Limitations of a New Drug Delivery System." *Journal of Magnetism and Magnetic Materials* 293 (1): 483–96. doi:10.1016/j.jmmm.2005.01.064.

Nigam, Saumya, K.C. Barick, and D. Bahadur. 2011. "Development of Citrate-Stabilized Fe3O4 Nanoparticles: Conjugation and Release of Doxorubicin for Therapeutic Applications." *Journal of Magnetism and Magnetic Materials* 323 (2). Elsevier: 237–43. doi:10.1016/j.jmmm.2010.09.009.

Oberdörster, Günter, Vicki Stone, and Ken Donaldson. 2007. "Toxicology of Nanoparticles: A Historical Perspective." *Nanotoxicology* 1 (1): 2–25. doi:10.1080/17435390701314761.

Owens, Donald E, and Nicholas a Peppas. 2006. "Opsonization, Biodistribution, and Pharmacokinetics of Polymeric Nanoparticles." *International Journal of Pharmaceutics* 307 (1): 93–102. doi:10.1016/j.ijpharm.2005.10.010.

Papaphilippou, Petri, Louiza Loizou, Nicolae C. Popa, Adelina Han, Ladislau Vekas, Andreani Odysseos, and Theodora Krasia-Christoforou. 2009. "Superparamagnetic Hybrid Micelles, Based on Iron Oxide Nanoparticles and Well-Defined Diblock Copolymers Possessing ??-Ketoester Functionalities." *Biomacromolecules* 10: 2662–71. doi:10.1021/bm9005936.

Park, Jongnam, Kwangjin An, Yosun Hwang, Je-Geun Park, Han-Jin Noh, Jae-Young Kim, Jae-Hoon Park, Nong-Moon Hwang, and Taeghwan Hyeon. 2004. "Ultra-Large-Scale Syntheses of Monodisperse Nanocrystals." *Nature Materials* 3 (12): 891–95. doi:10.1038/nmat1251.

Park, Shinyoung, Hye Sung Kim, Woo Jin Kim, and Hyuk Sang Yoo. 2012. "Pluronic@Fe3O4 Nanoparticles with Robust Incorporation of Doxorubicin by Thermo-Responsiveness." *International Journal of Pharmaceutics* 424 (1-2). Department of Biomaterials Engineering, Kangwon National University, Chuncheon, Republic of Korea.: 107–14. doi:10.1016/j.ijpharm.2011.12.044.

Patel, Daksha, Je Yong Moon, Yongmin Chang, Tae Jeong Kim, and Gang Ho Lee. 2008. "Poly(d,l-Lactide-Co-Glycolide) Coated Superparamagnetic Iron Oxide Nanoparticles: Synthesis, Characterization and in Vivo Study as MRI Contrast Agent." *Colloids and Surfaces A: Physicochemical and Engineering Aspects* 313-314 (February): 91–94. doi:10.1016/j.colsurfa.2007.04.078.

Petri-Fink, a, M Chastellain, L Juillerat-Jeanneret, a Ferrari, and H Hofmann. 2005. "Development of Functionalized Superparamagnetic Iron Oxide Nanoparticles for Interaction with Human Cancer Cells." *Biomaterials* 26 (15): 2685–94. doi:10.1016/j.biomaterials.2004.07.023.

Pirollo, Kathleen F., and Esther H. Chang. 2008. "Does a Targeting Ligand Influence Nanoparticle Tumor Localization or Uptake?" *Trends in Biotechnology* 26 (August): 552–58. doi:10.1016/j.tibtech.2008.06.007.

Prijic, Sara, Lara Prosen, Maja Cemazar, Janez Scancar, Rok Romih, Jaka Lavrencak, Vladimir B Bregar, et al. 2012. "Surface Modified Magnetic Nanoparticles for Immuno-Gene Therapy of Murine Mammary Adenocarcinoma." *Biomaterials* 33 (17). Elsevier Ltd: 4379–91. doi:10.1016/j.biomaterials.2012.02.061.

Qian, Zhong Ming, Hongyan Li, Hongzhe Sun, and Kwokping Ho. 2002. "Targeted Drug Delivery via the Transferrin Receptor-" 54 (4): 561–87.

Rahimi, Maham, Aniket Wadajkar, Khaushik Subramanian, Monet Yousef, Weina Cui, Jer-Tsong Hsieh, and Kytai Truong Nguyen. 2010. "In Vitro Evaluation of Novel Polymer-Coated Magnetic Nanoparticles for Controlled Drug Delivery." *Nanomedicine : Nanotechnology, Biology, and Medicine* 6 (5). Elsevier Inc.: 672–80. doi:10.1016/j.nano.2010.01.012.

Rosen, Joshua E, Lorena Chan, Dar-Bin Shieh, and Frank X Gu. 2012a. "Iron Oxide Nanoparticles for Targeted Cancer Imaging and Diagnostics." *Nanomedicine : Nanotechnology, Biology, and Medicine* 8 (3). Elsevier Inc.: 275–90. doi:10.1016/j.nano.2011.08.017.

Rosen, 2012b. "Iron Oxide Nanoparticles for Targeted Cancer Imaging and Diagnostics." *Nanomedicine : Nanotechnology, Biology, and Medicine* 8 (3). Elsevier Inc.: 275–90. doi:10.1016/j.nano.2011.08.017.

Rudge, S., C. Peterson, C. Vessely, J. Koda, S. Stevens, and L. Catterall. 2001. "Adsorption and Desorption of Chemotherapeutic Drugs from a Magnetically Targeted Carrier (MTC)." *Journal of Controlled Release* 74 (1-3): 335–40. doi:10.1016/S0168-3659(01)00344-3.

S. Santra, C.Kaittanis, J. Grimm, J. Manuel Perez. 2011. "Drug/Dye-Loaded, Multifunctional Iron Oxide Nanoparticles for Combined Targeted Cancer Therapy and Dual Optical/MRImaging." *NIH Public Access* 5 (16): 1862–68. doi:10.1002/smll.200900389.Drug/Dye-Loaded.

Salloum, Maher, Ronghui Ma, and Liang Zhu. 2008. "An in-Vivo Experimental Study of Temperature Elevations in Animal Tissue during Magnetic Nanoparticle Hyperthermia." *International Journal of Hyperthermia : The Official Journal of European Society for Hyperthermic Oncology, North American Hyperthermia Group* 24 (7): 589–601. doi:10.1080/02656730802203377.

Sartiano, G P, W E Lynch, and W D Bullington. 1979. "Mechanism of Action of the Anthracycline Anti-Tumor Antibiotics, Doxorubicin, Daunomycin and Rubidazone: Preferential Inhibition of DNA Polymerase Alpha." *The Journal of Antibiotics* 32: 1038–45.

Scherer. 2002. "Magnetofection: Enhancing and Targeting Gene Delivery by Magnetic Force in Vitro and in Vivo." *Gene Therapy* 9: 102–9. doi:10.1038/sj/gt/3301624.

Schweiger, Christoph, Clemens Pietzonka, Johannes Heverhagen, and Thomas Kissel. 2011. "Novel Magnetic Iron Oxide Nanoparticles Coated with Poly(ethylene Imine)-G-Poly(ethylene Glycol) for Potential Biomedical Application: Synthesis, Stability, Cytotoxicity and MR Imaging." *International Journal of Pharmaceutics* 408 (1-2). Elsevier B.V.: 130–37. doi:10.1016/j.ijpharm.2010.12.046.

Shkilnyy, Andriy, Emilie Munnier, Katel Herve, Martin Souce, Roland Benoit, Simone Cohen-jonathan, Patrice Limelette, et al. 2010. "Synthesis and Evaluation of Novel

Biocompatible Super-Paramagnetic Iron Oxide Nanoparticles as Magnetic Anticancer Drug Carrier and Fluorescence Active Label." *J. Phys. Chem.* 114: 5850–58.

Silva, André C, Tiago R Oliveira, Javier B Mamani, Suzana M F Malheiros, Luciana Malavolta, Lorena F Pavon, Tatiana T Sibov, et al. 2011. "Application of Hyperthermia Induced by Superparamagnetic Iron Oxide Nanoparticles in Glioma Treatment." *International Journal of Nanomedicine* 6 (January): 591–603. doi:10.2147/IJN.S14737.

Singh, Neenu, Gareth J S Jenkins, Romisa Asadi, and Shareen H Doak. 2010. "Potential Toxicity of Superparamagnetic Iron Oxide Nanoparticles (SPION)." *Nano Reviews* 1 (January): 1–15. doi:10.3402/nano.v1i0.5358.

Sjogren, Carl E, Karen Briley-saebra, Maj Hanson, and Christer Johansson. "Magnetic Characterization of Iron Oxides for Magnetic Resonance Imaging," no. 9.

Steitz, Benedikt, Heinrich Hofmann, Sarah W. Kamau, Paul O. Hassa, Michael O. Hottiger, Brigitte von Rechenberg, Magarethe Hofmann-Amtenbrink, and Alke Petri-Fink. 2007. "Characterization of PEI-Coated Superparamagnetic Iron Oxide Nanoparticles for Transfection: Size Distribution, Colloidal Properties and DNA Interaction." *Journal of Magnetism and Magnetic Materials* 311 (1): 300–305. doi:10.1016/j.jmmm.2006.10.1194.

Stolnik, S., L. Illum, and S.S. Davis. 1995. "Long Circulating Microparticulate Drug Carriers." *Advanced Drug Delivery Reviews* 16 (2-3): 195–214. doi:10.1016/0169-409X(95)00025-3.

Stroh, Albrecht, Claus Zimmer, Cindy Gutzeit, Manuela Jakstadt, Franziska Marschinke, Tobias Jung, Herbert Pilgrimm, and Tilman Grune. 2004. "Iron Oxide Particles for Molecular Magnetic Resonance Imaging Cause Transient Oxidative Stress in Rat Macrophages." *Free Radical Biology & Medicine* 36 (8): 976–84. doi:10.1016/j.freeradbiomed.2004.01.016.

Sumitani, Shogo, Motoi Oishi, Tatsuya Yaguchi, Hiroki Murotani, Yukichi Horiguchi, Minoru Suzuki, Koji Ono, Hironobu Yanagie, and Yukio Nagasaki. 2012. "Pharmacokinetics of Core-Polymerized, Boron-Conjugated Micelles Designed for Boron Neutron Capture Therapy for Cancer." *Biomaterials* 33 (13). Elsevier Ltd: 3568–77. doi:10.1016/j.biomaterials.2012.01.039.

Sun, Lin, Chi Huang, Tao Gong, and Shaobing Zhou. 2010. "A Biocompatible Approach to Surface Modification: Biodegradable Polymer Functionalized Super-Paramagnetic Iron Oxide Nanoparticles." *Materials Science and Engineering: C* 30 (4). Elsevier B.V.: 583–89. doi:10.1016/j.msec.2010.02.009.

Talelli, Marina, Cristianne J F Rijcken, Twan Lammers, Peter R Seevinck, Gert Storm, Cornelus F van Nostrum, and Wim E Hennink. 2009. "Superparamagnetic Iron Oxide Nanoparticles Encapsulated in Biodegradable Thermosensitive Polymeric Micelles: Toward a Targeted Nanomedicine Suitable for Image-Guided Drug Delivery." *Langmuir : The ACS Journal of Surfaces and Colloids* 25 (4): 2060–67. doi:10.1021/la8036499.

Tartaj, By Pedro, and Teresita Gonzµlez-carreæo. 2001. "Single-Step Nanoengineering of Silica Coated Maghemite Hollow Spheres with Tunable Magnetic Properties **." *Advanced Matarials* 13 (21): 1620–24.

Teja, Amyn S., and Pei-Yoong Koh. 2009. "Synthesis, Properties, and Applications of Magnetic Iron Oxide Nanoparticles." *Progress in Crystal Growth and Characterization of Materials* 55 (1-2). Elsevier Ltd: 22–45. doi:10.1016/j.pcrysgrow.2008.08.003.

Thoeny, Harriet C, Maria Triantafyllou, Frederic D Birkhaeuser, Johannes M Froehlich, Dechen W Tshering, Tobias Binser, Achim Fleischmann, Peter Vermathen, and Urs E Studer. 2009. "Combined Ultrasmall Superparamagnetic Particles of Iron Oxide-Enhanced and Diffusion-Weighted Magnetic Resonance Imaging Reliably Detect Pelvic Lymph Node Metastases in Normal-Sized Nodes of Bladder and Prostate Cancer Patients." *European Urology* 55 (4): 761–69. doi:10.1016/j.eururo.2008.12.034.

Thorek, Daniel L J, Antony K Chen, Julie Czupryna, and Andrew Tsourkas. 2006. "Superparamagnetic Iron Oxide Nanoparticle Probes for Molecular Imaging." *Annals of Biomedical Engineering* 34 (1): 23–38. doi:10.1007/s10439-005-9002-7.

Torchilin, Vladimir P. 2000. "Drug Targeting." *European Journal of Pharmaceutical Sciences* 11 (October): S81–91. doi:10.1016/S0928-0987(00)00166-4.

Ujiie, Kodai, Naoki Kanayama, Kei Asai, Mikio Kishimoto, Yusuke Ohara, Yoshimasa Akashi, Keiichi Yamada, et al. 2011. "Preparation of Highly Dispersible and Tumor-Accumulative, Iron Oxide Nanoparticles Multi-Point Anchoring of PEG-B-poly(4-Vinylbenzylphosphonate) Improves Performance Significantly." *Colloids and Surfaces. B, Biointerfaces* 88 (2). Elsevier B.V.: 771–78. doi:10.1016/j.colsurfb.2011.08.013.

Ulman, Abraham. 1996. "Formation and Structure of Self-Assembled Monolayers." *Chemical Reviews* 96 (4): 1533–54. doi:10.1021/cr9502357.

Unsoy, Gozde, Serap Yalcin, Rouhollah Khodadust, Gungor Gunduz, and Ufuk Gunduz. 2012. "Synthesis Optimization and Characterization of Chitosan-Coated Iron Oxide Nanoparticles Produced for Biomedical Applications." *Journal of Nanoparticle Research* 14 (11): 964. doi:10.1007/s11051-012-0964-8.

Valenzuela, Roberto, María Cecilia Fuentes, Carolina Parra, Jaime Baeza, Nelson Duran, S.K. Sharma, Marcelo Knobel, and Juanita Freer. 2009. "Influence of Stirring Velocity on the Synthesis of Magnetite Nanoparticles (Fe3O4) by the Co-Precipitation Method." *Journal of Alloys and Compounds* 488 (1): 227–31. doi:10.1016/j.jallcom.2009.08.087.

Van Doorslaer, S., I. Caretti, I. a. Fallis, and D. M. Murphy. 2009. "The Power of Electron Paramagnetic Resonance to Study Asymmetric Homogeneous Catalysts Based on Transition-Metal Complexes." *Coordination Chemistry Reviews* 253: 2116–30. doi:10.1016/j.ccr.2008.12.010.

Varanda, L. C., M. Jafelicci, P. Tartaj, K. O' Grady, T. González-Carreño, M. P. Morales, T. Muñoz, and C. J. Serna. 2002. "Structural and Magnetic Transformation of Monodispersed Iron Oxide Particles in a Reducing Atmosphere." *Journal of Applied Physics* 92 (4): 2079. doi:10.1063/1.1496124.

Veiseh, Omid, Jonathan W Gunn, and Miqin Zhang. 2010. "Design and Fabrication of Magnetic Nanoparticles for Targeted Drug Delivery and Imaging." *Advanced Drug Delivery Reviews* 62 (3). Elsevier B.V.: 284–304. doi:10.1016/j.addr.2009.11.002.

Veranth, John M, Erin G Kaser, Martha M Veranth, Michael Koch, and Garold S Yost. 2007. "Cytokine Responses of Human Lung Cells (BEAS-2B) Treated with Micron-Sized and Nanoparticles of Metal Oxides Compared to Soil Dusts." *Particle and Fibre Toxicology* 4 (January): 2. doi:10.1186/1743-8977-4-2.

Viali, Wesley Renato, Eloiza da Silva Nunes, Caio Carvalho dos Santos, Sebastião William da Silva, Fermin Herrera Aragón, José Antonio Huamaní Coaquira, Paulo César Morais, and Miguel Jafelicci. 2013. "PEGylation of SPIONs by Polycondensation Reactions: A New Strategy to Improve Colloidal Stability in Biological Media." *Journal of Nanoparticle Research* 15 (8): 1824. doi:10.1007/s11051-013-1824-x.

Vijayakumar, R, Yu Koltypin, I Felner, and A Gedanken. 2000. "Sonochemical Synthesis and Characterization of Pure Nanometer-Sized Fe 3 O 4 Particles." *Materials Science and Engineering A* 286: 101–5.

Wahajuddin. 2012. "Superparamagnetic Iron Oxide Nanoparticles : Magnetic Nanoplatforms as Drug Carriers." *International Journal of Nanomedicine* 7: 3445–71.

Wang, Y X, S M Hussain, and G P Krestin. 2001. "Superparamagnetic Iron Oxide Contrast Agents: Physicochemical Characteristics and Applications in MR Imaging." *European Radiology* 11 (11): 2319–31. doi:10.1007/s003300100908.

Wassel, Ronald a., Brian Grady, Richard D. Kopke, and Kenneth J. Dormer. 2007. "Dispersion of Super Paramagnetic Iron Oxide Nanoparticles in Poly(d,l-Lactide-Co-Glycolide) Microparticles." *Colloids and Surfaces A: Physicochemical and Engineering Aspects* 292 (2-3): 125–30. doi:10.1016/j.colsurfa.2006.06.012.

Weinstein, Jason S, Csanad G Varallyay, Edit Dosa, Seymur Gahramanov, Bronwyn Hamilton, William D Rooney, Leslie L Muldoon, and Edward a Neuwelt. 2010. "Superparamagnetic Iron Oxide Nanoparticles: Diagnostic Magnetic Resonance Imaging and Potential Therapeutic Applications in Neurooncology and Central Nervous System Inflammatory Pathologies, a Review." *Journal of Cerebral Blood Flow and Metabolism : Official Journal of the International Society of Cerebral Blood Flow and Metabolism* 30 (1). Nature Publishing Group: 15–35. doi:10.1038/jcbfm.2009.192.

Weissleder, Ralph, David D Stark, Barry L Engelstad, Bruce A Bacon, David L White, Paula Jacobs, and Jerome Lewis. 1989. "Superparamagnetic Pharmacokinetics Iron Oxide : And Toxicity."

Wu, Xiao, Jingyuan Tang, Yongcai Zhang, and Hao Wang. 2009. "Low Temperature Synthesis of Fe3O4 Nanocrystals by Hydrothermal Decomposition of a Metallorganic Molecular Precursor." *Materials Science and Engineering: B* 157 (1-3): 81–86. doi:10.1016/j.mseb.2008.12.021.

Xu, Cui-rong, Wen-ji Chen, Ning-na Chen, and Xiao-mao Li. 2009. "Daunorubicin-Loaded Magnetic Nanoparticles of Fe 3 O 4 Overcome Multidrug Resistance and Induce

Apoptosis of K562-N / VCR Cells in Vivo." *International Journal of Nanomedicine* 4: 201–8.

Yan, Juan, Shaobo Mo, Jiaorong Nie, Wenxuan Chen, Xinyu Shen, Jiming Hu, Guangming Hao, and Hua Tong. 2009. "Hydrothermal Synthesis of Monodisperse Fe3O4 Nanoparticles Based on Modulation of Tartaric Acid." *Colloids and Surfaces A: Physicochemical and Engineering Aspects* 340 (1-3): 109–14. doi:10.1016/j.colsurfa.2009.03.016.

Yang, Hee-Man, Byung Chang Oh, Jong Hun Kim, Taebin Ahn, Ho-Seong Nam, Chan Woo Park, and Jong-Duk Kim. 2011. "Multifunctional Poly(aspartic Acid) Nanoparticles Containing Iron Oxide Nanocrystals and Doxorubicin for Simultaneous Cancer Diagnosis and Therapy." *Colloids and Surfaces A: Physicochemical and Engineering Aspects* 391 (1-3). Elsevier B.V.: 208–15. doi:10.1016/j.colsurfa.2011.04.032.

Ying, Xiao-Ying, Yong-Zhong Du, Ling-Hong Hong, Hong Yuan, and Fu-Qiang Hu. 2011. "Magnetic Lipid Nanoparticles Loading Doxorubicin for Intracellular Delivery: Preparation and Characteristics." *Journal of Magnetism and Magnetic Materials* 323 (8). Elsevier: 1088–93. doi:10.1016/j.jmmm.2010.12.019.

Yoffe, Serge, Tim Leshuk, Perry Everett, and Frank Gu. 2013. "Superparamagnetic Iron Oxide Nanoparticles (SPIONs): Synthesis and Surface Modification Techniques for Use with MRI and Other Biomedical Applications." *Current Pharmaceutical Design* 19 (3): 493–509. doi:10.2174/138161213804143707.

Yoshitomi, Toru, Daisuke Miyamoto, and Yukio Nagasaki. 2009. "Design of Core--Shell-Type Nanoparticles Carrying Stable Radicals in the Core." *Biomacromolecules* 10 (3): 596–601. doi:10.1021/bm801278n.

Zhang, DongEn, ZhiWei Tong, ShanZhong Li, XiaoBo Zhang, and Ailing Ying. 2008. "Fabrication and Characterization of Hollow Fe3O4 Nanospheres in a Microemulsion." *Materials Letters* 62 (24): 4053–55. doi:10.1016/j.matlet.2008.05.023.

Zhang, Yong, Nathan Kohler, and Miqin Zhang. 2002. "Surface Modification of Superparamagnetic Magnetite Nanoparticles and Their Intracellular Uptake." *Biomaterials* 23: 1553–61.

Zhao, Hong, Katayoun Saatchi, and Urs O. Häfeli. 2009. "Preparation of Biodegradable Magnetic Microspheres with Poly(lactic Acid)-Coated Magnetite." *Journal of Magnetism and Magnetic Materials* 321 (10): 1356–63. doi:10.1016/j.jmmm.2009.02.038.

Zou, Peng, Yanke Yu, Y Andrew Wang, Yanqiang Zhong, and Amanda Welton. 2010. "Articles Superparamagnetic Iron Oxide Nanotheranostics for Targeted Cancer Cell Imaging and pH-Dependent Intracellular Drug Release." *Molecular Pharmaceutics* 7 (6): 1974–84.